LA-7932-MS (ENDF-283)
Informal Report

3



# Evaluated Data for n + $^{9}$Be Reactions



LOS ALAMOS SCIENTIFIC LABORATORY
Post Office Box 1663 Los Alamos, New Mexico 87545

This report was not edited by the Technical Information staff.

This work was supported by the US Department of Energy, Offices of Magnetic Fusion, Military Affairs, and Energy Research.



UNITED STATES
DEPARTMENT OF ENERGY
CONTRACT W-7405-ENG. 36

LA-7932-MS (ENDF-283)
Informal Report

UC-34c
Issued: July 1979

# Evaluated Data for n + $^{9}$Be Reactions

P. G. Young
L. Stewart

# EVALUATED DATA FOR n + $^{9}$Be REACTIONS

by

P. G. Young and L. Stewart

ABSTRACT

A new evaluation of neutron-induced reactions on $^{9}$Be has been completed for the energy range $10^{-5}$ eV to 20 MeV. Particular emphasis is placed on accurately representing new measurements of secondary neutron-emission spectra and scattering data between 6 and 15 MeV. Additionally, adjustments to the total, (n,γ), and (n,t) cross sections in previous ENDF/B evaluations have been made, and covariance data files that contain error correlations for the cross sections and emission spectra are included in the evaluation. The data are available in ENDF/B format from the ENDF/A library at the National Nuclear Data Center at Brookhaven National Laboratory and from the Radiation Shielding Information Center at Oak Ridge National Laboratory.

---

## I. INTRODUCTION

The main purpose of this work is to provide an evaluated data set for neutron-induced reactions on $^{9}$Be that accurately represents new measurements of neutron-emission spectra (Dr77) and elastic and inelastic scattering (Ho78a) for incident energies in the 6-15 MeV range. Additionally, the neutron total cross section was updated to better represent both older and more recent measurements (Fo67, Sc71, Au77), and the (n,t) cross section was modified on the basis of existing data (Wy58, My61). Finally, a set of data covariances was developed that not only permits description of the cross-section uncertainties but also provides correlated errors for the secondary neutron energy distributions.

The standard formats* for both Version IV and V of ENDF/B do not provide sufficient flexibility to accurately represent energy-angle correlations of neutron-emission spectra from light-element reactions. The deficiencies in the formats are discussed in detail by Howerton and Perkins (Ho78b). These limitations can be overcome in a straightforward manner for light-element reactions that involve only one emitted neutron by representing continuum-neutron emission as a sum of discrete inelastic scatterings to groups of levels (or excitation energy bins) in the residual nucleus. This method, which is sometimes referred to as the pseudo-level technique, has been used successfully for $^{6}$Li, $^{10}$B, $^{14}$N, $^{16}$O, and $^{27}$Al evaluations in ENDF/B-V (St76, Yo79).

For the present evaluation, we have extended the use of excitation energy bins to include secondary neutron emission from the $^{9}$Be(n,2n) reaction. While there is no particular difficulty in applying this technique for (n,2n) reactions, bookkeeping in processing the data is slightly more complicated, and ENDF/B procedures have customarily required a separate representation of (n,2n) reactions. Therefore, because of the ENDF/B procedural restriction, this evaluation is not part of the official ENDF/B data set but is available from the ENDF/A library maintained at Brookhaven National Laboratory and from the Radiation Shielding Information Center at Oak Ridge National Laboratory.

The evaluated cross sections for each of the possible reaction types are discussed and compared to experiment and ENDF/B-V (Ho78c) in Sec. II. Sec. III includes a summary of the elastic and inelastic angular distribution evaluations, again with detailed comparisons to experiment and ENDF/B-V. The (n,2n) emission spectra are described in detail in Sec. IV, and the gamma-ray production data are summarized in Sec. V. The covariance data file provided with the evaluation is discussed in Sec. VI. Finally, a brief summary and concluding remarks are given in Sec. VII.

## II. NEUTRON CROSS SECTIONS

The thresholds and Q-values (Wa77) for the possible neutron reactions below 20 MeV are given in Table I. Data are not included in the evaluation for the $^{9}$Be(n,np)$^{8}$Li, $^{9}$Be(n,nd)$^{7}$Li, and $^{9}$Be(n,nt)$^{6}$Li reactions because the (unmeasured)

*It is always possible to represent energy-angle correlations precisely by the use of File 6 in ENDF/B. However, the use of File 6 has been avoided because of its complexity and because standard ENDF/B processing codes do not presently handle it.

TABLE I

Q-VALUES AND THRESHOLDS FOR $^{9}Be$ NEUTRON-INDUCED REACTIONS

| Reaction | Q (MeV) | Threshold (MeV) |
|---|---|---|
| $^{9}Be(n,\gamma)^{10}Be$ | 6.812 | 1.749 |
| $^{9}Be(n,2n)2\alpha$ | - 1.573 | 1.749 |
| $^{9}Be(n,p)^{9}Li$ | -12.824 | 14.259 |
| $^{9}Be(n,d)^{8}Li$ | -14.663 | 16.304 |
| $^{9}Be(n,t)^{7}Li$ | -10.439 | 11.607 |
| $^{9}Be(n,\alpha)^{6}He$ | - 0.6025 | 0.6699 |
| $^{9}Be(n,np)^{8}Li$ | -16.888 | 18.778 |
| $^{9}Be(n,nd)^{7}Li$ | -16.696 | 18.565 |
| $^{9}Be(n,nt)^{6}Li$ | -17.689 | 19.669 |
| $^{9}Be(n,n\alpha)^{5}He$ | - 2.463 | 2.739 |

cross sections are expected to be very small. The $^{9}Be(n,n\alpha)^{5}He$ reaction is combined into the $^{9}Be(n,2n)2\alpha$ data, since $^{5}He$ decays immediately into a neutron and an alpha particle.

## A. Total Cross Section

In the energy region below 0.5 MeV, the present evaluation was essentially taken from ENDF/B-IV (Ho74). The values near thermal neutron energies and below are slightly lower than ENDF/B-IV (and V) since this evaluation is based on more recent experimental data for the $(n,\gamma)$ cross section (see Sec. II. G below). The results in the range 1-400 keV are compared to the available experimental data and to ENDF/B-V (Ho78c) in Fig. 1. There is very little difference between the two evaluations, and both agree reasonably with experiment. Above 0.5 MeV, the present evaluation is based mainly on the experimental data of Auchampaugh et al. (Au79) and Schwartz et al. (Sc71). The results from 0.4 to 2 MeV are compared to experiment and ENDF/B-V in Fig. 2; from 2 to 6 MeV in Fig. 3; and from 6 to 20 MeV in Fig. 4. The differences between the present evaluation and ENDF/B-V are relatively minor except for limited energy regions, particularly near 16 MeV.

B. (n,2n) Cross Section

The (n,2n) reaction on $^{9}$Be leads to $^{8}$Be, which immediately breaks up into two alpha particles. Although the neutron emission spectrum is continuous in energy, a well-defined peak is observed (Dr77, Ho78a) corresponding to a cluster of levels near an excitation energy of 2.43 MeV in $^{9}$Be. Accordingly, the (n,2n) reaction was represented in the evaluation as a continuum plus a single broad level at $E_x$ = 2.43 MeV. As discussed in Sec. IV, the data are given in excitation energy bins using ENDF/B reaction types MT=51-83, with an LR flag of 16 to indicate that the reactions are in fact (n,2n) rather than (n,n'). The cluster of real levels is included in MT=52.

The neutron emission cross section corresponding to the cluster of levels near 2.43 MeV is illustrated in Fig. 5. The spread in the experimental data is somewhat large, possibly because the various measurements had different detector resolutions, and continuum components had to be subtracted from the observed peaks (e.g., see Dr77). In the present evaluation, emphasis was placed on representing the total (n,2n) cross-section measurements as accurately as possible and, at the same time, maintaining reasonable agreement with the Drake et al. (Dr77) measurements of the continuum component of the emission spectra. The integrated or total (n,2n) cross section is shown in Fig. 6 with the available experimental data. The evaluated curve was taken from ENDF/B-IV, which is the same as ENDF/B-V. The evaluation emphasizes the data of Bloser et al. (Bl72) and Holmberg et al. (Ho69) and is in good agreement with the more recent Drake measurement.

C. (n,p) Cross Section

The $^{9}$Be(n,p)$^{9}$Li reaction cross section was taken from ENDF/B-IV, which is also the same as ENDF/B-V. As shown in Fig. 7, the evaluated curve is based on the single measurement of Alburger (Al63) near 15.5 MeV, with a rough extrapolation to 20 MeV.

D. (n,d) Cross Section

The evaluated $^{9}$Be(n,d)$^{8}$Li cross section is based upon the experimental data of Scobel et al. (Sc69) and is shown in Fig. 8. Again, the evaluation was taken from ENDF/B-IV and is the same as ENDF/B-V.

## E. (n,t) Cross Section

The $^{9}Be(n,t)^{7}Li$ cross-section evaluation is based upon the measurements of Wyman et al. (Wy58) and Myachkova and Perelygin (My61) near 14 MeV. The results are shown in Fig. 9. The total (n,t) cross section is the sum of $(n,t_0)$ and $(n,t_1)$, which are also included in the evaluation. The $(n,t_1)$ evaluation is based upon the experimental data of Dietrich et al. (Di75), although both the $(n,t_0)$ and $(n,t_1)$ cross sections were adjusted somewhat to agree with the total (n,t) cross-section measurements (Wy58, My61) given in Fig. 9. The ENDF/B-V (n,t) evaluation is based upon the present work.

## F. (n,α) Cross Section

The $^{9}Be(n,\alpha)^{6}He$ cross-section data are shown in Fig. 10. The evaluation is taken from ENDF/B-IV (same as ENDF/B-V) and is based mainly on the experimental data of Stelson et al. (St57), Bass et al. (Ba61), Battat and Ribe (Ba53), Paik et al. (Pa67), and Myachkova et al. (My61).

## G. (n,γ) Cross Section

The $^{9}Be(n,\gamma)^{10}Be$ cross section for thermal neutrons (0.0253 eV) is taken from the measurement of Jurney (Ju74), which gives a value of $7.6 \pm 0.8$ mb. The cross section is assumed to follow a 1/v energy dependence from $10^{-5}$ to 100 eV. Because no experimental data are available at energies other than thermal, the cross section is extrapolated logarithmically to a value of 0.1 mb at 1 keV and is held constant at this value to 20 MeV.

## H. Nonelastic Cross Section

The nonelastic cross section for the present evaluation is compared with ENDF/B-V and available experimental data in Fig. 11. The present results were obtained by summing the cross sections from the various nonelastic reactions, and they correspond closely to the ENDF/B-V evaluation.

## I. Elastic Cross Section

The evaluated elastic cross section was obtained at all energies by subtracting the evaluated nonelastic results from the total cross section. Below 1.75 MeV, the only nonelastic process is the very small (n,γ) reaction so the elastic is essentially equal to the total cross section at those energies.

Below 10 keV, the elastic was constrained to equal a constant 6 b, in agreement with ENDF/B-V.

The results from 20 keV to 2 MeV are compared to direct elastic measurements and to ENDF/B-V in Fig. 12. Similar comparisons are given in Fig. 13 for the energy range up to 20 MeV. The results are consistent within experimental accuracies with the new data of Drake et al. (Dr77) and Hogue et al. (Ho78a), although the evaluation is systematically lower than the latter (mean deviation = -3%).

## III. NEUTRON ANGULAR DISTRIBUTIONS

### A. Elastic Scattering

The elastic scattering angular distributions were evaluated by fitting all available measurements in terms of Legendre expansions and passing smooth curves through the resulting energy-dependent coefficients. Measurements at a total of 160 neutron energies were included in the analysis. Below 50 keV, the distributions were assumed isotropic. Above 15 MeV, the Legendre coefficients were obtained from optical-model calculations using the parameters of Wilmore and Hodgson (Wi64). In order to match the coefficients determined from experimental data near 14 MeV, it was necessary to renormalize some of the calculated coefficients slightly.

The evaluated $\ell = 1$ and $\ell = 2$ coefficients at energies below 1.5 MeV are compared to those extracted from experimental data in Fig. 14. Similarly, the $\ell = 1$-4 coefficients for 1-20 MeV are presented in Fig. 15, and the $\ell = 5$-8 coefficients are given in Fig. 16. In the energy range 7-15 MeV, the evaluation is based entirely on the experimental data of Hogue et al. (Ho78a). These results are consistent with the recent measurements of Drake et al. (Dr77). Coefficients from the latter measurement are not shown at 10.1 and 14.2 MeV because that experiment was directed mainly at measuring the emission spectrum down to as low an energy as possible, and not enough angles were included for reliable Legendre fitting of the elastic data at the higher energies.

Comparisons of the present evaluation with experimental angular distributions and with ENDF/B-V are given in Figs. 17-33. The two evaluations are in good agreement below 2 MeV, but differences of 20% or more occur at some angles for the higher neutron energies.

## B. Inelastic Scattering

As with elastic scattering, the angular distributions for inelastic scattering to the cluster of states near $E_x(^9Be)$ = 2.43 MeV (MT=52) are represented with Legendre coefficients obtained by fitting the available experimental results. The Legendre coefficients for $\ell$ = 1-4 are compared to experiment in Fig. 34. Angular distributions calculated from the evaluation are shown with the measurements in Figs. 35-38.

# IV. NEUTRON EMISSION SPECTRA

Because of problems associated with accurately representing energy-angle correlations in the emitted neutron spectra, the (n,2n) data are given as excitation cross sections and angular distributions for a series of excitation energy bins in the evaluation. That is, cross sections and secondary angular distributions for populating particular ranges of excitation energies in the residual nucleus are tabulated as functions of incident-neutron energy. In the parlance of the ENDF/B format, the data are given in Files 3 and 4 using reaction types MT=51-83, each with an LR flag of 16 to indicate that the reactions are (n,2n) rather than (n,n'). Except for MT=52, which represents the cluster of real levels near $E_x(^9Be)$ = 2.43 MeV, the excitation energy bins for all MT sections have a width of 0.5 MeV.

The excitation cross sections and associated angular distributions were determined from the experimental data of Drake et al. (Dr77) at 5.9, 10.1, and 14.2 MeV. Neutron emission spectra down to an emission energy of 400 keV were measured at seven or eight angles for each incident energy. In the evaluation, smooth interpolations and extrapolations of the data were made to other energies. The sum of the excitation cross sections was constrained to equal the total (n,2n) cross section shown in Fig. 6. Anisotropic, forward-peaked angular distributions were required to fit most of the experimental data, with the most pronounced effects occurring for the lowest excitation energy bins. The angular data are included as tabulated distributions in File 4.

The emission spectra calculated from the evaluated results and from ENDF/B-V are compared to the experimental data in Figs. 39-44. Only the continuum or smooth portions of the experimental emission spectra are shown in the figures; that is, the peaks in the measured spectra due to inelastic scattering to levels near $E_x(^9Be)$ = 2.43 MeV have been removed (see Fig. 5). The calculated curves

show the total (n,2n) emission spectrum and only exclude the elastic scattering peak.

The results in Figs. 39-44 show that the present technique of grouping the data in excitation energy bins represents the experimental spectra far more accurately than does ENDF/B-V. The large discrepancies between experiment and the ENDF/B-V curves result in part from the special format that was used to represent the data, as described by Howerton and Perkins (Ho78b). In that format, the $^{9}Be(n,n')^{9}Be^{*}$ neutrons (or first neutrons) are given as four discrete inelastic scattering lines with zero width. The second neutrons that result after neutron emission from the $^{9}Be^{*}$ states are then described in four sets of continuous energy spectra, each of which has its own angular distribution. The requirement of zero width for the discrete first neutrons, the use of just four levels, and the inability to incorporate energy-angle correlations in the second-neutron continuous spectra are too restrictive to adequately describe the experimental results.

An additional problem with ENDF/B-V is the particular choice of $^{9}Be$ discrete states that were included ($E_x$ = 1.68, 2.43, 6.76, and 11.28 MeV). The new measurements (Dr77, Ho78a) show no evidence for the $E_x$ = 1.68 MeV state, which appears as the highest energy peak in the dashed curves in Figs. 39-44. In addition, Anderson and his coworkers at Livermore (Ba64, An70) have searched for the isobaric analogue state in $^{9}B$ that would be implied by the existence of the 1.68-MeV state in $^{9}Be$. Although they employed three different reaction mechanisms and covered a wide range in incident energies with detectors at several different reaction angles, they observed an upper limit of about 100μ b/sr for the production of an ∿1.7-MeV state in $^{9}B$. Therefore, for the present evaluation we have concluded that even if the 1.68-MeV state exists, its excitation cross section is negligible, and the corresponding emission spectrum is given by the weak continuum measured by Drake et al. (Dr77).

Finally, it should be mentioned that simply broadening the discrete first neutron peaks in the ENDF/B-V spectra is still not sufficient to produce agreement with experiment. Calculations which include finite widths for the discrete states using level widths compiled by Ajzenberg-Selove (Aj74) are compared to the Drake measurements in Fig. 45. While the discrepancies with experiment are somewhat reduced, the ENDF/B-V results still differ substantially from the measured spectra.

## V. GAMMA-RAY PRODUCTION DATA

The only reactions that result in gamma-ray production of any consequence when neutrons interact with $^{9}Be$ are the $^{9}Be(n,\gamma)^{10}Be$ and the $^{9}Be(n,t\gamma)^{7}Li$ processes. In the latter reaction, 0.4776-MeV gamma rays from deexcitation of the first excited state in $^{7}Li$ occur. These data are represented in the evaluation with a multiplicity of one relative to the $^{9}Be(n,t_1)$ cross section.

The gamma-ray production evaluation for the $^{9}Be(n,\gamma)^{10}Be$ reaction is based on the spectrum measurements of Jurney (Ju74). The decay scheme used for the evaluation is shown in Fig. 46. Intensities are given in photons/100 neutron captures, and the capturing state for the thermal neutron measurement is represented by the dashed line at the top. Minor adjustments were made in the measured intensities to exactly conserve energy, and two unobserved transitions (dashed lines) were added for the same reason. The gamma-ray energies in the evaluation have been corrected for recoil of the residual nuclei. A total gamma-ray multiplicity of 1.5811 was used in the evaluation.

For the evaluation, all gamma rays from both the $(n,t\gamma)$ and the $(n,\gamma)$ reactions were assumed isotropic in the laboratory system.

## VI. COVARIANCES

Correlated error information is included in the evaluation for all neutron cross-section types. The energy-correlated errors are generally composed of short-range and long-range components, which are based on quoted experimental uncertainties, scatter of the various measurements, and the particular choice of measurements used in different energy ranges covered by the evaluation. All error data are given explicitly except for elastic scattering, which can be derived from the other reactions by subtracting the total and nonelastic error matrices in the same manner that the elastic cross section was obtained.

Correlations across reaction type are included in the excitation energy bins used to describe the (n,2n) reaction, that is, in MT=51-83. Because these data are based mainly on the Drake et al. (Dr77) measurement, the systematic uncertainties in that experiment were used to infer the MT=51-83 correlations. The elastic scattering error matrix is also correlated with the other reactions from which it is derived.

Standard deviations obtained from the variances of the error matrices are included for a selection of incident neutron energies in Table II. In order to

TABLE II

EVALUATED STANDARD DEVIATIONS IN PERCENT

| $E_L$ (MeV) | $E_H$ (MeV) | Total | Elastic | (n,γ) | (n,2n) | (n,p) | (n,d) | (n,t) | (n,α) |
|---|---|---|---|---|---|---|---|---|---|
| 1.0-11 | 1.0-4 | 3 | 3 | 11 | | | | | |
| 1.0-4 | 1.0-3 | 3 | 3 | 25 | | | | | |
| 1.0-3 | 0.25 | 3 | 3 | 50 | | | | | |
| 0.25 | 0.5 | 4 | 4 | 60 | | | | | |
| 0.5 | 0.7 | 4 | 4 | 70 | | | | | 80 |
| 0.7 | 0.9 | 4 | 4 | 80 | | | | | 50 |
| 0.9 | 1.1 | 4 | 4 | 90 | | | | | 41 |
| 1.1 | 1.3 | 4 | 4 | 100 | | | | | 31 |
| 1.3 | 1.5 | 4 | 4 | 110 | | | | | 21 |
| 1.5 | 2.0 | 4 | 4 | 120 | | | | | 12 |
| 2.0 | 2.3 | 4 | 4 | 130 | | | | | 10 |
| 2.3 | 2.6 | 5 | 5 | 140 | 25 | | | | 10 |
| 2.6 | 3.0 | 5 | 6 | 150 | 25 | | | | 10 |
| 3.0 | 3.4 | 4 | 6 | 160 | 17 | | | | 10 |
| 3.4 | 3.7 | 6 | 9 | 170 | 17 | | | | 10 |
| 3.7 | 4.0 | 6 | 11 | 180 | 17 | | | | 10 |
| 4.0 | 4.4 | 6 | 10 | 190 | 11 | | | | 10 |
| 4.4 | 5.0 | 4 | 8 | 200 | 11 | | | | 12 |
| 5.0 | 5.5 | 4 | 8 | 200 | 10 | | | | 12 |
| 5.5 | 6.5 | 4 | 8 | 200 | 10 | | | | 12 |
| 6.5 | 7.5 | 4 | 8 | 200 | 8 | | | | 12 |
| 7.5 | 8.5 | 4 | 9 | 200 | 11 | | | | 15 |
| 8.5 | 9.5 | 4 | 8 | 200 | 9 | | | | 20 |
| 9.5 | 10.5 | 4 | 9 | 200 | 11 | | | | 30 |
| 10.5 | 11.5 | 4 | 8 | 200 | 9 | | | | 30 |
| 11.5 | 12.5 | 4 | 10 | 200 | 13 | | | 50 | 30 |
| 12.5 | 13.5 | 4 | 9 | 200 | 10 | | | 50 | 20 |
| 13.5 | 14.5 | 4 | 10 | 100 | 13 | 100 | | 50 | 15 |
| 14.5 | 15.5 | 4 | 9 | 50 | 11 | 50 | | 50 | 20 |
| 15.5 | 16.5 | 4 | 11 | 50 | 16 | 50 | 50 | 50 | 30 |
| 16.5 | 18.0 | 4 | 10 | 100 | 14 | 100 | 12 | 50 | 40 |
| 18.0 | 20.0 | 4 | 15 | 100 | 25 | 100 | 12 | 50 | 50 |

keep the size of the error files to a minimum, rather coarse groupings were used for the evaluated error data. As a result, the matching of the standard deviations in Table II with those inferred from the experimental data base is somewhat approximate.

The standard deviations for elastic scattering in Table II, which were derived entirely from the other reaction types in the evaluation, vary from 8-10% over the energy range 7-15 MeV. The quoted experimental errors for the measurements of Hogue et al. (Ho78a) vary from 3-6% over the same energy range. We therefore conclude that a more detailed error analysis for the evaluation would probably result in somewhat smaller variances overall, and in this sense the present covariances are conservative.

## VII. SUMMARY

Use of excitation energy bins in the present evaluation to represent all (n,2n) reactions for $^{9}$Be has resulted in a more accurate description of neutron-emission spectra than is available in the ENDF/B-V (Ho78c) evaluation. Adjustments have been made in the total, elastic, (n,$\gamma$), and (n,t) cross sections to better conform with recent experimental data. A Legendre analysis of elastic and discrete inelastic angular distributions that were incorporated in the evaluation results in improved agreement with experiment above $E_n$ = 2 MeV. Finally, evaluated covariance data are provided in a form that includes correlated errors in the secondary neutron-energy distributions.

Hendricks (He78) has validated a version of the present evaluation for neutron energies in the fission spectrum region by calculating $^{9}$Be-reflected uranium and plutonium critical assemblies, as well as reactivity contributions from $^{9}$Be to the GODIVA (bare uranium) and JEZEBEL (bare plutonium) critical assemblies. Using the $S_n$ code ONETRAN (Hi75), Hendricks also finds that the present evaluation describes the Livermore pulsed-sphere experiments (Wo72) better than ENDF/B-IV. In the latter measurements, time-of-flight neutron-emission spectra were measured from $^{9}$Be spheres that were pulsed at the center with 14-MeV neutrons. The calculation of these experiments is therefore sensitive to the representation of neutron-emission spectra from (n,2n) reactions used in the evaluations.

ACKNOWLEDGMENTS

It is a pleasure to thank D. C. George for her assistance in developing the graphics capability used in this report and R. J. LaBauve for calculating the standard deviations given in Table II from the basic ENDF/B file. We also wish to thank D. M. Drake for several helpful discussions regarding the LASL measurements of neutron emission spectra.

REFERENCES

Ad49 R. K. Adair, H. H. Barschall, C. K. Bockelman, and O. Sala, "Total Cross Section of Be, O, Na, and Ca for Fast Neutrons," Phys. Rev. 75, 1124 (1949).

Ad60 B. Adams, private communication to R. J. Howerton, Lawrence Livermore Laboratory (1960). Referenced in AWRE-O-27/60 by K. Parker (1960).

Aj74 F. Ajzenberg-Selove and T. Lauritsen, "Energy Levels of Light Nuclei A=5-10," Lemon Aid Preprint series LAP-124 (1974).

Al63 D. E. Alburger, "Beta Decay of $Li^9$," Phys. Rev. 132, 328 (1963).

An58 J. D. Anderson, C. C. Gardner, J. W. McClure, M. P. Nakada, and C. Wong, "Inelastic Scattering of 14-MeV Neutrons from Carbon and Beryllium," Phys. Rev. 111, 572 (1958).

An70 J. D. Anderson, C. Wong, B. A. Pohl, and J. W. McClure, "Fast-Neutron Spectroscopy of the Reaction $^9Be(p,n)^9B$ at 20 MeV," Phys. Rev. C2, 319 (1970).

As58 V. J. Ashby, H. C. Catron, L. L. Newkirk, and J. C. Taylor, "Absolute Measurement of (n,2n) Cross Sections at 14.1 MeV," Phys. Rev. 111, 616 (1958).

Au79 G. F. Auchampaugh, S. Plattard, and N. W. Hill, "Neutron Total Cross-Section Measurements of $^9Be$, $^{10,11}B$, and $^{12,13}C$ From 1.0 to 14 MeV Using the $^9Be(d,n)^{11}B$ Reaction as a 'White' Neutron Source," Nucl. Sci. Eng. 69, 30 (1979).

Ba53 M. E. Battat and F. L. Ribe, "Formation of He-6 By 14-MeV Neutron Bombardment of Li and Be," Phys. Rev. 89, 80 (1953).

Ba57 W. P. Ball, M. MacGregor, and R. Booth, "Neutron-Nonelastic Cross Section for 14 MeV Neutrons, Phys. Rev. 110, 1392 (1958).

Ba61 R. Bass, T. W. Bonner, and H. P. Haenni, "Cross Section for the $Be^9(n,\alpha)He^6$ Reaction," Nucl. Phys. 23, 122 (1961).

Ba64 R. W. Bauer, J. D. Anderson, and C. Wong, "A Search for an Excited State in $^9B$ near 1.7-MeV," Nucl. Phys. 56, 117 (1964).

Be55 J. R. Beyster, R. L. Henkel, R. A. Nobles, and J. M. Kister, "Inelastic Collison Cross Sections at 1.0, 4.0, and 4.5 MeV Neutron Energies," Phys. Rev. 98, 1216 (1955).

Be56a J. R. Beyster, M. Walt, and E. W. Salmi, "Interaction of 1.0 MeV to 7.0 MeV Neutrons with Nuclei, Angular Distributions," Phys. Rev. 104, 1319 (1956).

Be56b R. L. Becker and H. H. Barschall, "Total Cross Sections of Light Elements for (α,n) Neutrons," Phys. Rev. 102, 1384 (1956).

Bi62 E. G. Bilpuch, Duke University, Physics Department, personal communication (1962).

Bl72 M. Bloser, "Absolute Messung des $^{9}$Be(n,2n) Wirkungsquerschnitts im Energiebereich Von 2.37 Bis 3.34 MeV," Atomkernenergie 20, 309 (1972).

Bo50 C. K. Bockelman, "Total Cross Sections of Be, B, O, and F for Fast Neutrons," Phys. Rev. 80, 1011 (1950).

Bo51 C. K. Bockelman, D. W. Miller, R. K. Adair, and H. H. Barschall, "Total Cross Sections for Light Nuclei for P-T-Neutrons," Phys. Rev. 84, 69 (1951).

Bo57 R. O. Bondelid, K. L. Dunning, and F. L. Talbott, "Total Neutron Cross Sections of Be, C, F, Co, and Ge," Phys. Rev. 105, 193 (1957).

Bo66 R. Bouchez, F. Merchez, V. Regis, V. S. Nguyen, R. Darves-Blanc, and D. L. Pham, "Etude de la Diffusion Elastique et Inelastic des Neutrons de 14 MeV par les Noyaux $^{6}$Li, $^{7}$Li, and $^{9}$Be," (paper CN-23/75) IAEA Conf. on Nuclear Data, Paris (1966).

Ca61 H. C. Catron, M. D. Goldberg, R. W. Hill, J. M. LeBlanc, J. P. Stoering, C. J. Taylor, and M. A. Williamson, "Deuterium and Beryllium (n,2n) Cross Sections Between 6 and 10 MeV," Phys. Rev. 123, 218 (1961).

Ch59 C. X. Chaun, "Etude de la Reaction Be(n,2n)2α," J. Phys. Radium 20, 621 (1959).

Co54 C. F. Cook and T. W. Bonner, "Scattering of Fast Neutrons in Light Nuclei," Phys. Rev. 94, 651 (1954).

Co58 H. O. Cohn and J. L. Fowler, "Differential Elastic Neutron Scattering From Beryllium," Bull. Am. Phys. Soc. 3, 305 (1958).

Co61 A. V. Cohen, "The Non-Elastic Neutron Cross Section for Uranium at 13-19 MeV and Beryllium at 14 MeV," J. Nucl. Energy, Parts A/B 14, 180 (1961).

Di63 D. Didier, H. Dillemann, P. Thouvenin, and E. Fort, in "Progess Report on Nuclear Data Research in the Euratom Community," Commissariat a L'Energie Atomique report EANDC(E)-49L, p. 85 (1963).

Di75 F. S. Dietrich, L. F. Hansen, and R. P. Koopman, "Cross Section for the $^{9}$Be $(n,t_1)^{7}$Li Reaction for $E_n$ Between 13.5 and 15 MeV," Bull. Am. Phys. Soc. 20, 85 (1975).

Dr77 D. M. Drake, G. F. Auchampaugh, E. D. Arthur, C. E. Ragan, and P. G. Young, "Double-Differential Beryllium Neutron Cross Sections at Incident Neutron Energies of 5.9, 10.1, and 14.2 MeV," Nucl. Sci. Eng. 63, 401 (1977).

Ea68 J. R. P. Eaton and J. Walker, "The Non-Elastic Cross Section of Beryllium for Neutrons from 2.3 to 5.2 MeV," Conf. on Neutron Cross Section Tech., Washington, D.C., 1, 169 (1968).

Fi57 G. J. Fischer, "Cross Section for the (n,2n) Reaction in $Be^{9}$," Phys. Rev. 108, 99 (1957).

Fl56 N. N. Flerov and V. M. Talyzin, "Cross Section for Inelastic Interactions of 14.5 MeV Neutrons with Various Elements," At. Energ. (Sov. J. At. Energy) 1, 155 (1956).

Fl58 N. N. Flerov and V. M. Talyzin, "Measurement of the Cross Section for the (n,2n) Reactions for 14-MeV Neutrons in Beryllium, Lead, and Bismuth," At. Energ. (Sov. J. At. Energy) 5, 657 (1958).

Fo55 J. M. Fowler, S. S. Hanna, and G. E. Owen, Johns Hopkins Hospital, personal communication (1955). Also "$Be^{9}$(n,2n)$Be^{8}$ Reaction," Phys. Rev. 98, 249 (1955).

Fo59 J. L. Fowler and H. O. Cohn, "Scattering of Neutrons from Beryllium," Bull. Am. Phys. Soc. 4, 385 (1959).

Fo61 D. B. Fossan, R. L. Walter, W. E. Wilson, and H. H. Barschall, "Neutron Total Cross Sections of Be, $B^{10}$, B, C, and O," Phys. Rev. 123, 209 (1961).

Fo67 D. G. Foster, Jr., and D. W. Glasgow, Los Alamos Scientific Laboratory, personal communication (1967).

Go58 V. M. Gorbachev and L. B. Poretskii, "Cross Section for Inelastic Interaction of 14 MeV Neutrons with Some Light Elements," Sov. J. Atomic Energy 4, 259 (1958).

Go64 G. V. Gorlov, N. S. Lebedeva, and V. M. Morozov, "Elastic Scattering of Polarized Neutrons by $Be^{9}$, $C^{12}$, $Co^{59}$, $Ni^{62}$, $Se^{80}$, $Nb^{93}$, $Cd^{114}$, $In^{115}$, $Sn^{118}$, $I^{127}$, Pb, and $Bi^{209}$ Nuclei," Dokl. Akad, Nauk SSSR (Sov. Phys.-Doklady) 158, 574 (1964).

He78 J. S. Hendricks, "Validation of a New $^{9}$Be Pseudolevel Evaluation," Trans. Am. Nucl. Soc. 30, 732 (1978).

Hi54 C. T. Hibdon and A. S. Langsdorf, Argonne National Laboratory, personal communication to Brookhaven National Laboratory Sigma Center (1954).

Hi75 T. R. Hill, "ONETRAN: A Discrete Ordinates Finite Code for the Solution of the One-Dimensional Multigroup Transport Equation," Los Alamos Scientific Laboratory report LA-5990-MS (1975).

Ho52 E. R. Hodgson, J. F. Gallagher, and E. M. Bowey, "Neutron Total Cross Sections," Proc. Phys. Soc. (London) 65, 992 (1952).

Ho69 M. Holmberg and J. Hansen, "The (n,2n) Cross Section of $^{9}$Be in the Energy Region 2.0-6.4 MeV," Nucl. Phys. 129, 305 (1969).

Ho74 R. J. Howerton and S. T. Perkins, ENDF/B-IV Evaluation MAT 1289, available from the National Nuclear Data Center at Brookhaven National Laboratory.

Ho78a H. H. Hogue, P. L. Von Behren, D. H. Epperson, S. G. Glendinning, P. W. Lisowski, C. E. Nelson, H. W. Newson, F. O. Purser, W. Tornow, C. R. Gould, and L. W. Seagondollar, "Differential Elastic and Inelastic Scattering of 7- to 15-MeV Neutrons from Beryllium," Nuc. Sci. Eng. 68, 38 (1978).

Ho78b R. J. Howerton and S. T. Perkins, "Comments on Beryllium (n,2n) Cross Sections in ENDF/B-IV and -V," Nucl. Sci. Eng. 65, 201 (1978).

Ho78c R. J. Howerton and S. T. Perkins, ENDF/B-V Evaluation, MAT 1304, available from the National Nuclear Data Center, Brookhaven National Laboratory.

Ju74 E. T. Jurney, "Weak Gamma Transitions from $^{9}$Be(n,$\gamma$)$^{10}$Be and Radiative Capture of Thermal Neutrons by $^{9}$Be," USNDC-11, 149 (1974).

La50 A. S. Langsdorf, Jr., and M. T. Burgy, Argonne National Laboratory Physics Division Quarterly report ANL-4476, p. 28 (1950).

La57 A. Langsdorf, Jr., R. O. Lane, and J. E. Monahan, "Angular Distributions of Scattered Neutrons," Phys. Rev. 107, 1077 (1957).

La60 R. O. Lane, A. S. Langsdorf, J. E. Monahan, and A. J. Elwyn, "Angular Distributions of Neutrons Scattered from Various Nuclei," Argonne National Laboratory report ANL-6172 (1960).

La64 R. O. Lane, A. J. Elwyn, and A. Langsdorf, Jr., "Polarization and Differential Cross Section of Neutrons Scattered from $^{9}$Be: Parities of the 7.37- and 7.54-MeV States in $^{10}$Be," Phys. Rev. 133B, 409 (1964).

Le60 J. S. Levin and L. Cranberg, Los Alamos Scientific Laboratory, personal communication to R. J. Howerton (1960).

Ma59 J. B. Marion, J. S. Levin, and L. Cranberg, "Elastic and Nonelastic Neutron Cross Sections for Beryllium," Phys. Rev. 114, 1584 (1959).

Mc57 M. H. MacGregor, W. P. Ball, and Rex Booth, "Nonelastic Neutron Cross Sections at 14 MeV," Phys. Rev. 108, 726 (1957).

Mc63 M. H. McTaggart and H. Goodfellow, "Measurements at 14 MeV Neutron Energy of the n,2n Cross Section of Beryllium and the n,3n Cross Section of Thorium," J. Nucl. Energy Parts A/B 17, 437.

My61 S. A. Myachkova and V. P. Perelygin, "Interaction of 14.1-MeV Neutrons with $^{9}$Be," J. Expmtl. Theor. Phys. (USSR) 40, 1244 (1961).

Na58 M. P. Nakada, J. D. Anderson, C. C. Gardner, and C. Wong, "Elastic Scattering of 14-MeV Neutrons from Beryllium and Carbon," Phys. Rev. 110, 1439 (1958).

Ne54 N. G. Nereson and S. E. Darden, "Survey of Average Neutron Total Cross Sections from 3 to 13 MeV," Los Alamos Scientific Laboratory report LA-1655 (1954).

Pa67 G. Paik, D. Rendic, and P. Tomas, "The $^{9}Be(n,\alpha_0)^{6}He$ Reaction Induced by 14.4 MeV Neutrons," Nucl. Phys. A96, 476 (1967).

Pe60 J. M. Peterson, A. Bratenahl, and J. P. Stoering, "Neutron Total Cross Sections in the 17- to 29-MeV Range," Phys. Rev. 120, 521 (1960).

Pe62 A. Perrin, G. Surget, C. Thibault, and F. Verriere, "Section Efficace Neutronique du Beryllium au Voisinage de 200 keV," C. R. Acad. Sci (Paris) 255, 277 (1962).

Ph49 D. D. Phillips, "Inelastic Collision Cross Sections of Various Elements for 14-MeV Neutrons," Los Alamos Scientific Laboratory report ACCU-404 (LA-740) (1949).

Ph61 D. D. Phillips, Los Alamos Scientific Laboratory, personal communication to Brookhaven National Laboratory Data Center (1961).

Ph64 D. D. Phillips, Los Alamos Scientific Laboratory, personal communication to R. J. Howerton (1964).

Ro57 L. Rosen, and L. Stewart, "Neutron Emission Probabilities from the Interaction of 14-MeV Neutrons with Be, Ta, and Bi," Phys. Rev. 107, 824 (1957).

Ro68 R. Roturier, University of Bordeau, France, personal communication to Brookhaven National Laboratory Cross Section Center (1968).

Sa59 M. Sakisaka, "Be-9(n,2n)Be-8 and Be-11(n,α)Li-8(B)Be-8 Reactions by 14 MeV Neutrons," J. Phys. Soc. Japan 14, 554 (1959).

Sc69 W. Scobel, "Wirkungsquerschnitt der Reaction $^{9}Be(n,d)^{8}Li$ Zwischen 16.3 und 18.7 MeV," Z. Naturforsch 24, 289 (1969).

Sc71 R. B. Schwartz, personal communication; see also R. A. Schrack, R. B. Schwartz, and H. T. Heaton, "Total Neutron Cross Sections of Silicon and Beryllium," Bull. Am. Phys. Soc. 16, 495 (1971).

Sm66 A. B. Smith, Argonne National Laboratory, personal communication (1966).

St51 C. H. Stafford, "Total Cross Sections of Al, S, and Pb for Neutrons of Energies from 2 MeV to 6 MeV," Proc. Phys. Soc. (London) 64, 388 (1951).

St57 P. H. Stelson and E. C. Campbell, "Cross Section for the $Be^{9}(n,\alpha)He^{6}$ Reactions," Phys. Rev. 106, 1252 (1957).

St64 P. H. Stelson, Massachusetts Institute of Technology, personal communication to Brookhaven National Laboratory Sigma Center (1964).

St76 Leona Stewart and Phillip G. Young, "Evaluated Nuclear Data for CRT Applications," Trans. Am. Nucl. Soc. 23, 22 (1976).

Ta55 H. L. Taylor, O. Lonsjo, and T. W. Bonner, "Nonelastic Scattering Cross Sections for Fast Neutrons," Phys. Rev. 100, 174 (1955).

Th67 C. Thibault, "Use of the Fast Coincidence (n,$^{3}$He) in (d,d) Reactions. Measurements of Various Total Cross Sections," Commissariat a L'Energie Atomic report CEA-R-3124 (1967).

Va58 S. S. Vasilev, V. V. Kumarov, and A. M. Popova, "An Investigation of the (n,$\alpha$) and (n,t) Reactions in Be$^{9}$" Dokl. Akad. Nauk SSSR (Sov. Phys.-Doklady) 119, 914 (1958); also, J. Expmtl. Theoret. Phys. (USSR) 33, 527 (1957).

Wa55 M. Walt and J. R. Beyster, "Interaction of 4.1-MeV Neutrons with Nuclei," Phys. Rev. 98, 677 (1955).

Wa77 A. H. Wapstra and K. Bos, Atomic Data and Nuclear Data Tables 19, 175 (1977).

We73 D. R. Weaver and J. Walker, "The Non-Elastic Cross Sections of $^{9}$Be for Neutrons Between 2.4 and 3.9 MeV," U. of Birmingham Phys. Dept. report 73-02 (1973).

Wi55 Harvey B. Willard, Joe K. Bair, and Joe D. Kingston, "Elastic Scattering Angular Distributions of Fast Neutrons on Light Nuclei," Phys. Rev. 98, 699 (1955).

Wi64 D. Wilmore and P. E. Hodgson, The Calculation of Neutron Cross Sections from Optical Potentials," Nucl. Phys. 55, 673 (1964).

Wo72 C. Wong, J. D. Anderson, P. Brown, L. F. Hansen, J. L. Kammerdiener, C. Logan and B. Pohl, "Livermore Pulsed Sphere Program: Program Summary Through July 1971," University of California Research Laboratory report UCRL-51144, Rev. 1 (Feb. 1972).

Wy58 M. E. Wyman, E. M. Freyer, and M. M. Thorpe, "(n,t) Cross Sections for B-10, B-11, and Be-9," Phys. Rev. 112, 1264 (1958).

Yo79 P. G. Young, Ed., "Summary Documentation of LASL Nuclear Data Evaluations for ENDF/B-V," Los Alamos Scientific Laboratory report LA-7663-MS (1979).

Zu61 Yu. G. Zubov, N. S. Lebedov, and V. M. Morozov, "Inelastic Scattering of Neutrons with Energies 3.2-4.5 MeV on Beryllium," Soviet Progress in Neutron Physics, p. 219 (1961).

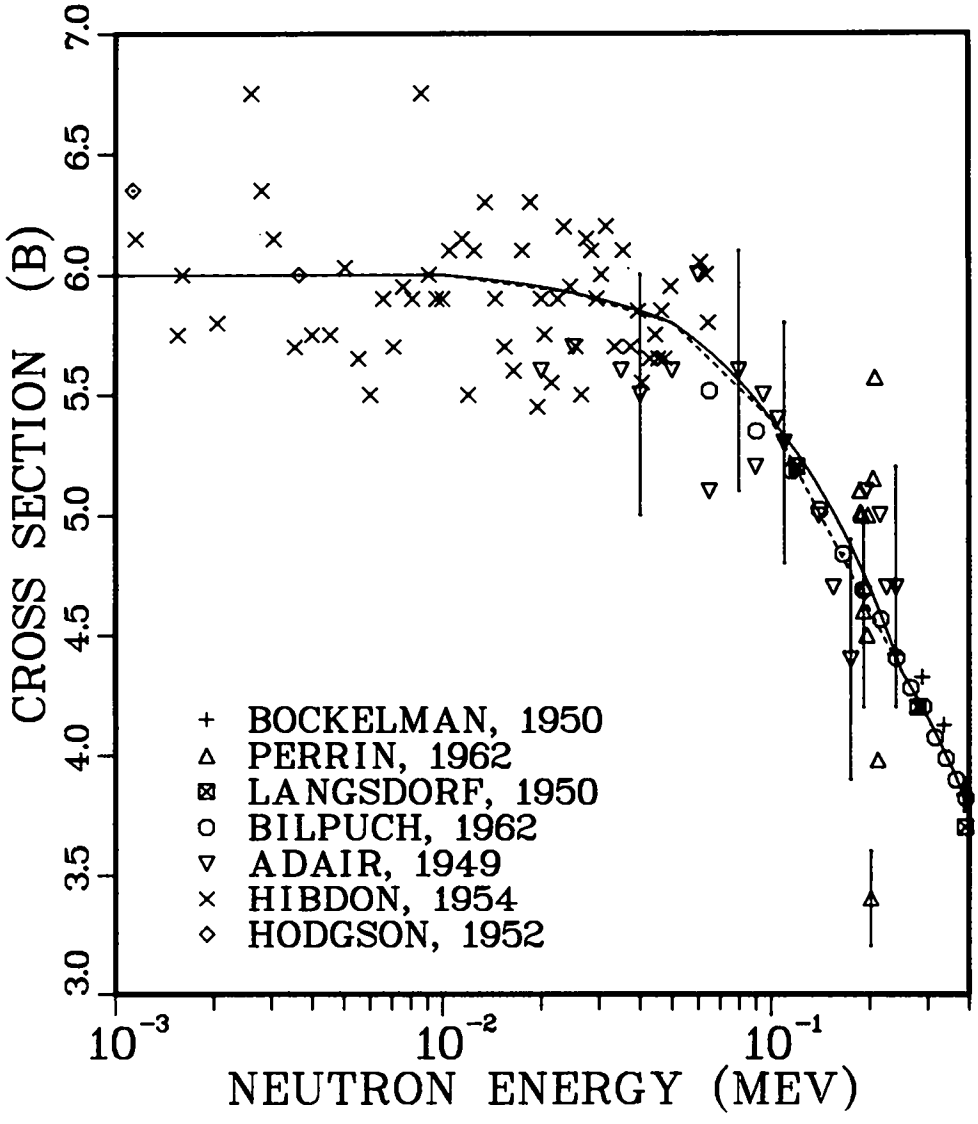


Fig. 1.
Measured and evaluated total cross sections from 1 to 400 keV. The dashed curve is ENDF/B-V, and the solid curve is the present evaluation.

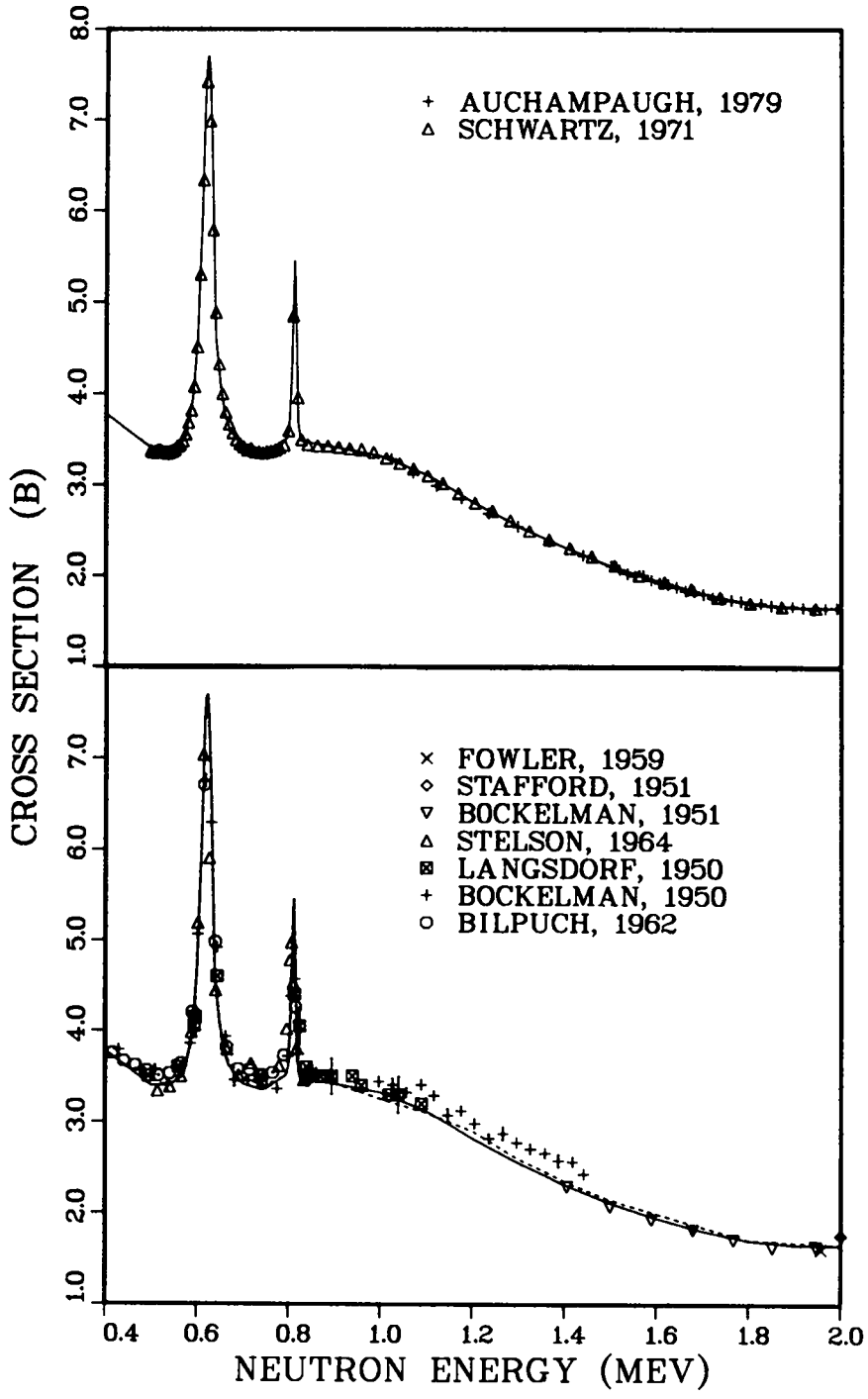


Fig. 2.
Measured and evaluated total cross sections from 0.4 to 2.0 MeV. The dashed curve is ENDF/B-V, and the solid curve is the present evaluation.

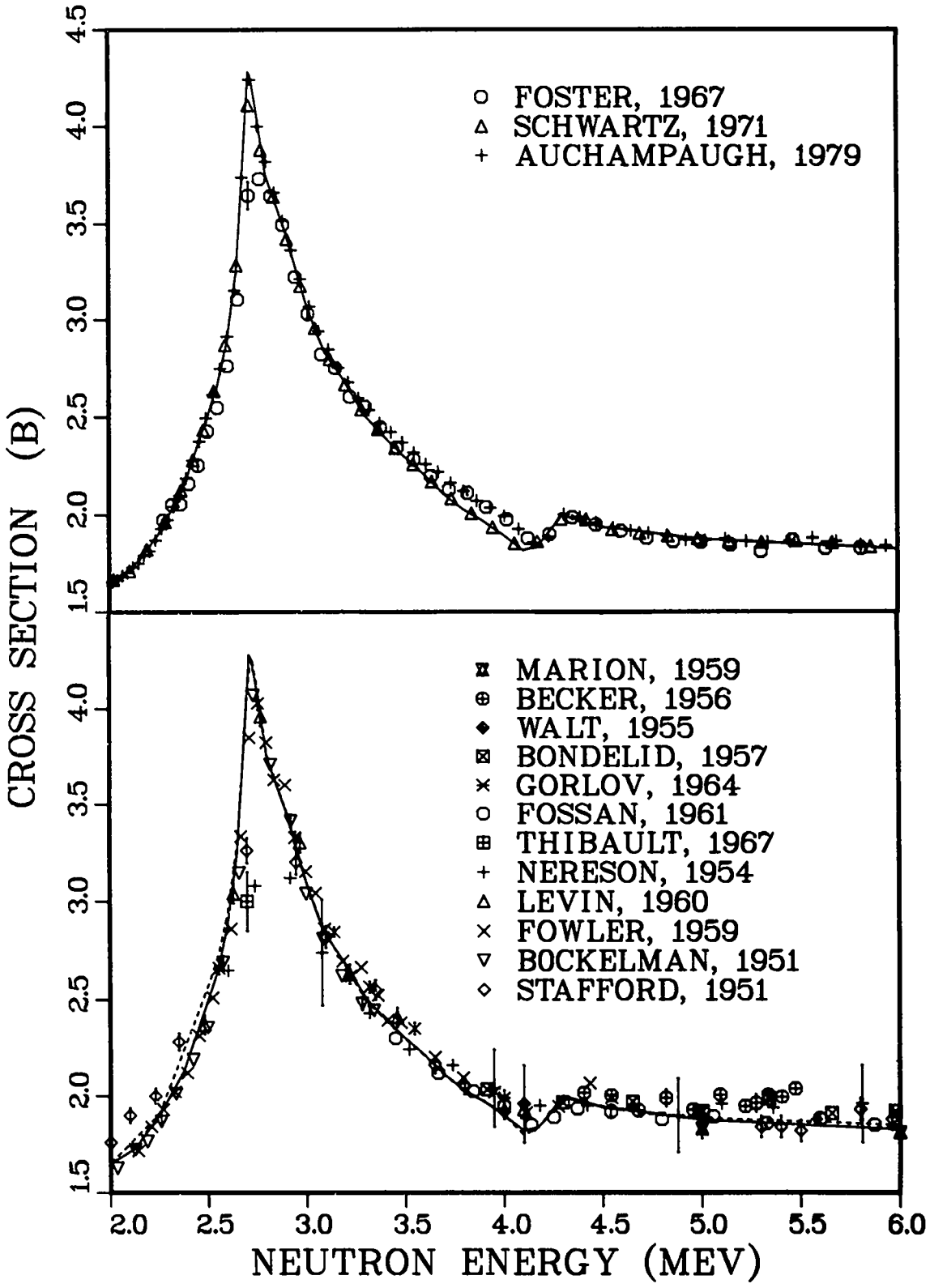


Fig. 3.
Measured and evaluated total cross sections from 2 to 6 MeV. The dashed curve is ENDF/B-V, and the solid curve is the present evaluation.

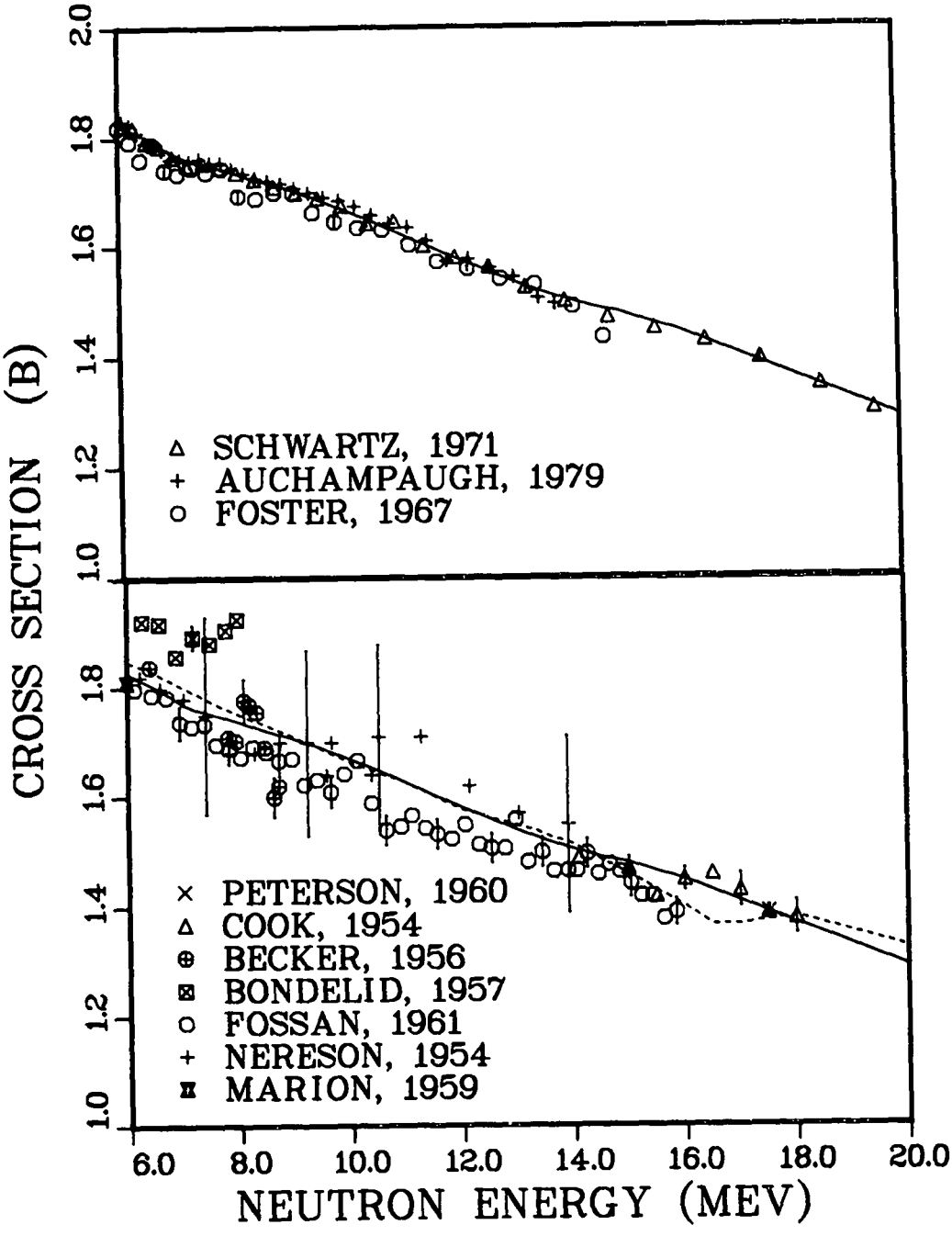


Fig. 4.
Measured and evaluated total cross sections from 6 to 20 MeV. The dashed curve is ENDF/B-V, and the solid curve is the present evaluation.

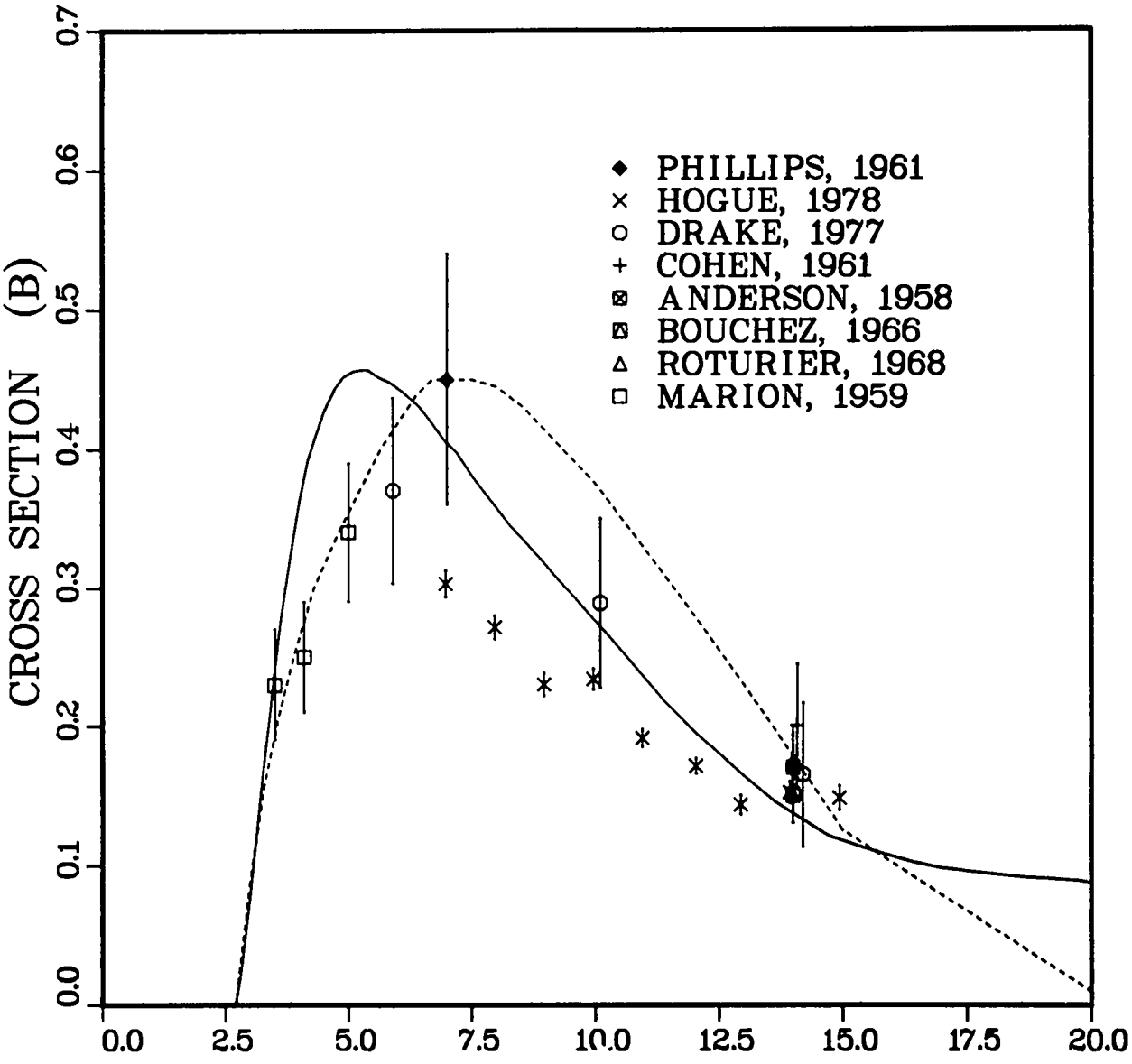


Fig. 5.
Measured and evaluated (n,n') cross sections to the 2.43-MeV cluster of levels in $^{9}$Be. The dashed and solid curves are ENDF/B-V and the present evaluation, respectively.

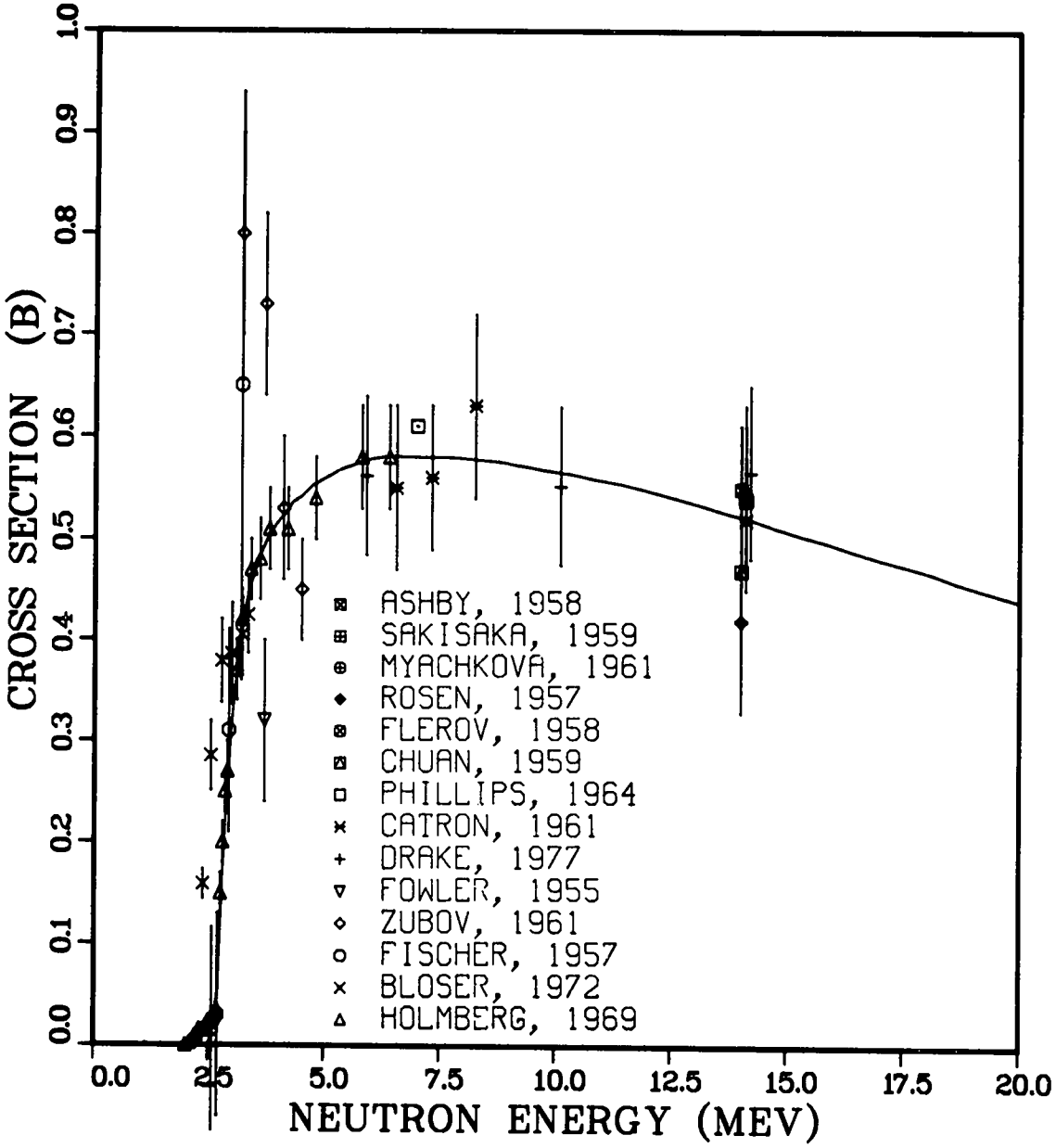


Fig. 6.
Measured and evaluated (n,2n) cross sections from threshold to 20 MeV. The dashed and solid curves are ENDF/B-V and the present evaluation, respectively,

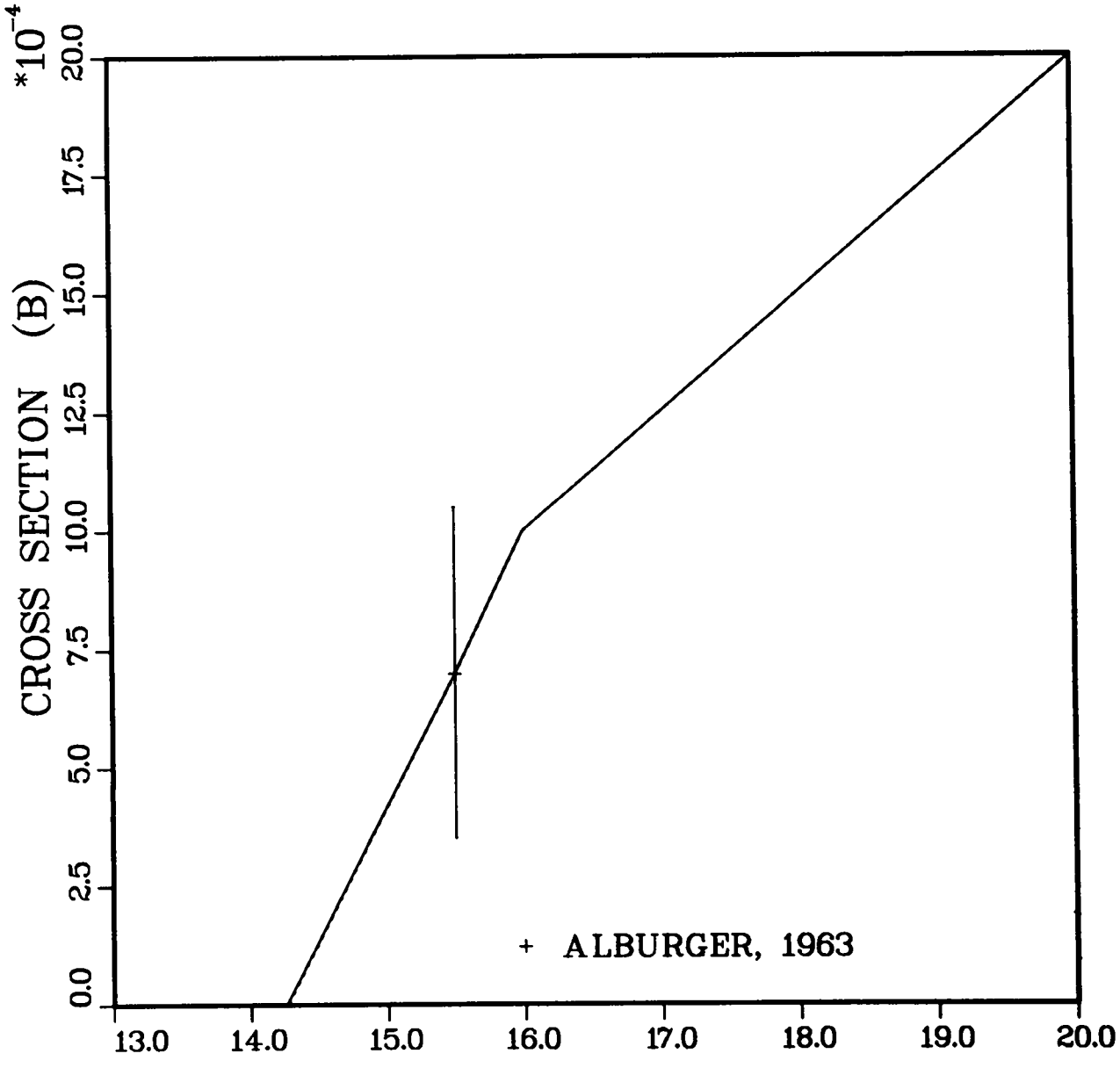


Fig. 7.
Measured and evaluated (n,p) cross sections from threshold to 20 MeV. The solid curve represents the present evaluation.

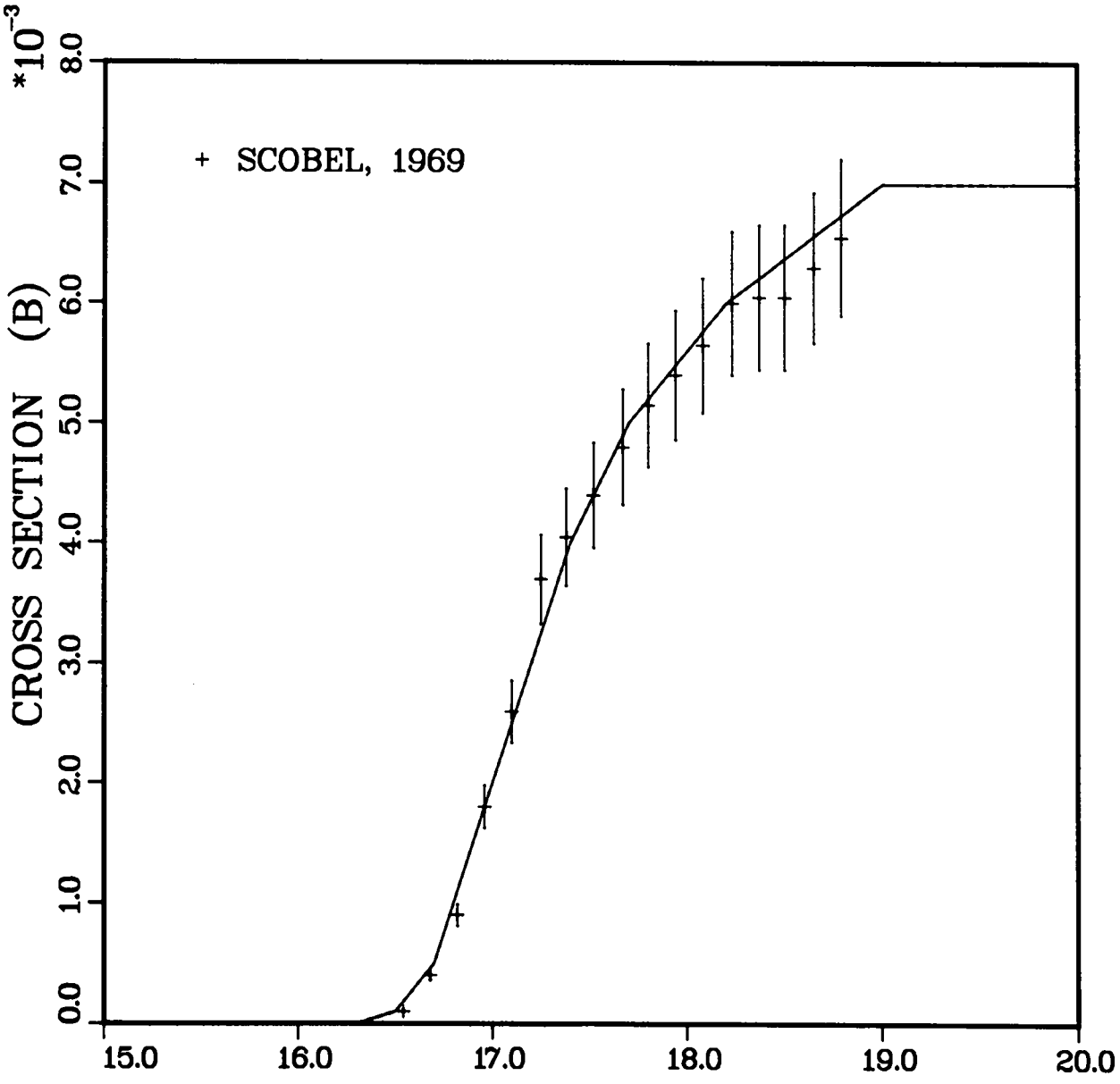


Fig. 8.
Measured and evaluated (n,d) cross sections from threshold to 20 MeV. The solid curve represents the present evaluation.

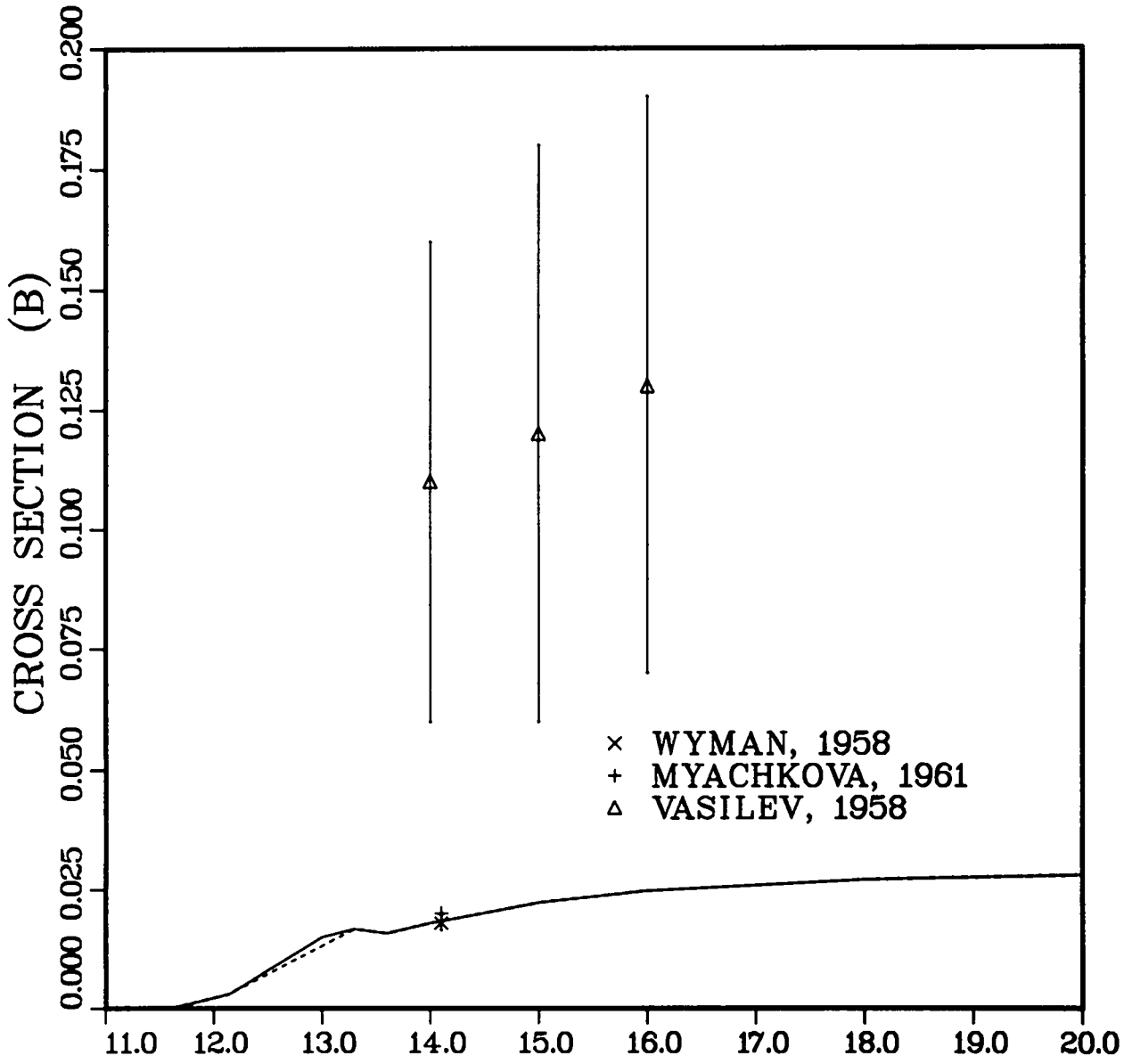


Fig. 9.
Measured and evaluated (n,t) cross sections from threshold to 20 MeV. The dashed and solid curves are ENDF/B-V and the present evaluation, respectively.

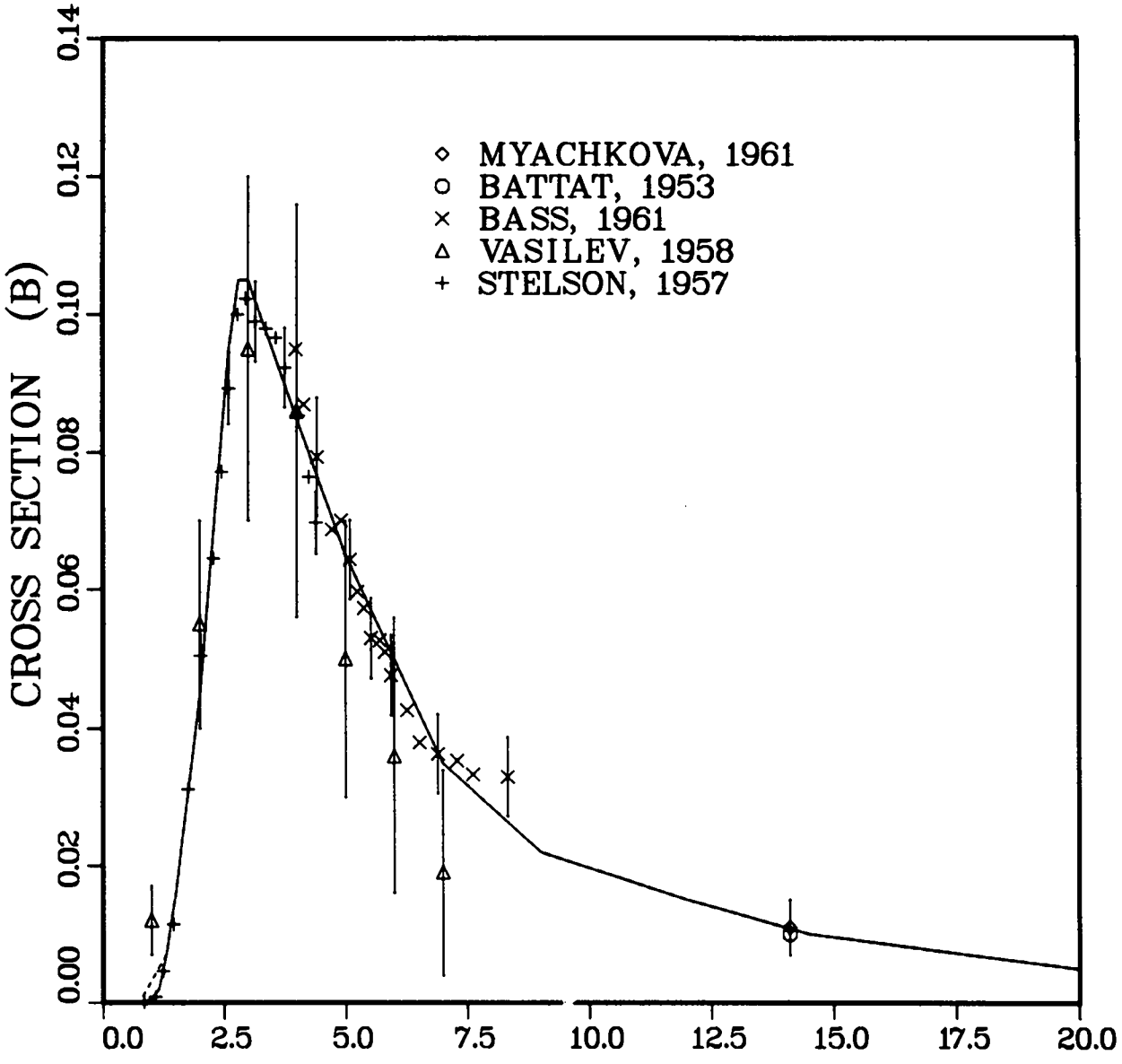


Fig. 10.
Measured and evaluated (n,α) cross sections from threshold to 20 MeV. The dashed and solid curves are ENDF/B-V and the present evaluation, respectively.

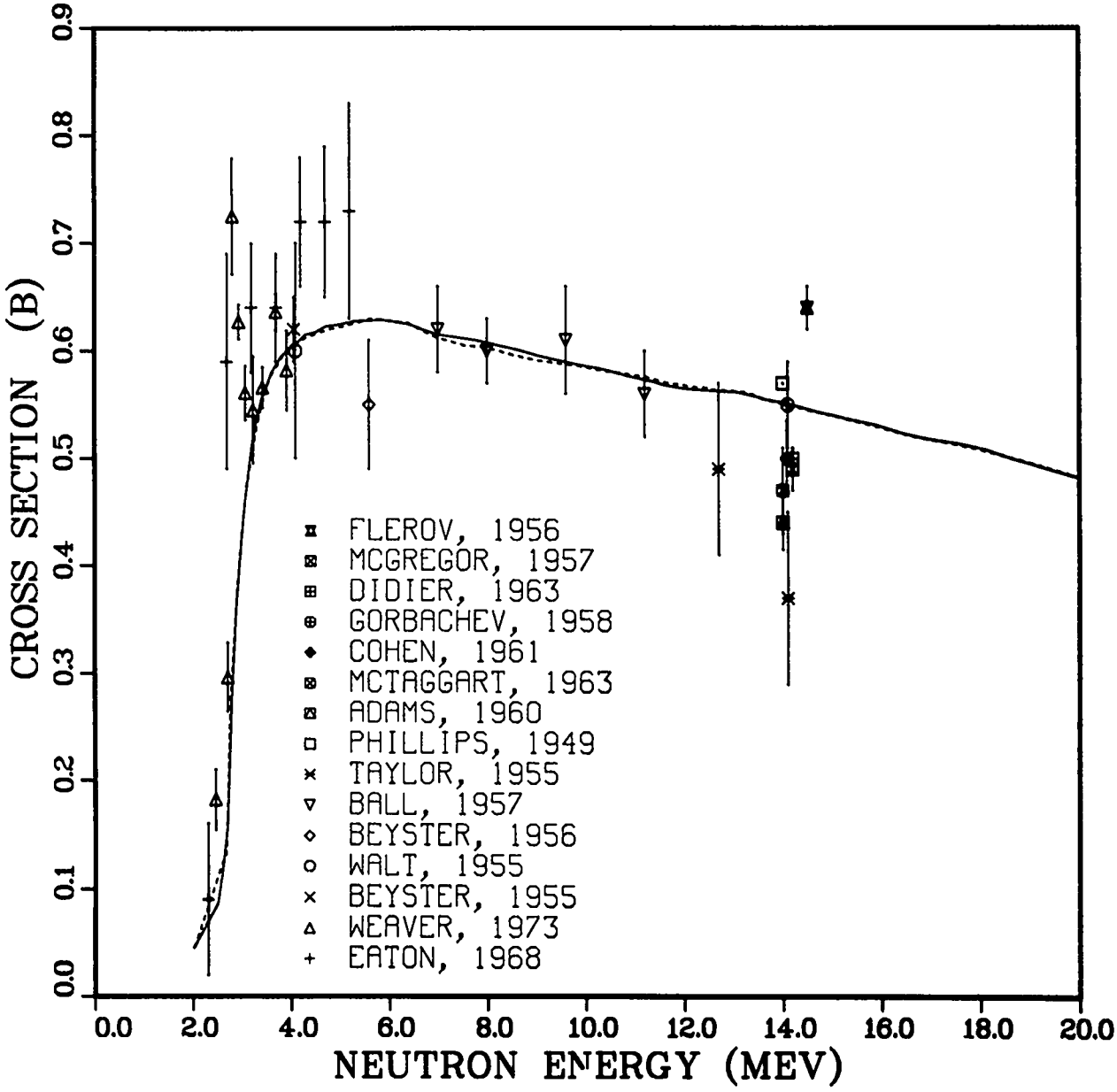


Fig. 11.
Measured and evaluated nonelastic cross sections from threshold to 20 MeV. The dashed and solid curves are ENDF/B-V and the present evaluation, respectively.

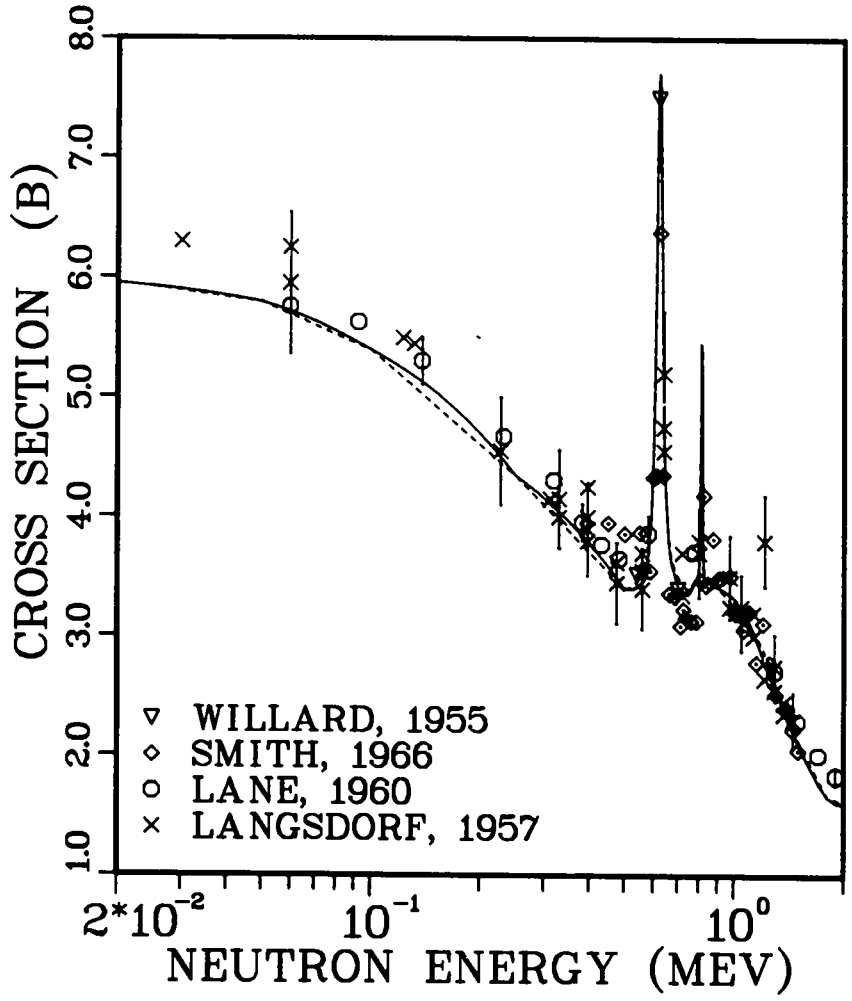


Fig. 12
Measured and evaluated elastic cross section from 0.02 to 2 MeV. The dashed curve is ENDF/B-V, and the solid curve is the present evaluation.

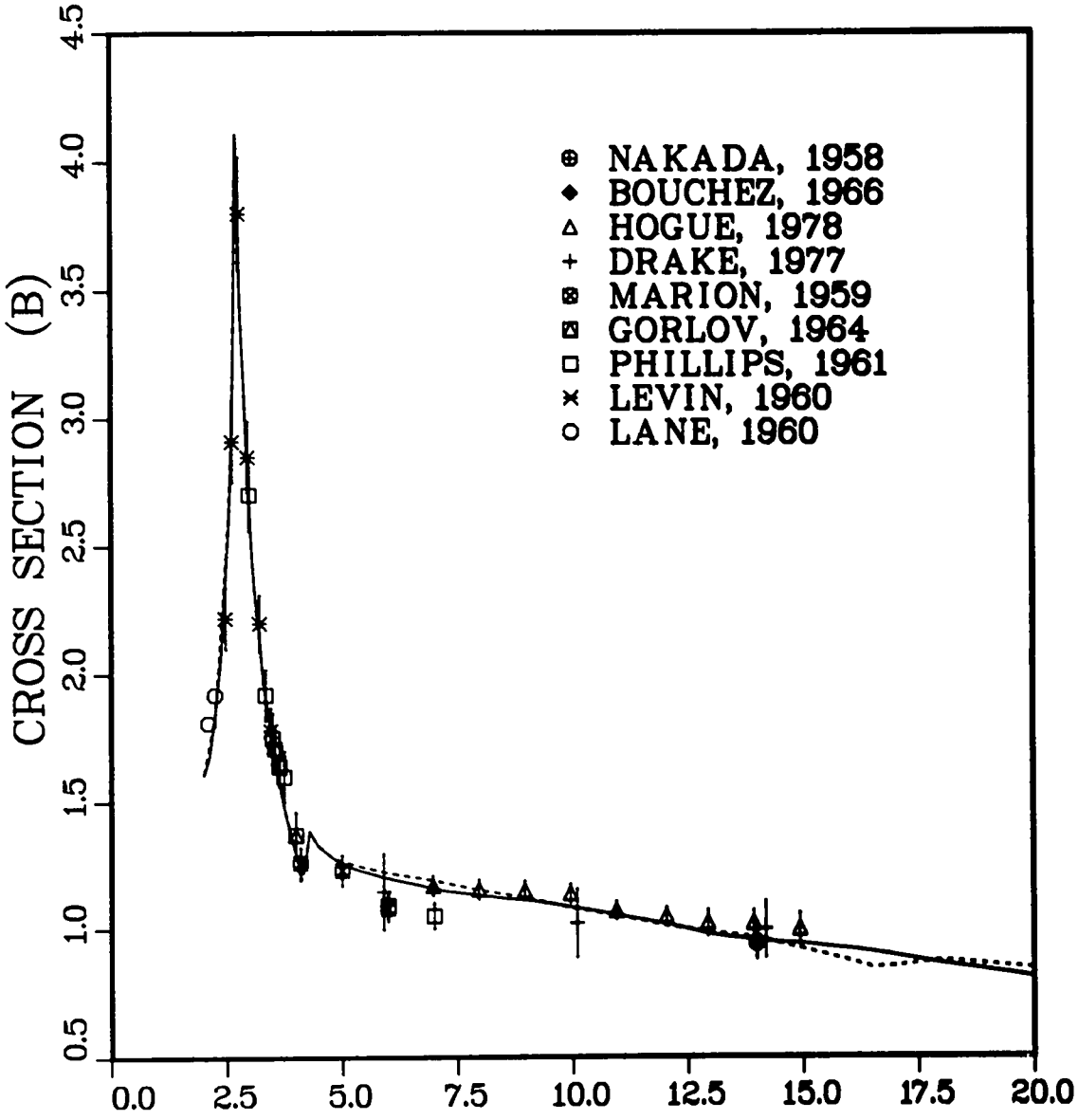


Fig. 13
Measured and evaluated elastic cross sections from 2 to 20 MeV. The dashed curve is ENDF/B-V, and the solid curve is the present evaluation.

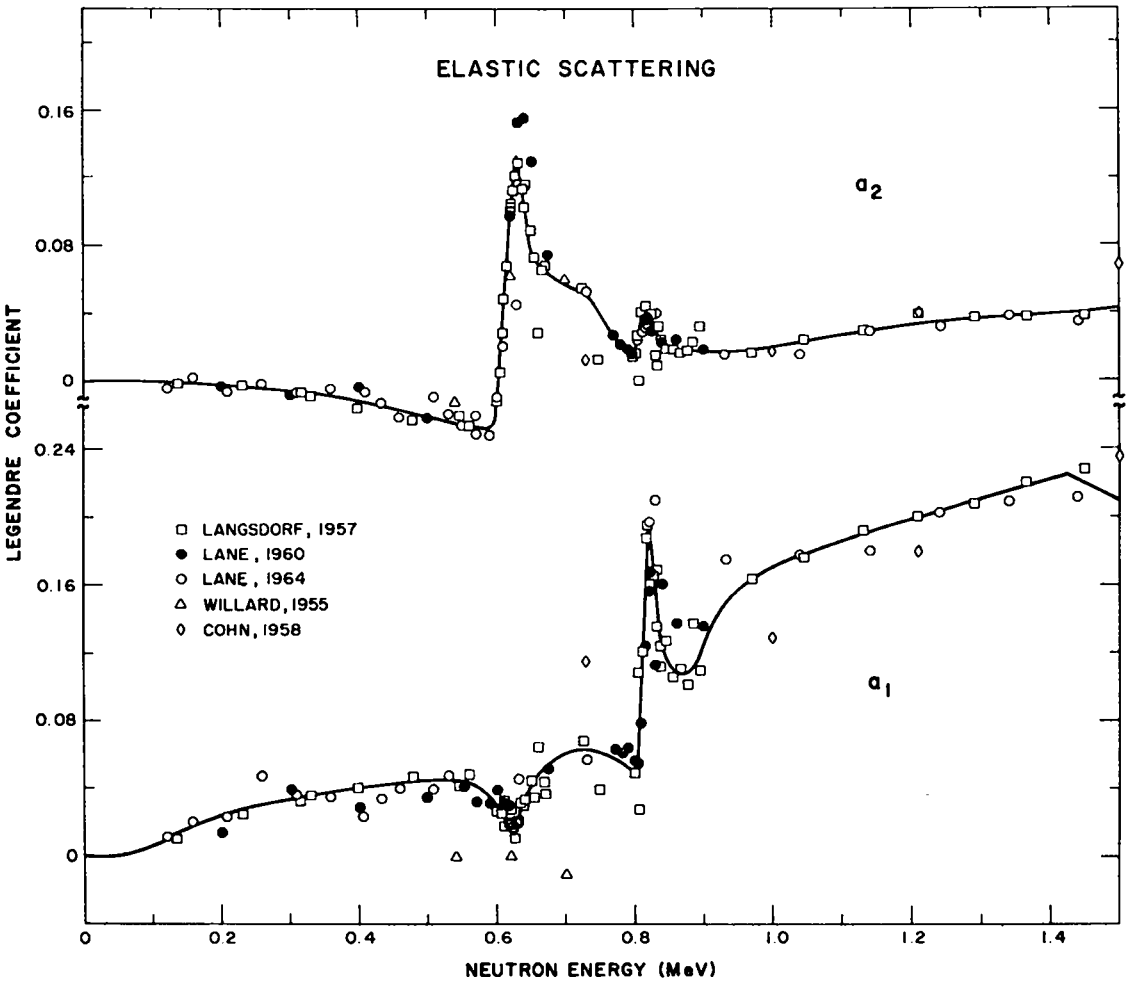


Fig. 14.
Evaluated $\ell$ = 1,2 Legendre coefficients for elastic scattering from 0 to 1.5 MeV. The points represent fits to measured angular distributions.

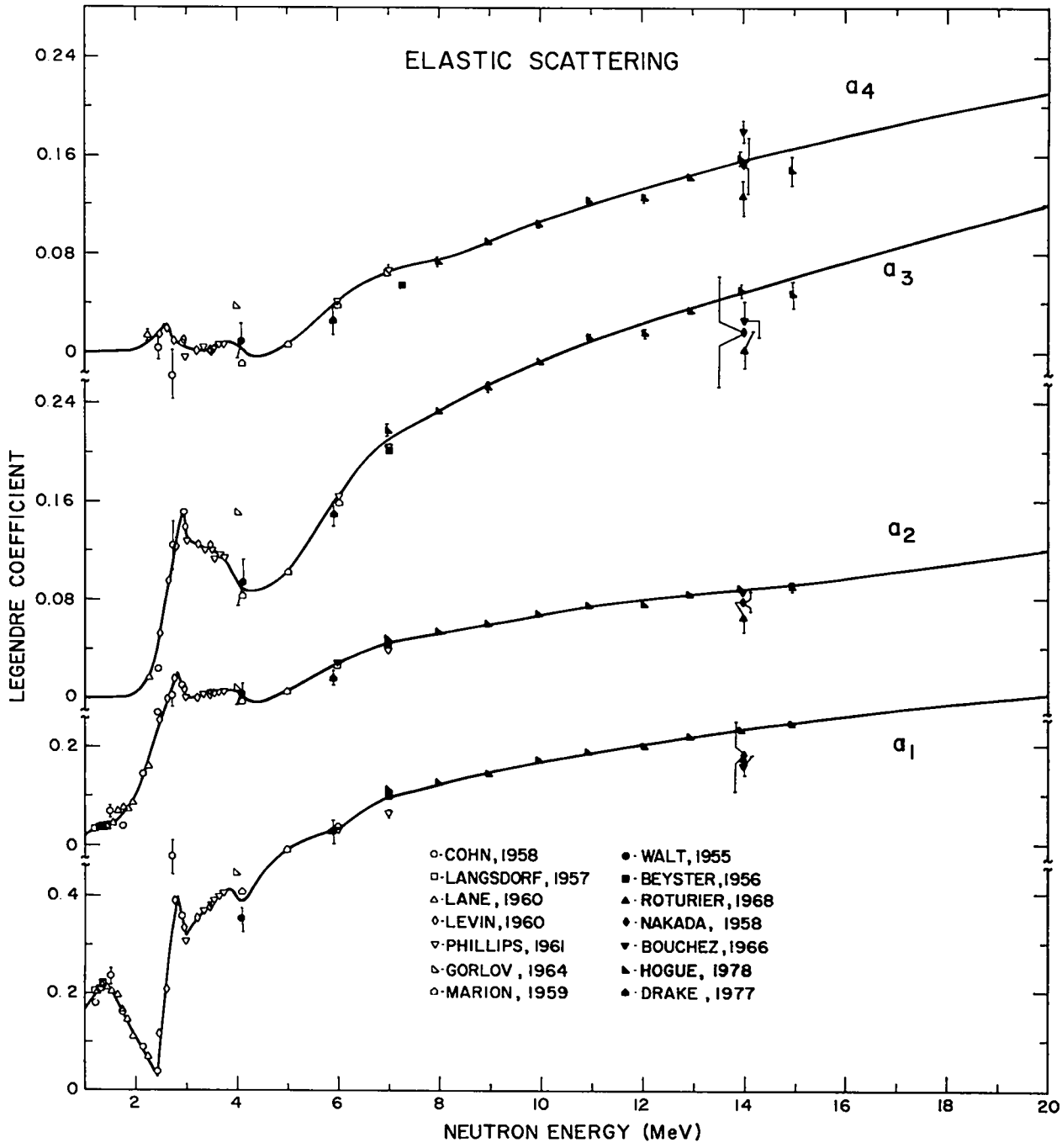


Fig. 15.
Evaluated $\ell$ = 1-4 Legendre coefficients for elastic scattering from 1 to 20 MeV. The points represent fits to measured angular distributions.

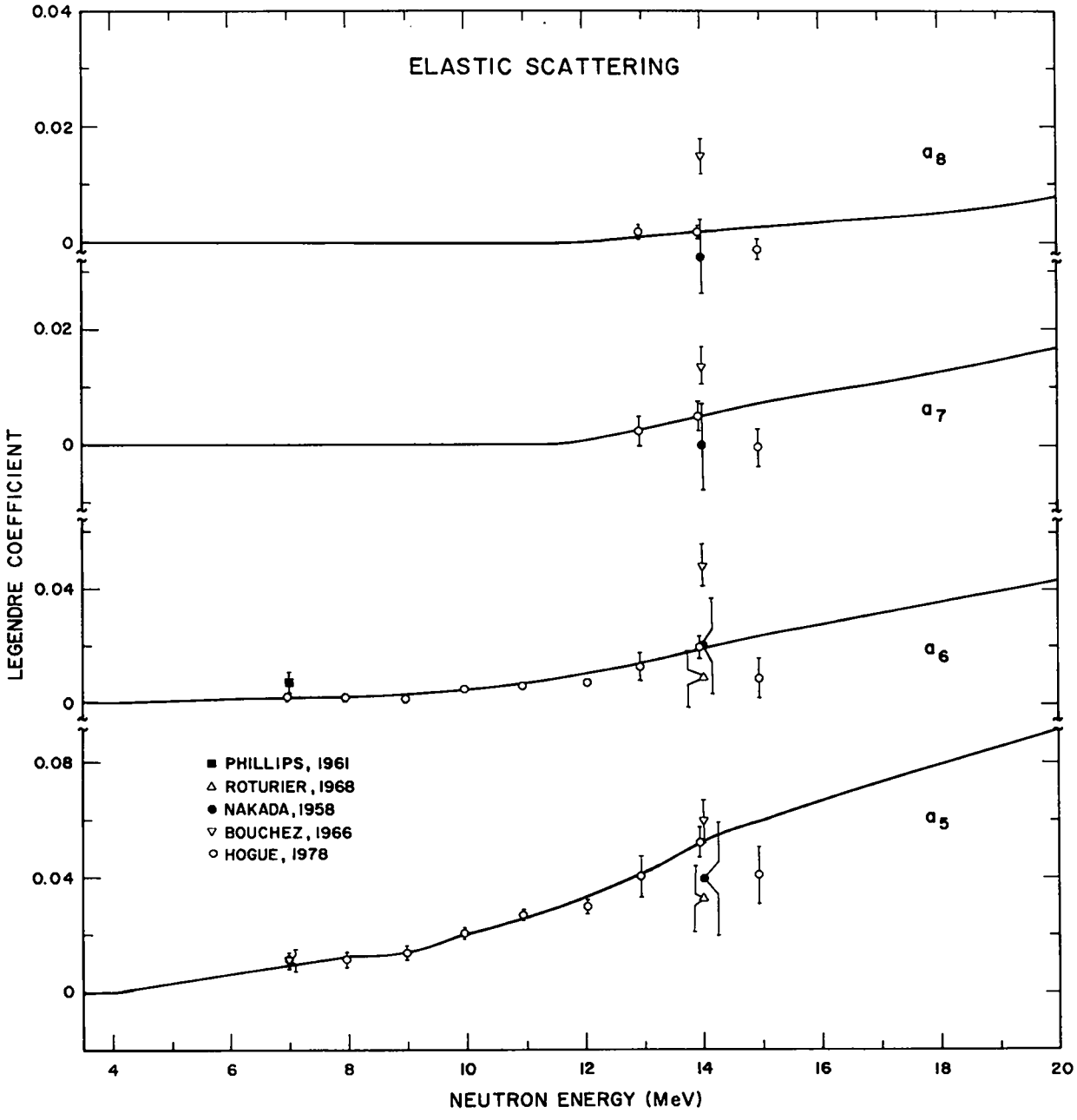


Fig. 16.
Evaluated $\ell$ = 5-8 Legendre coefficients for elastic scattering from 1 to 20 MeV. The points represent fits to measured angular distributions.

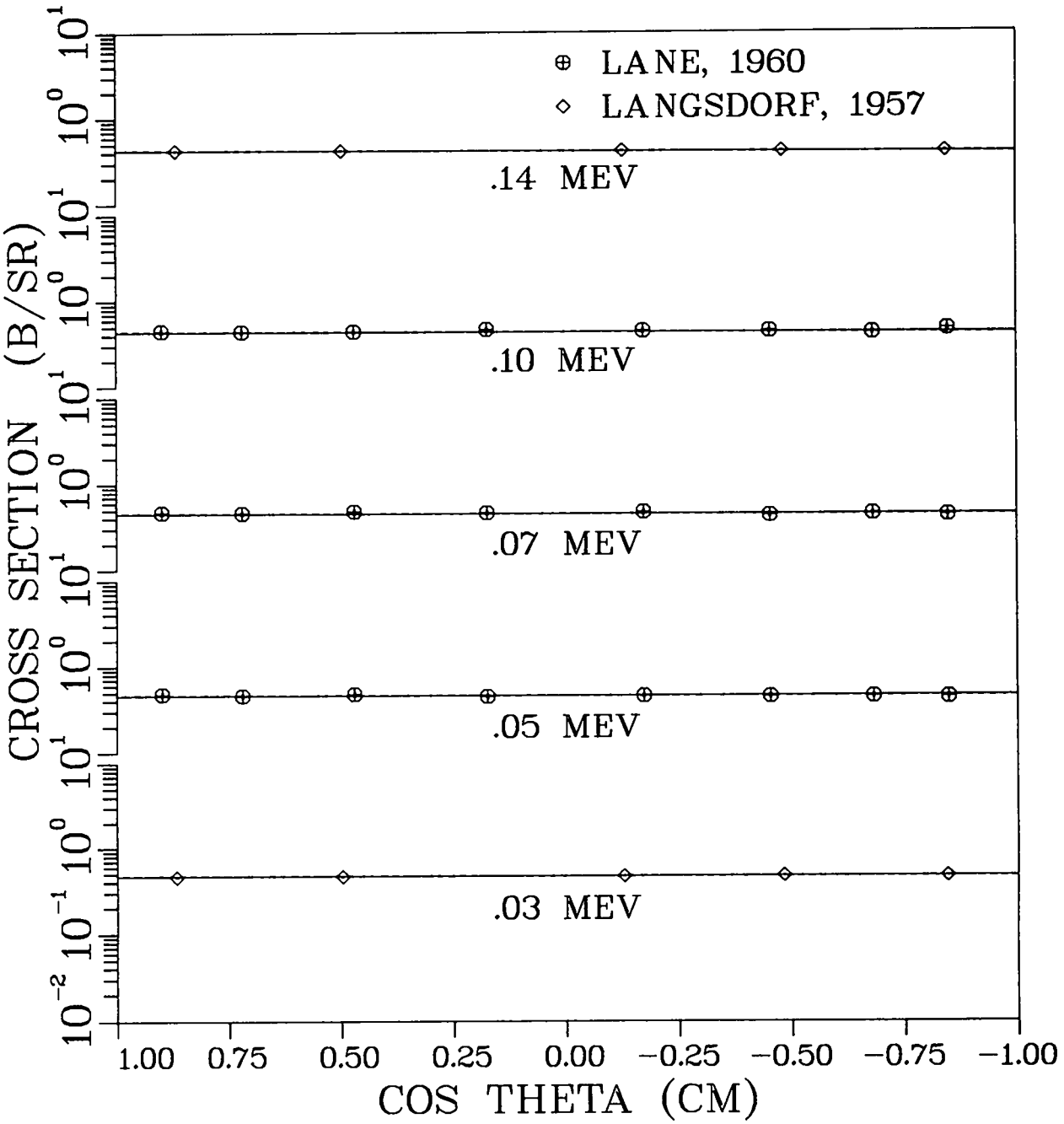


Fig. 17.
Measured and evaluated elastic angular distributions from 0.03 to 0.14 MeV. The solid curve is the present evaluation, and the dashed curve is ENDF/B-V.

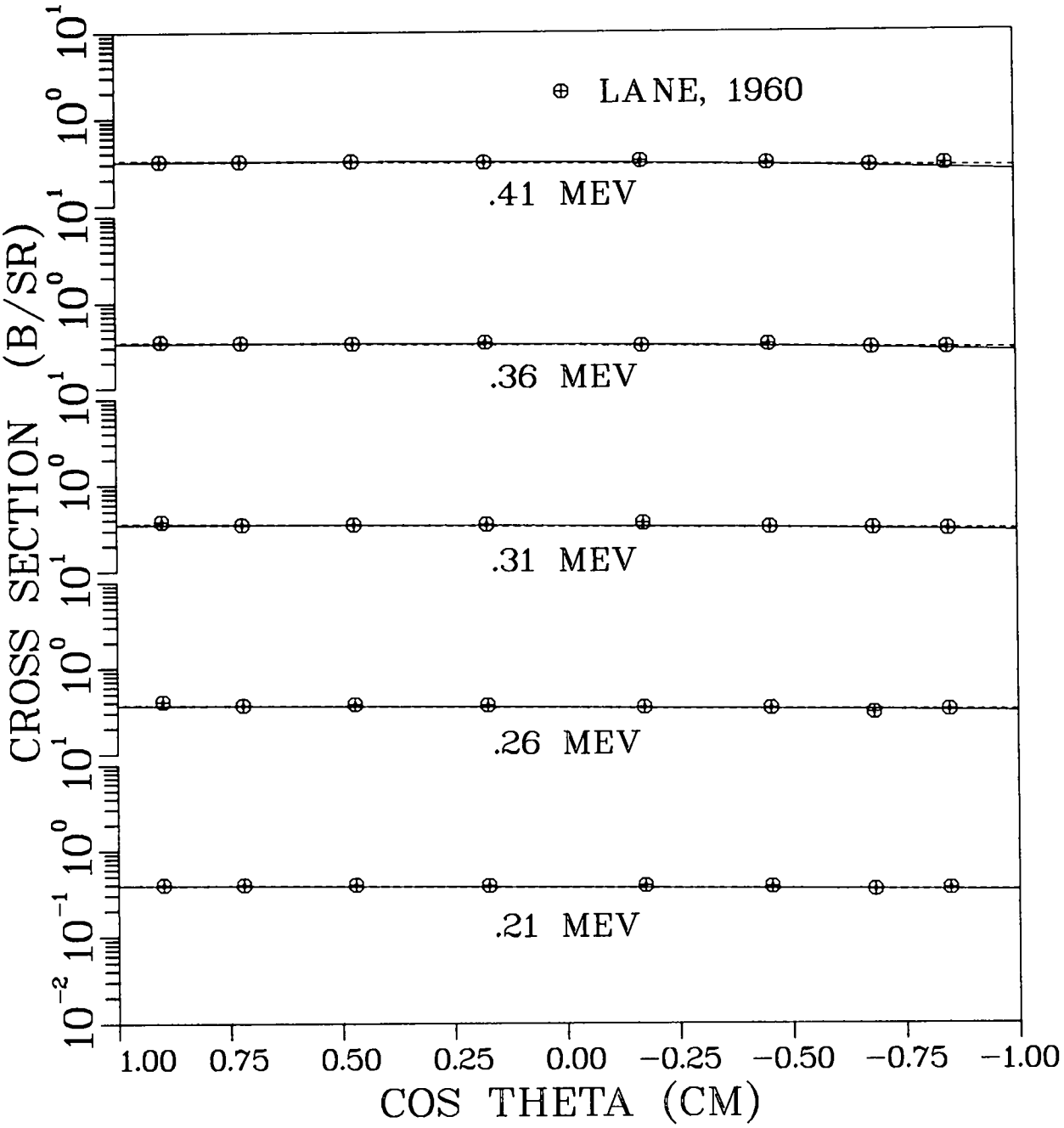


Fig. 18.
Measured and evaluated elastic angular distributions from 0.21 to 0.41 MeV. The solid curve is the present evaluation, and the dashed curve is ENDF/B-V.

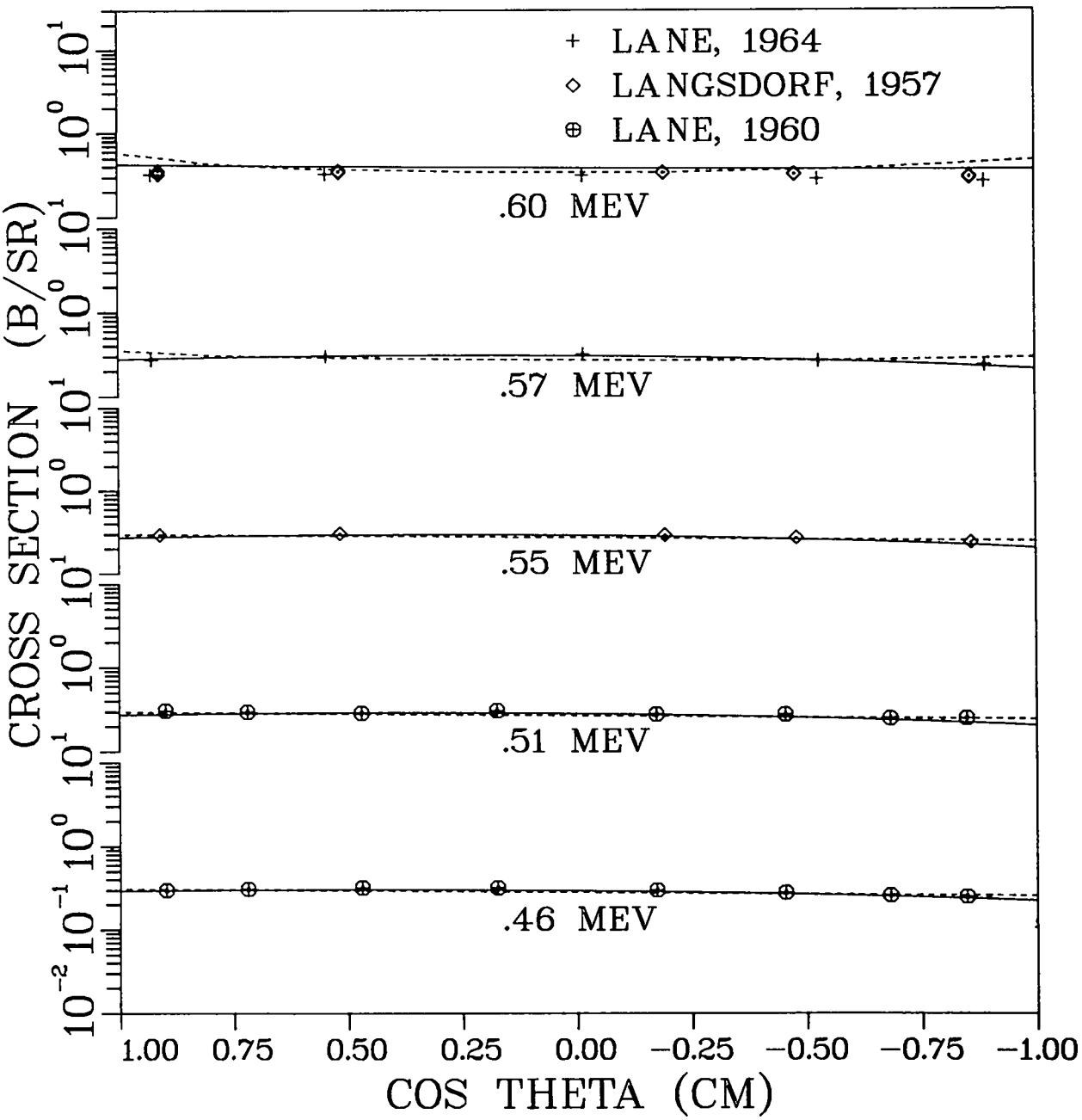


Fig. 19.
Measured and evaluated elastic angular distributions from 0.46 to 0.60 MeV. The solid curve is the present evaluation, and the dashed curve is ENDF/B-V.

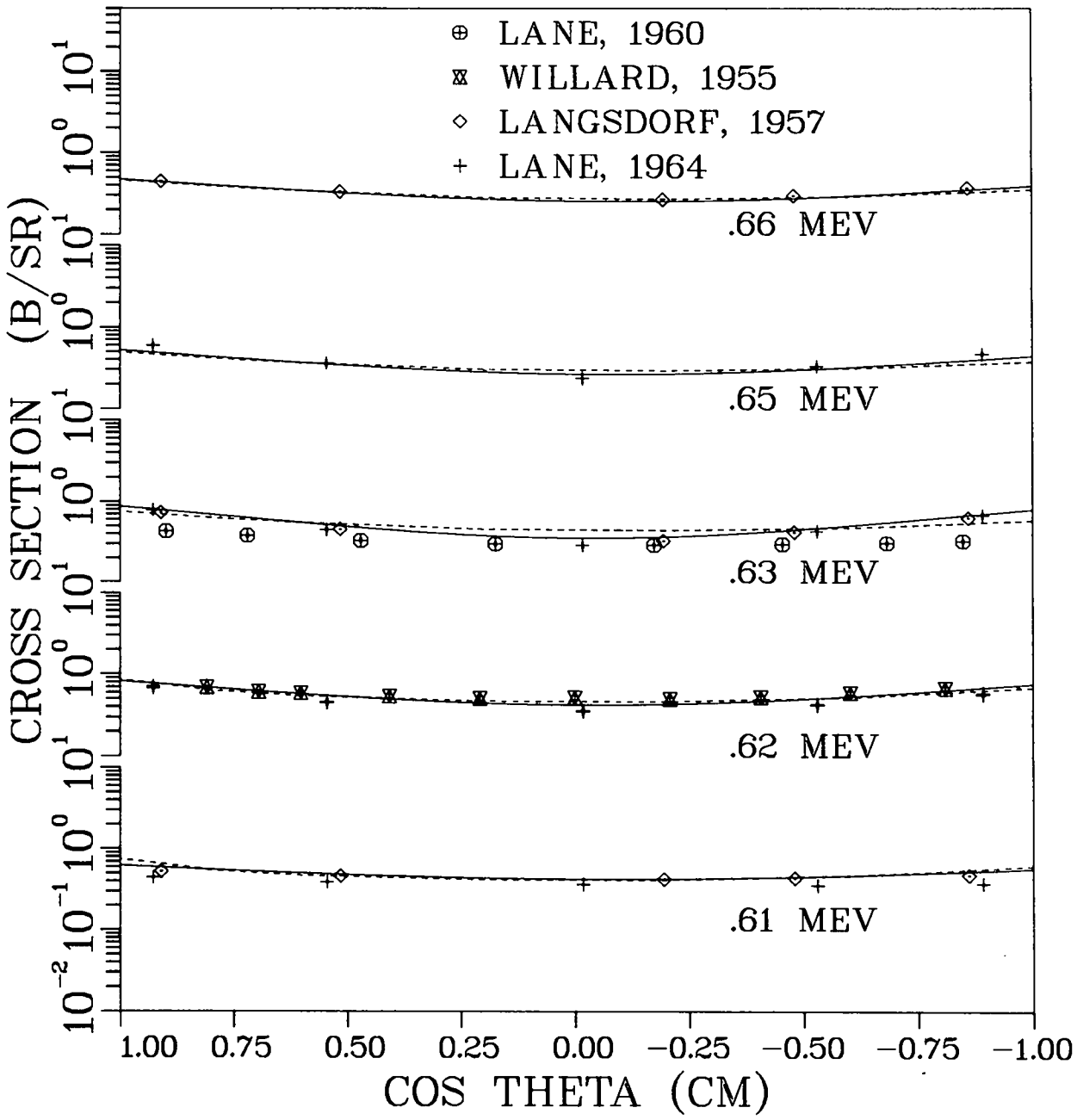


Fig. 20.
Measured and evaluated elastic angular distributions from 0.61 to 0.66 MeV. The solid curve is the present evaluation, and the dashed curve is ENDF/B-V.

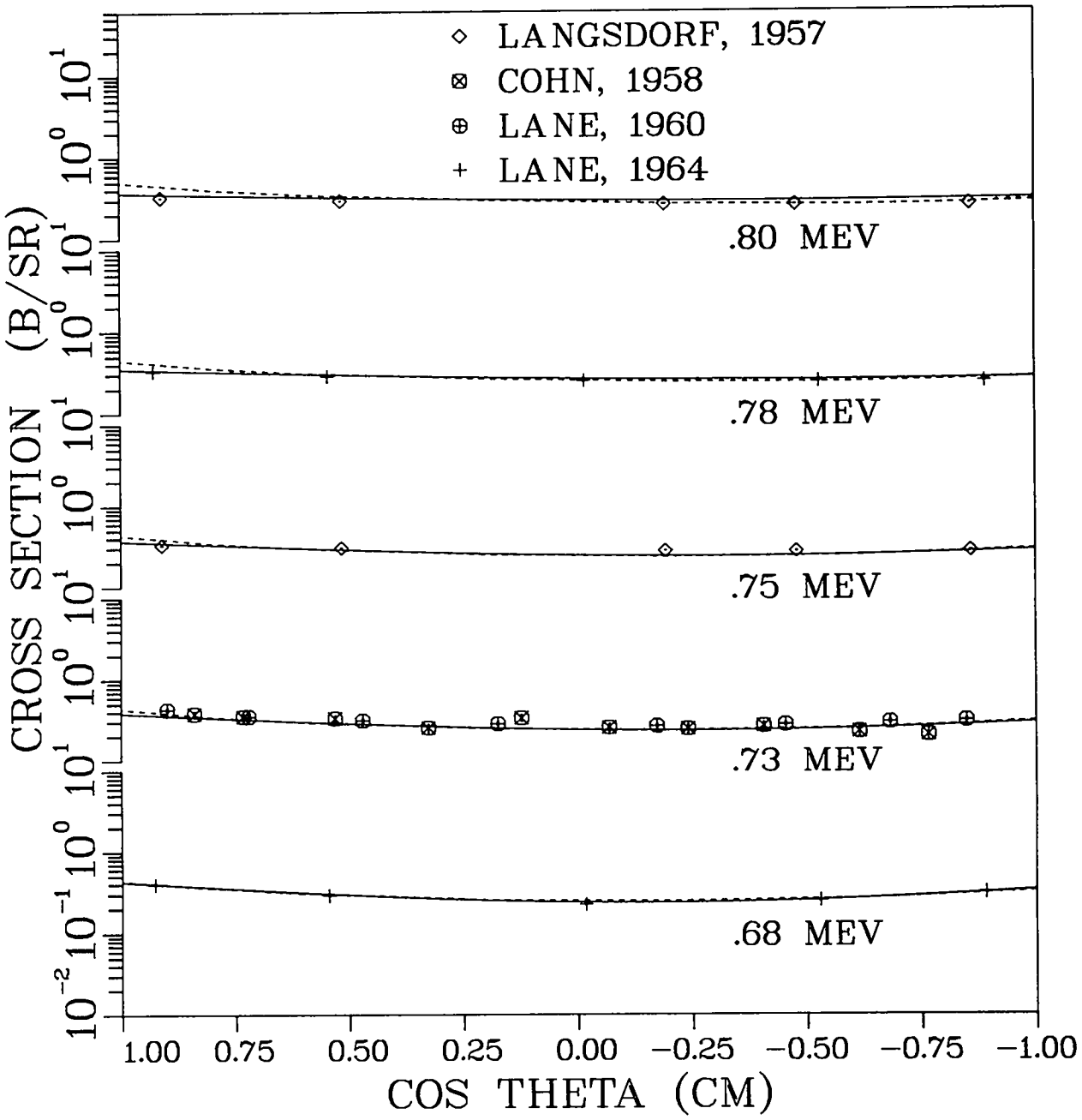


Fig. 21.
Measured and evaluated elastic angular distributions from 0.68 to 0.80 MeV. The solid curve is the present evaluation, and the dashed curve is ENDF/B-V.

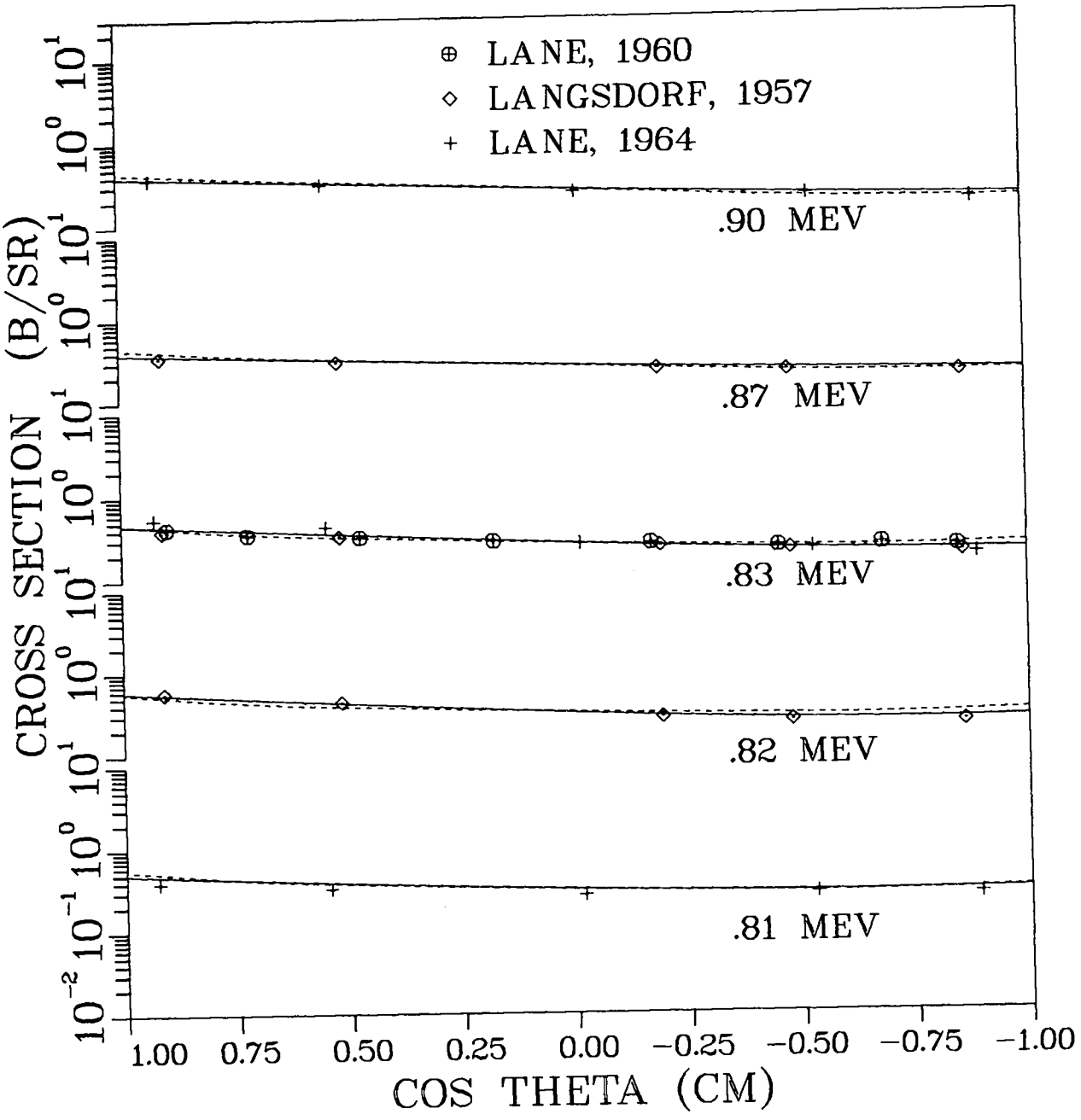


Fig. 22.
Measured and evaluated elastic angular distributions from 0.81 to 0.90 MeV. The solid curve is the present evaluation, and the dashed curve is ENDF/B-V.

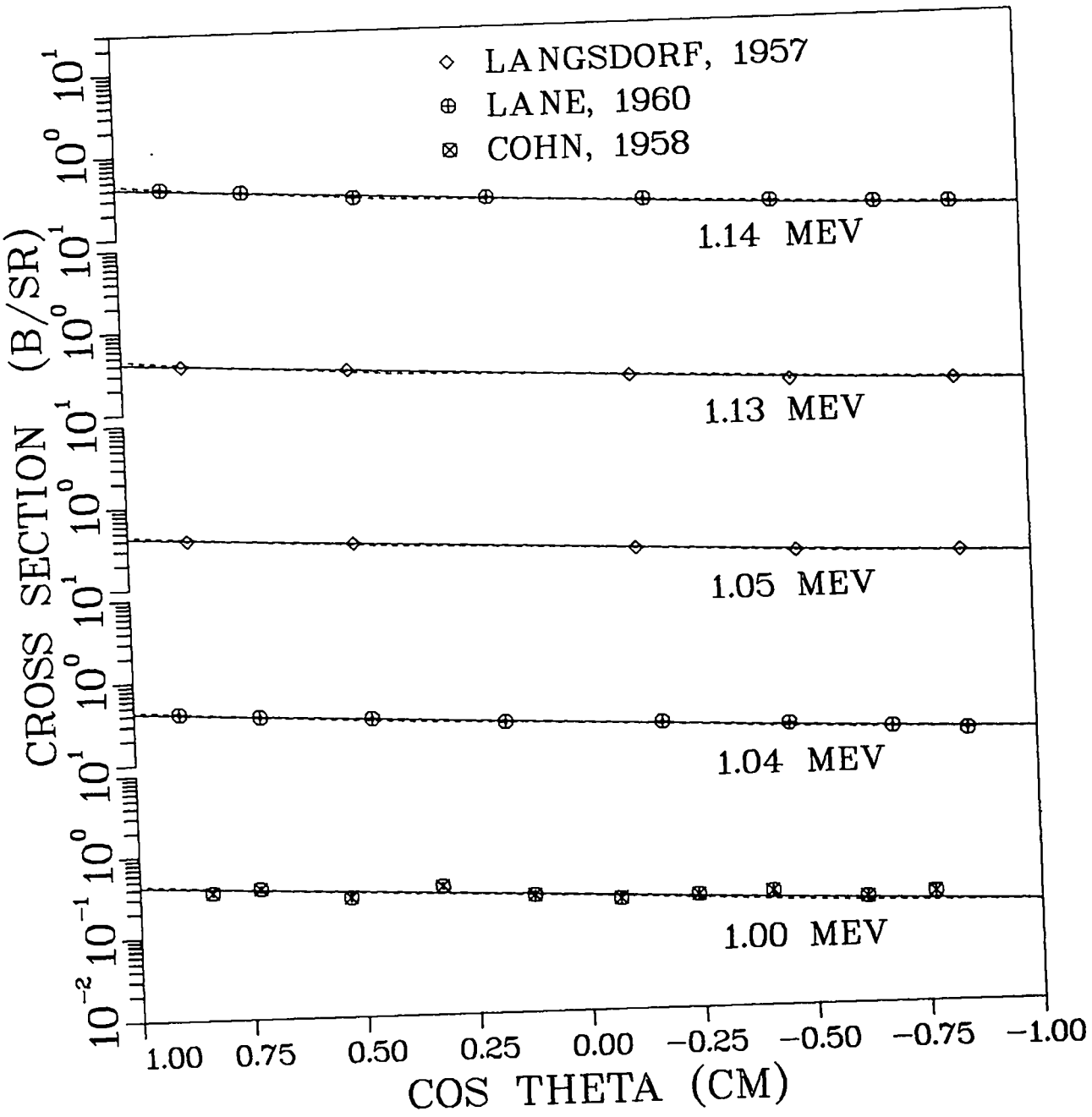


Fig. 23.
Measured and evaluated elastic angular distributions from 1.00 to 1.14 MeV. The solid curve is the present evaluation, and the dashed curve is ENDF/B-V.

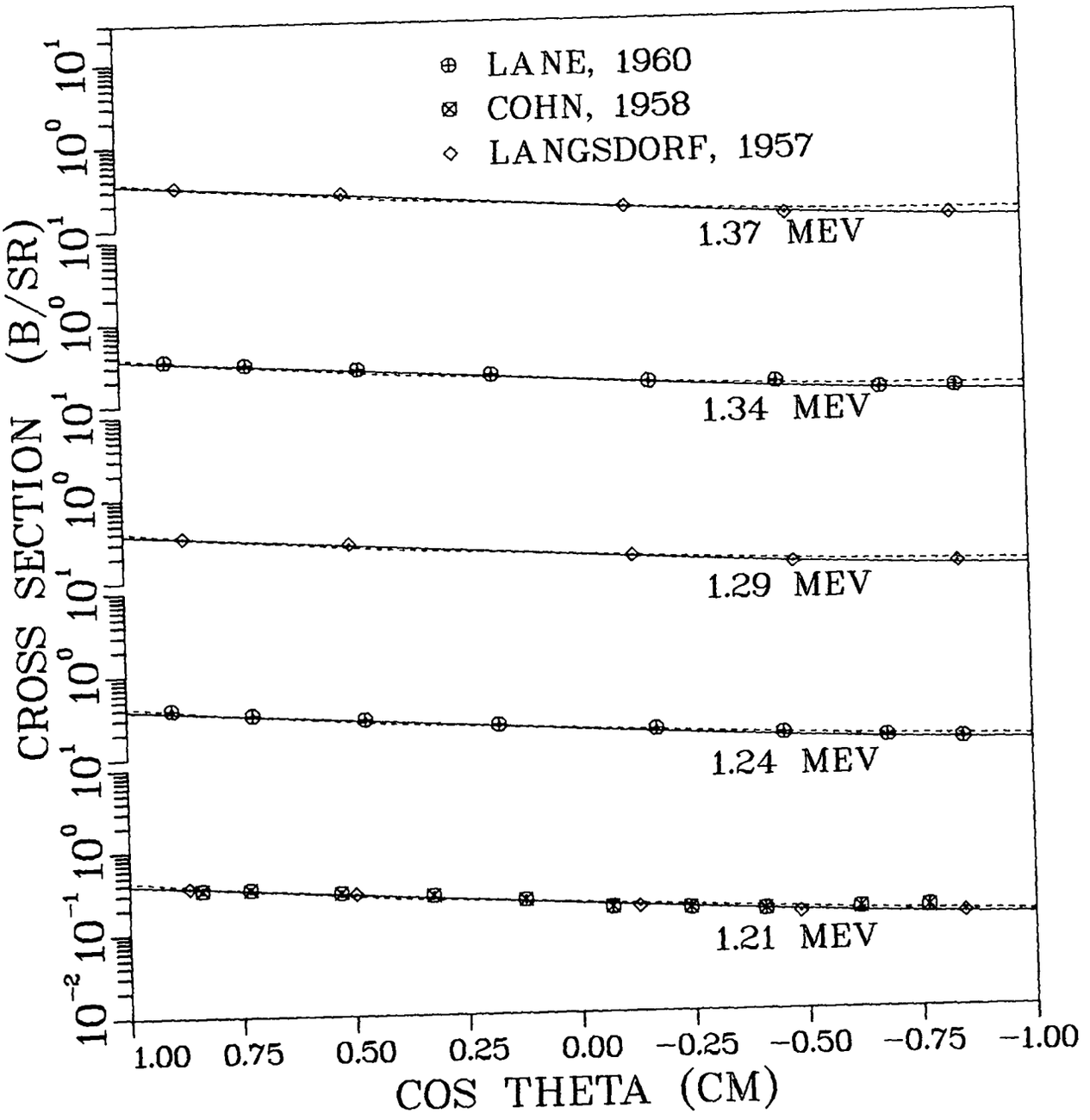


Fig. 24.
Measured and evaluated elastic angular distributions from 1.21 to 1.37 MeV. The solid curve is the present evaluation, and the dashed curve is ENDF/B-V.

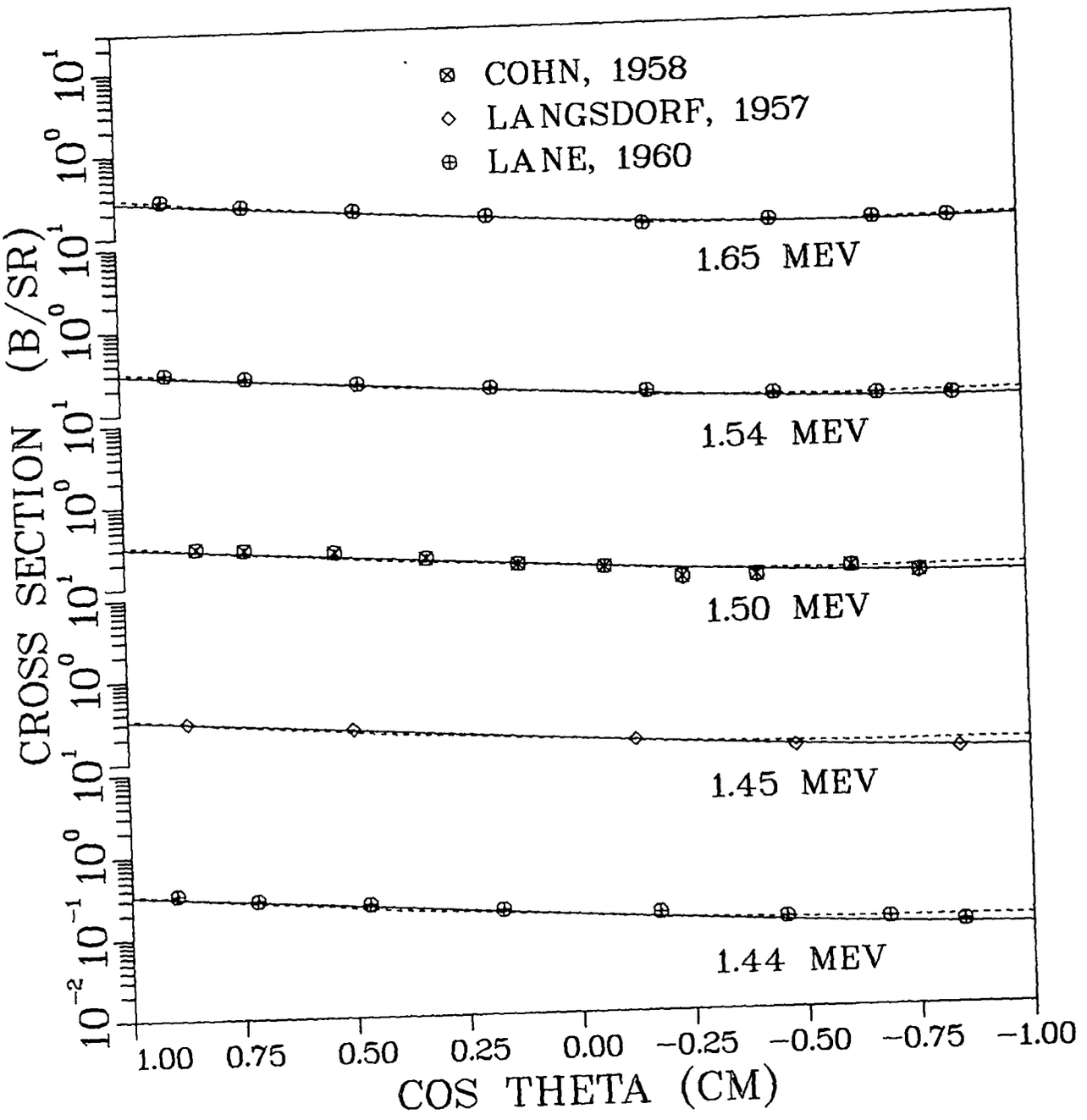


Fig. 25.
Measured and evaluated elastic angular distributions from 1.44 to 1.65 MeV. The solid curve is the present evaluation, and the dashed curve is ENDF/B-V.

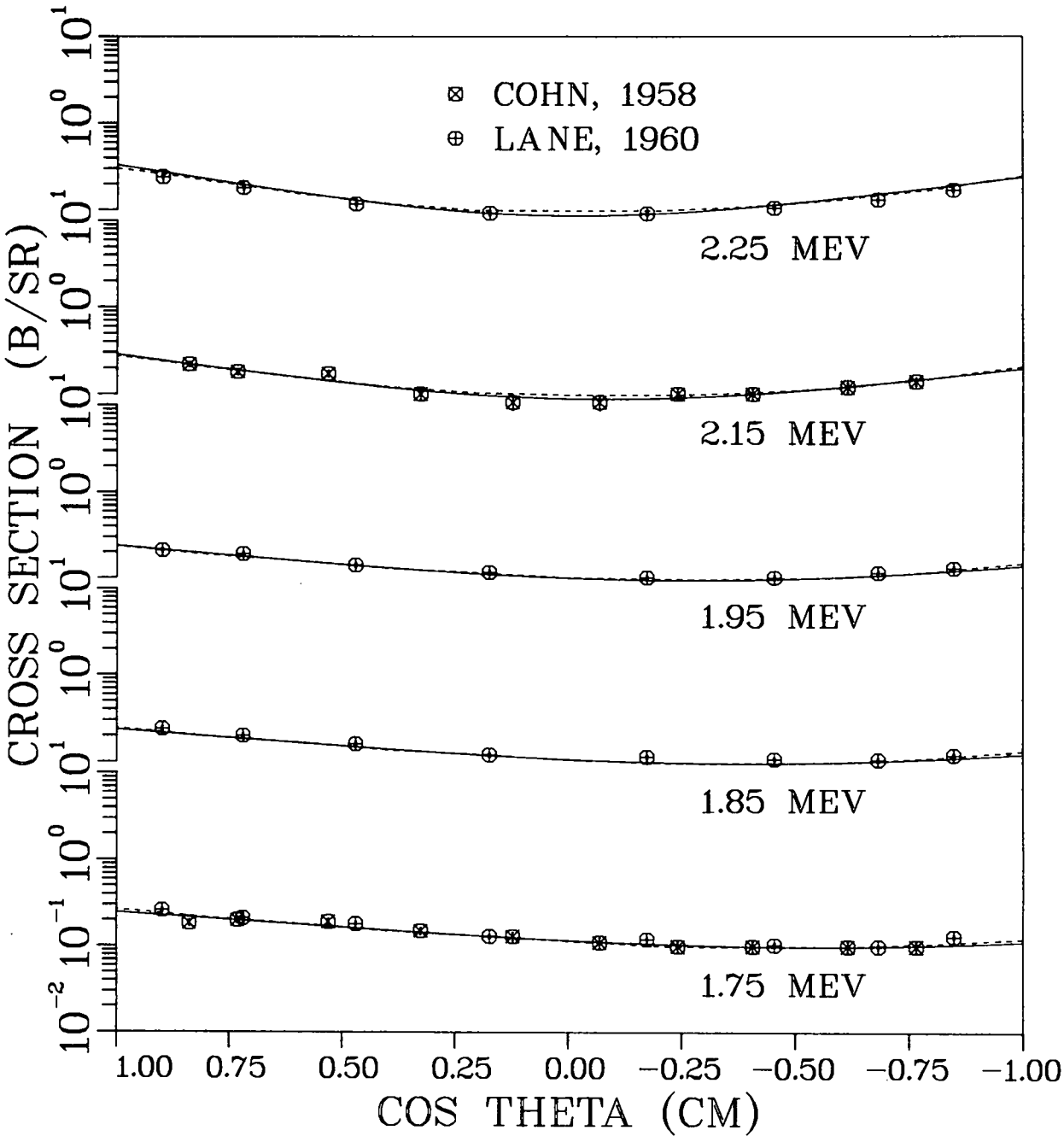


Fig. 26.
Measured and evaluated elastic angular distributions from 1.75 to 2.25 MeV. The solid curve is the present evaluation, and the dashed curve is ENDF/B-V.

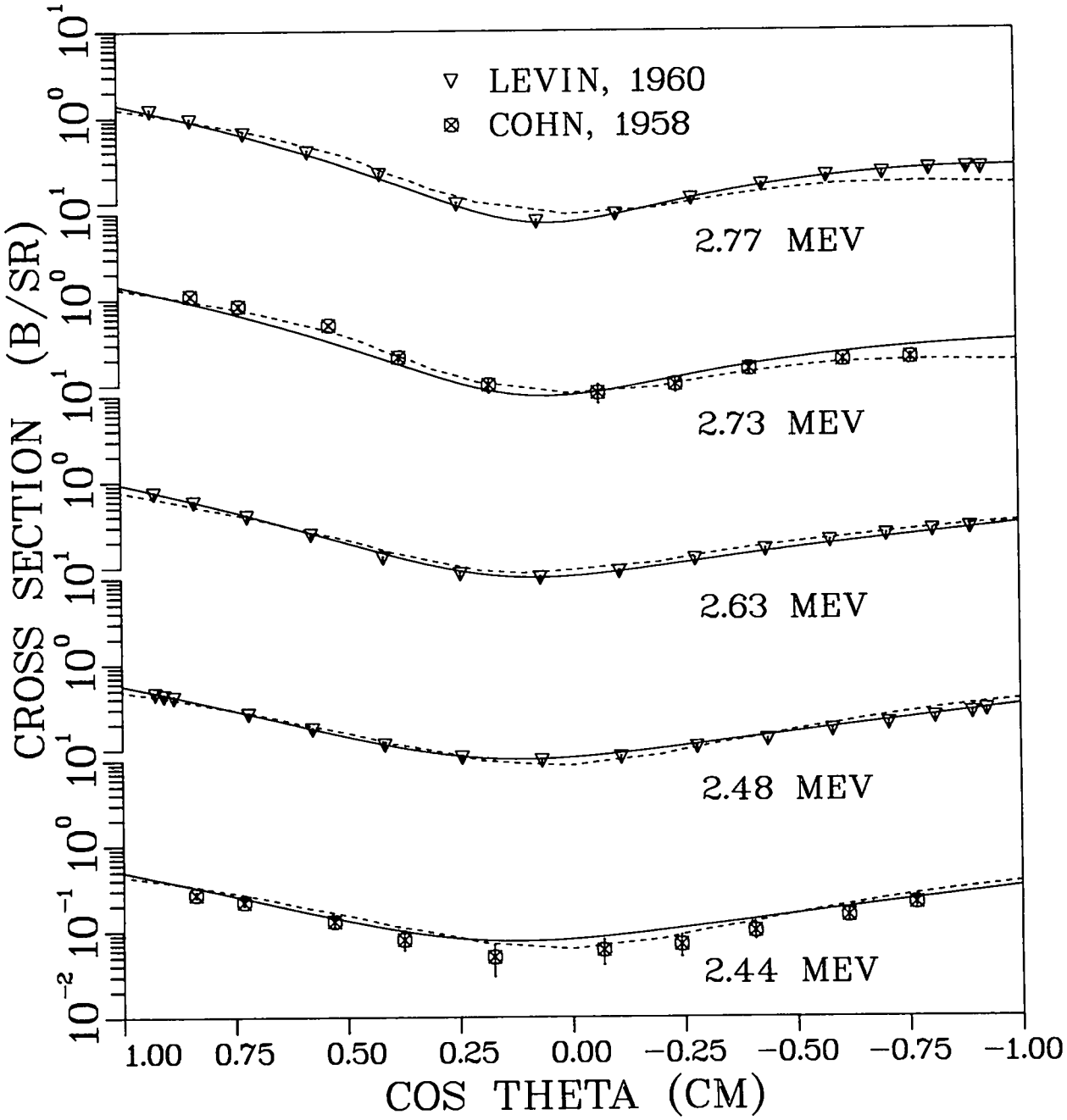


Fig. 27.
Measured and evaluated elastic angular distributions from 2.44 to 2.77 MeV. The solid curve is the present evaluation, and the dashed curve is ENDF/B-V.

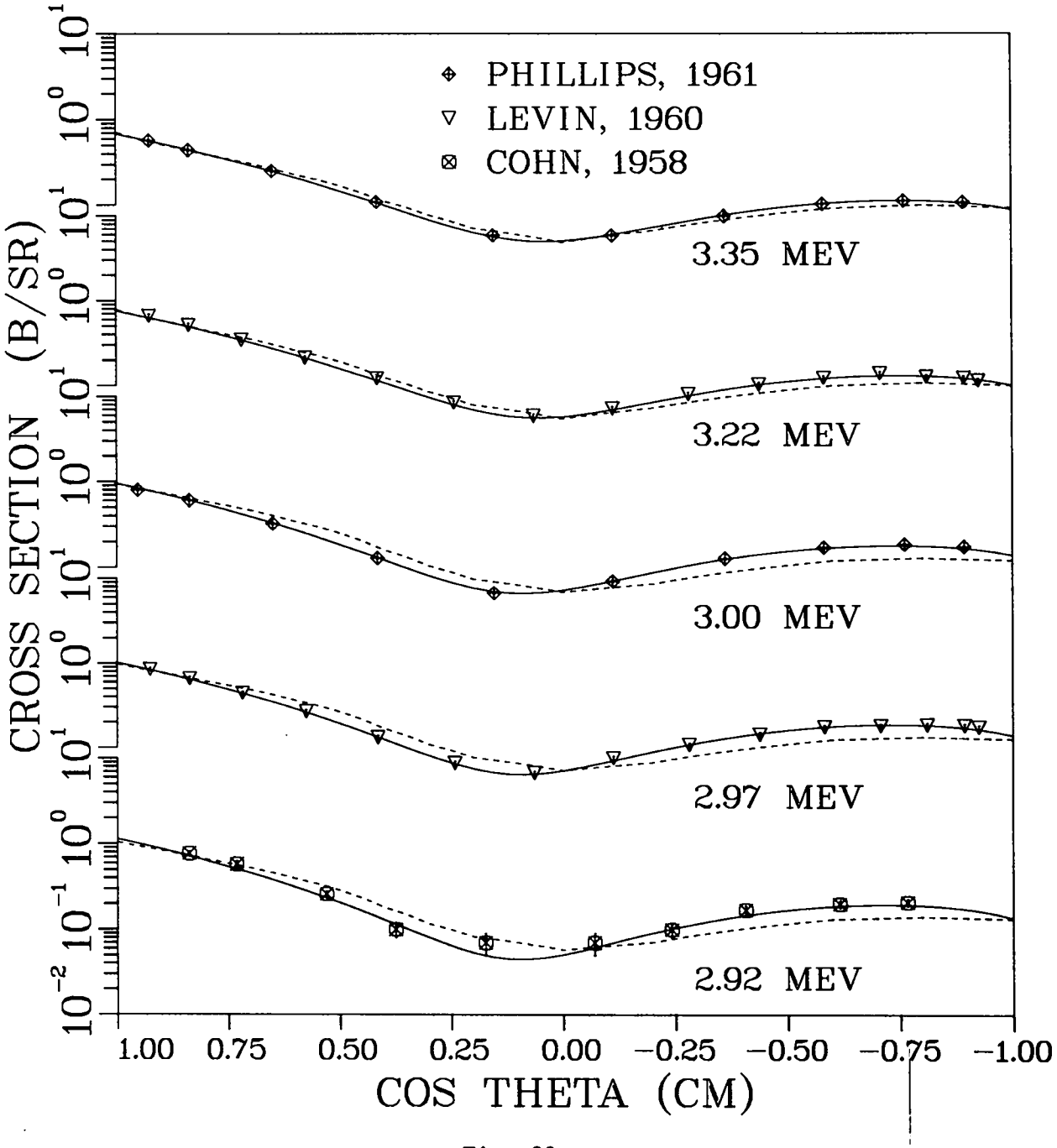


Fig. 28.
Measured and evaluated elastic angular distributions from 2.92 to 3.35 MeV. The solid curve is the present evaluation, and the dashed curve is ENDF/B-V.

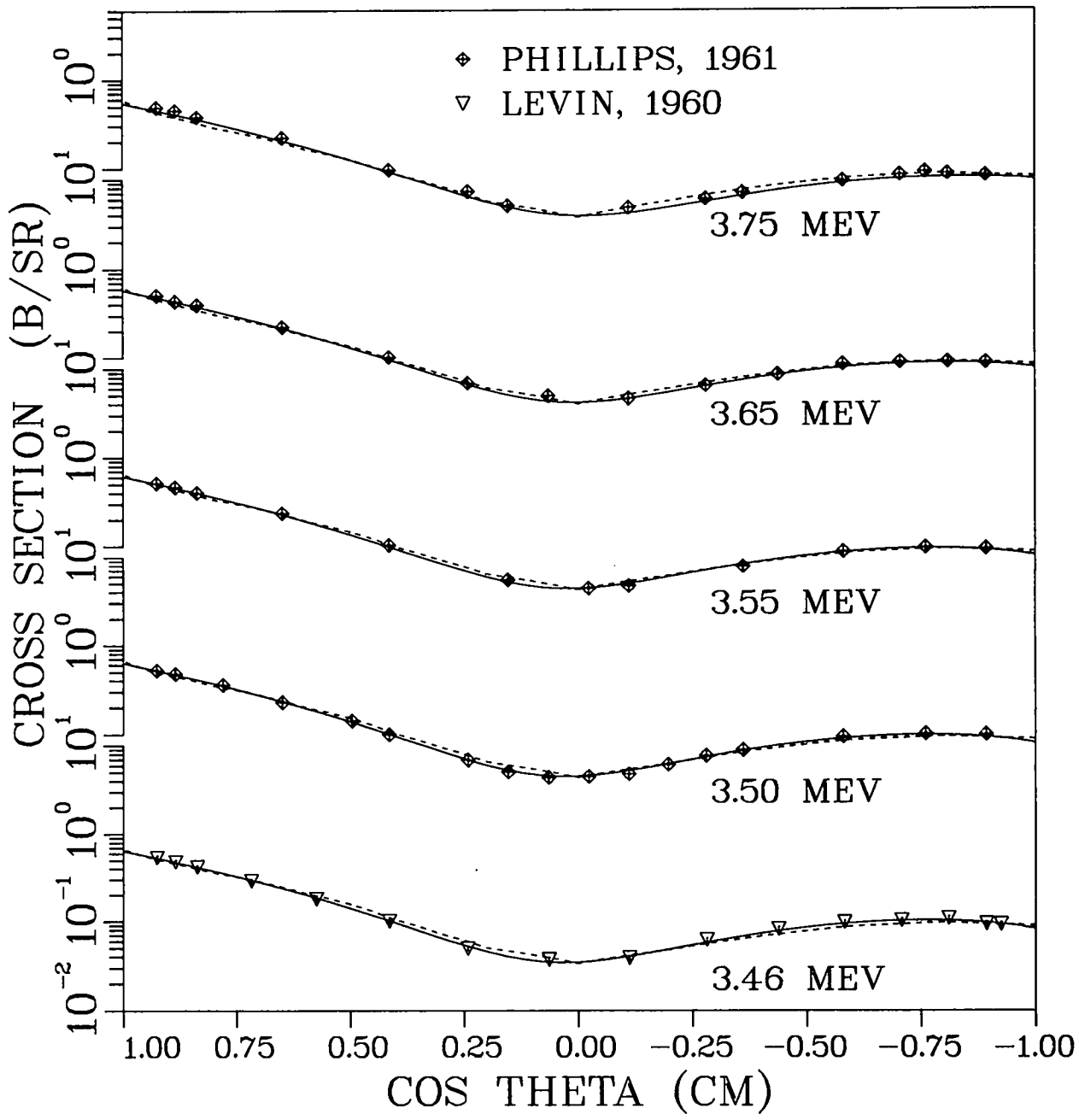


Fig. 29.
Measured and evaluated elastic angular distributions from 3.46 to 3.75 MeV. The solid curve is the present evaluation, and the dashed curve is ENDF/B-V.

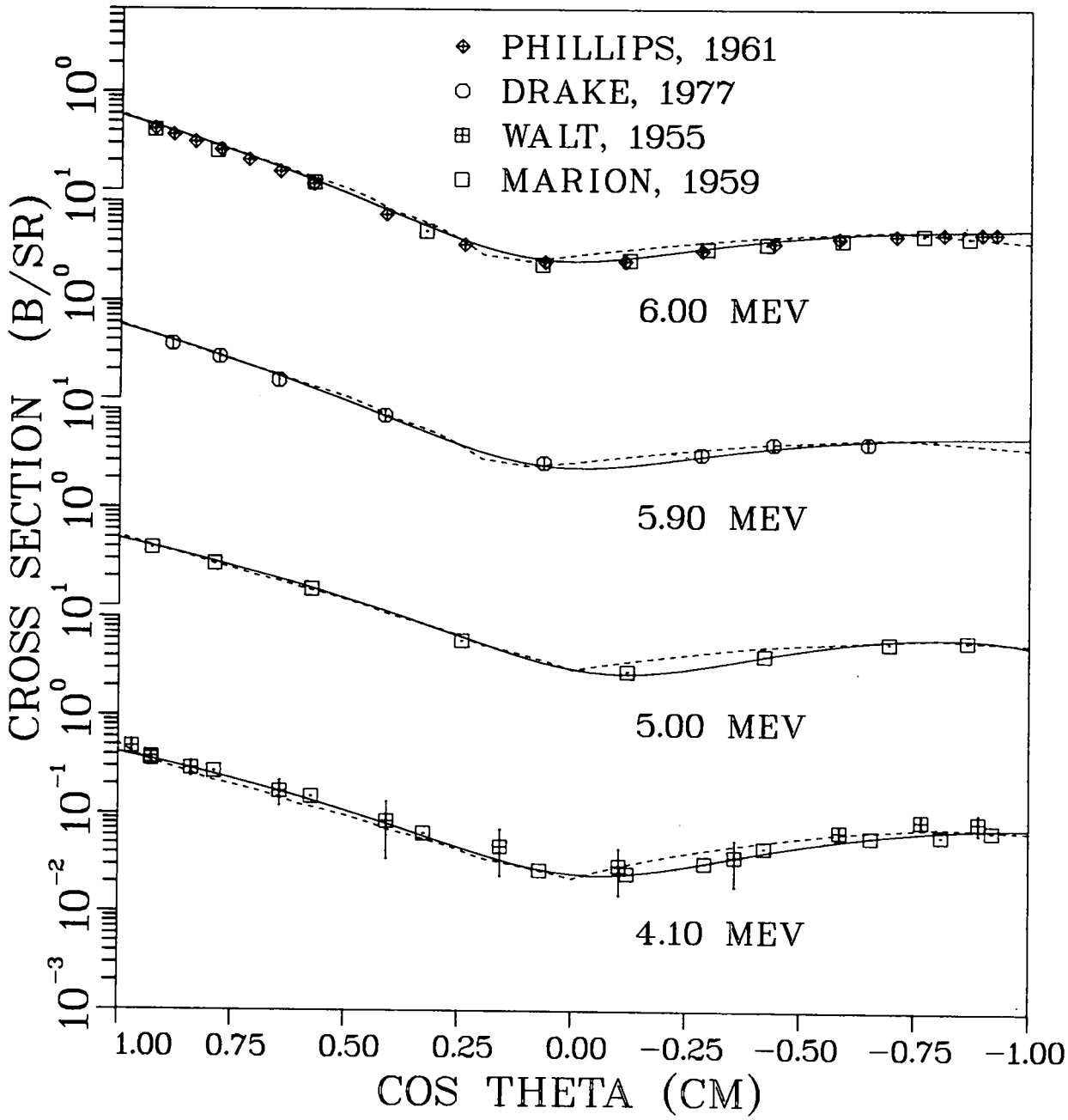


Fig. 30.
Measured and evaluated elastic angular distributions from 4.10 to 6.00 MeV. The solid curve is the present evaluation, and the dashed curve is ENDF/B-V.

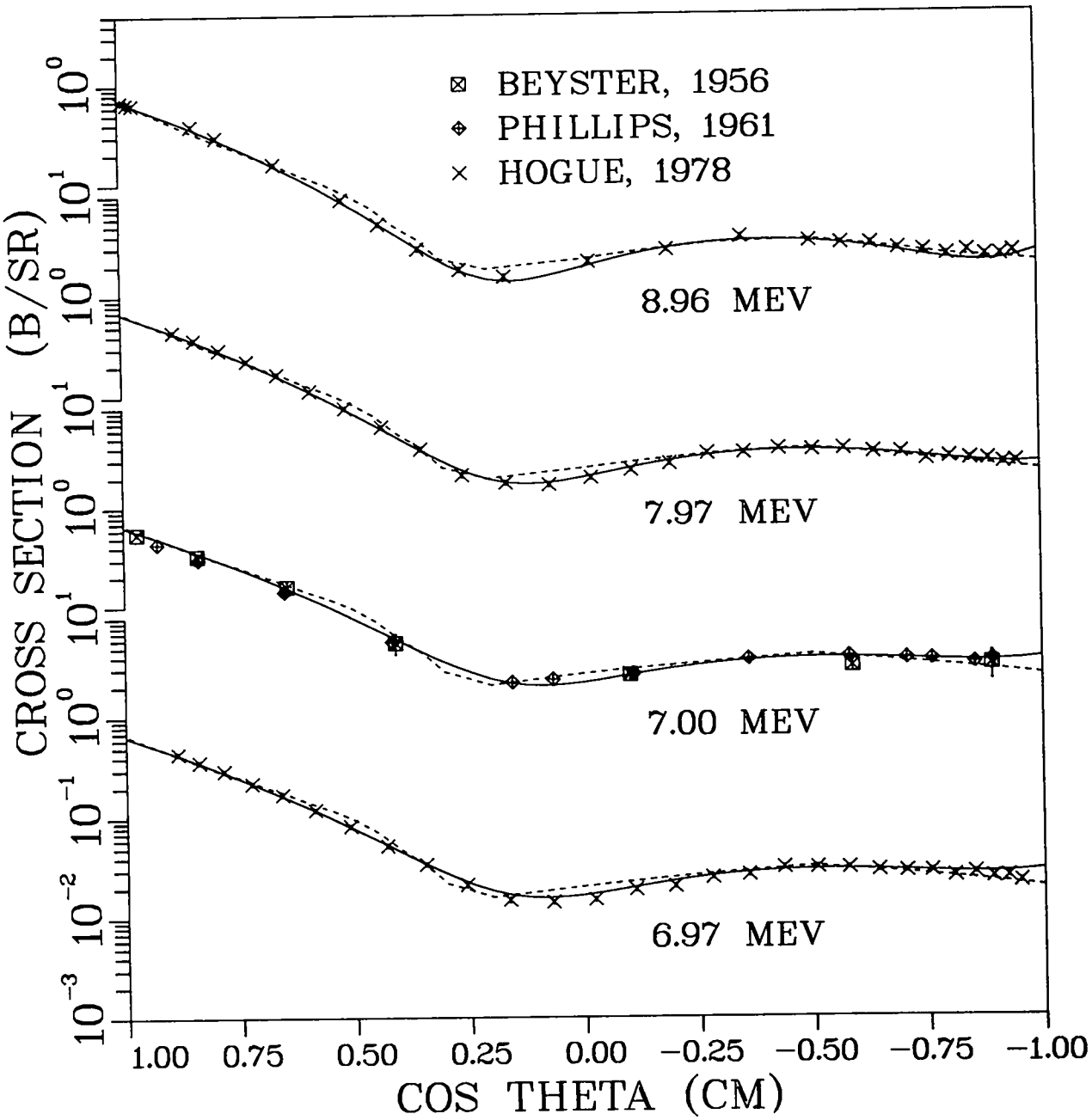


Fig. 31.
Measured and evaluated elastic angular distributions from 6.97 to 8.96 MeV. The solid curve is the present evaluation, and the dashed curve is ENDF/B-V.

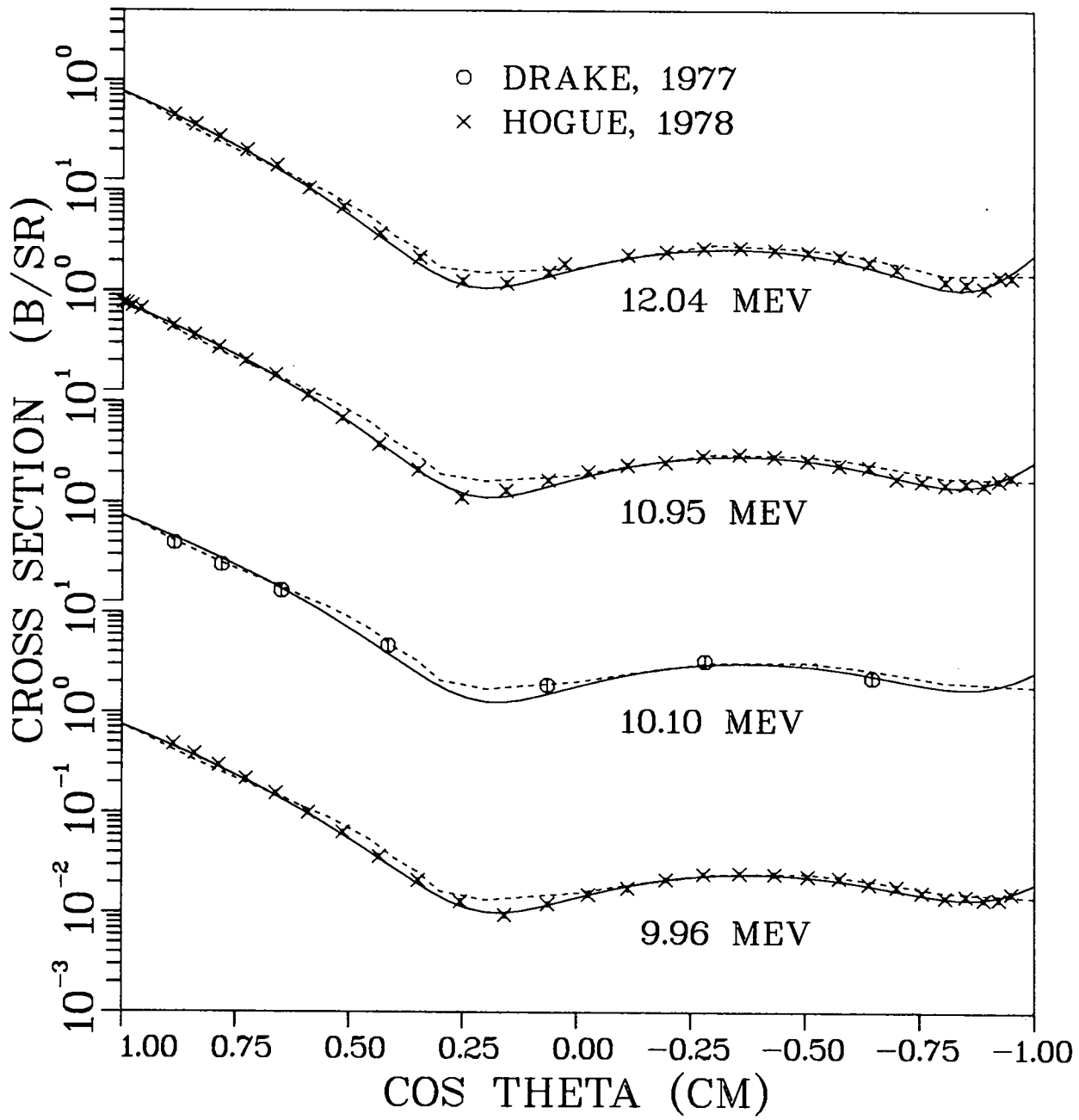


Fig. 32.
Measured and evaluated elastic angular distributions from 9.96 to 12.04 MeV. The solid curve is the present evaluation, and the dashed curve is ENDF/B-V.

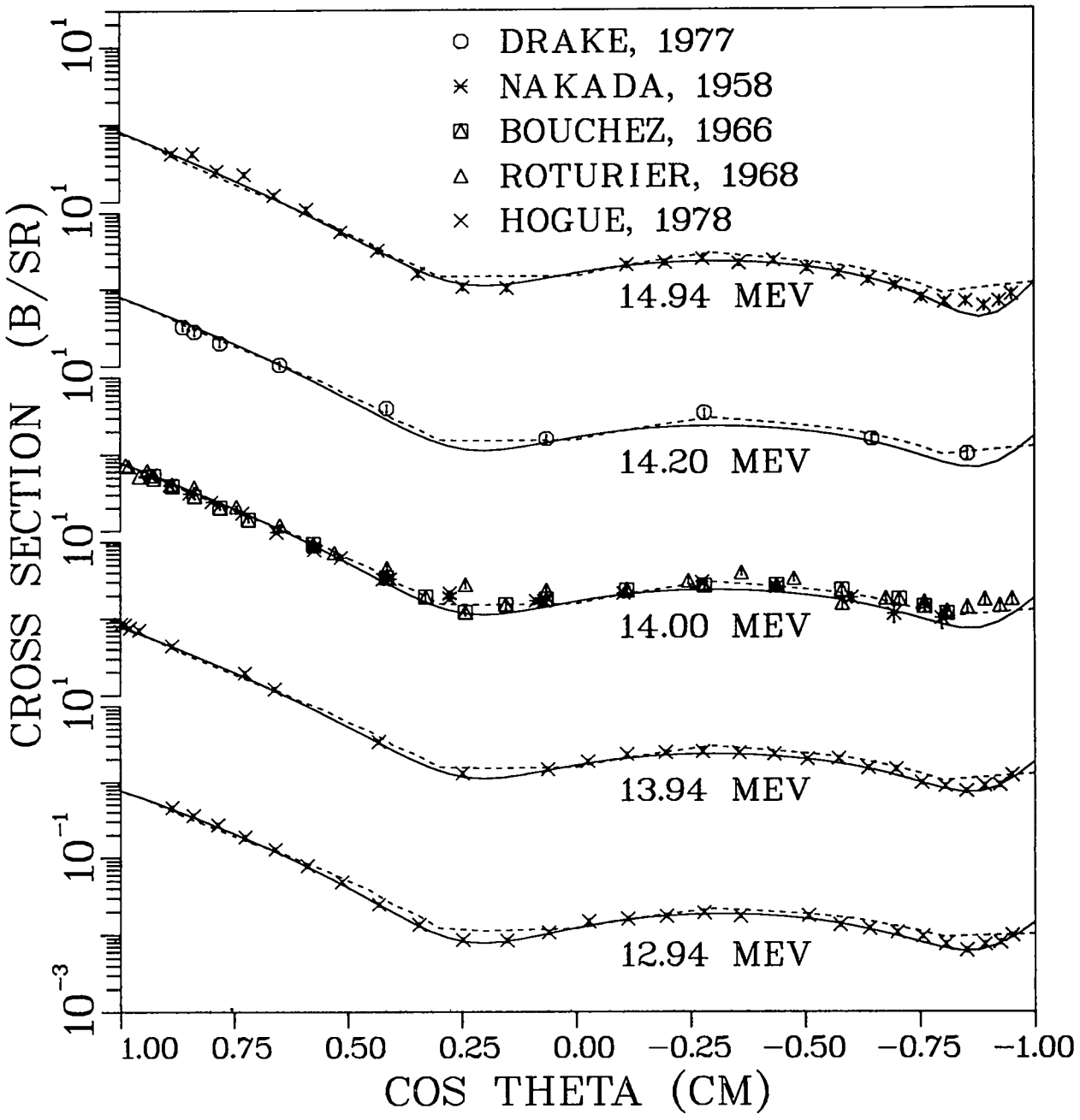


Fig. 33.
Measured and evaluated elastic angular distributions from 12.94 to 14.94 MeV. The solid curve is the present evaluation, and the dashed curve is ENDF/B-V.

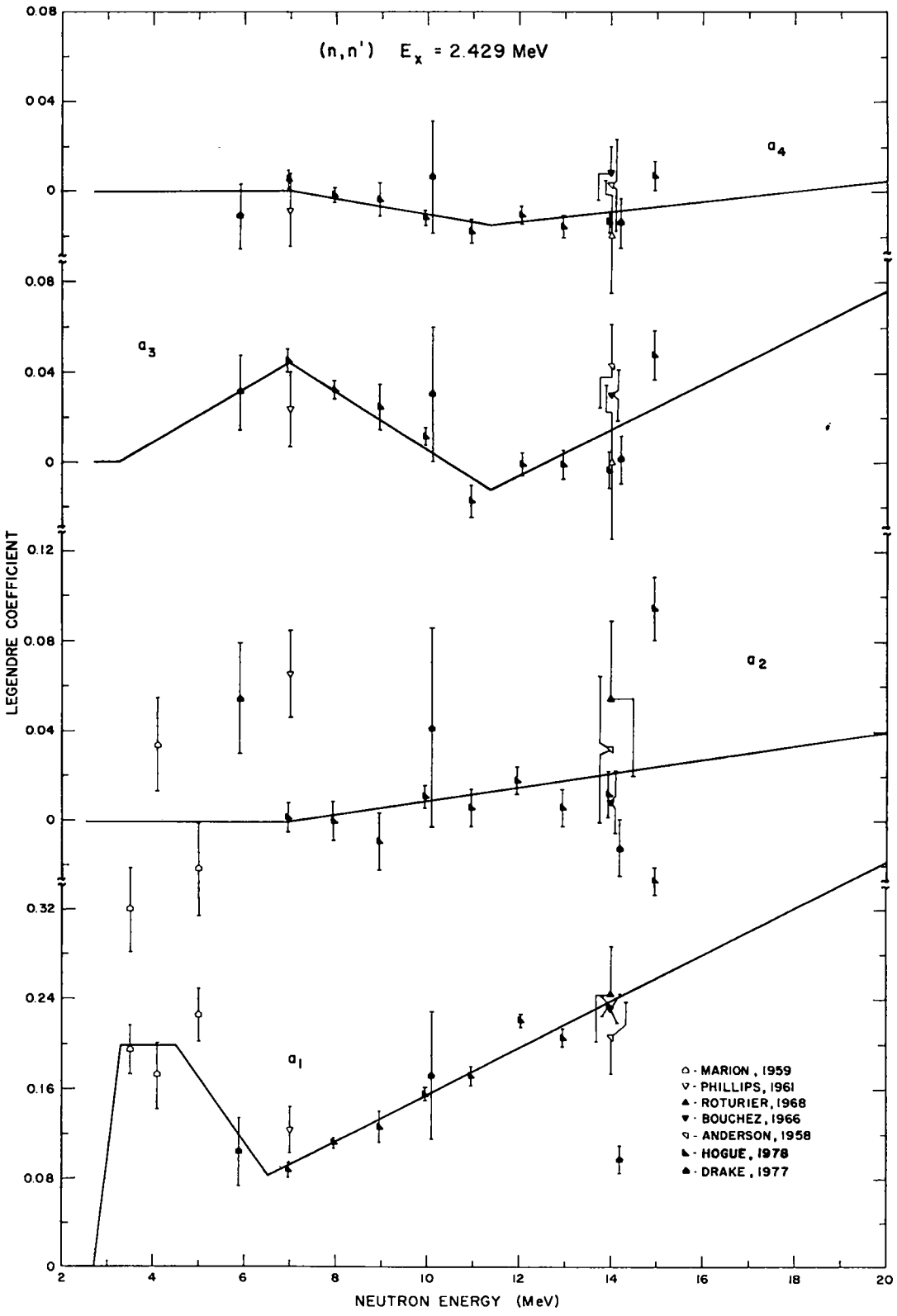


Fig. 34.
Evaluated Legendre coefficients for inelastic scattering to the cluster of states near 2.43-MeV excitation energy in $^9$Be.

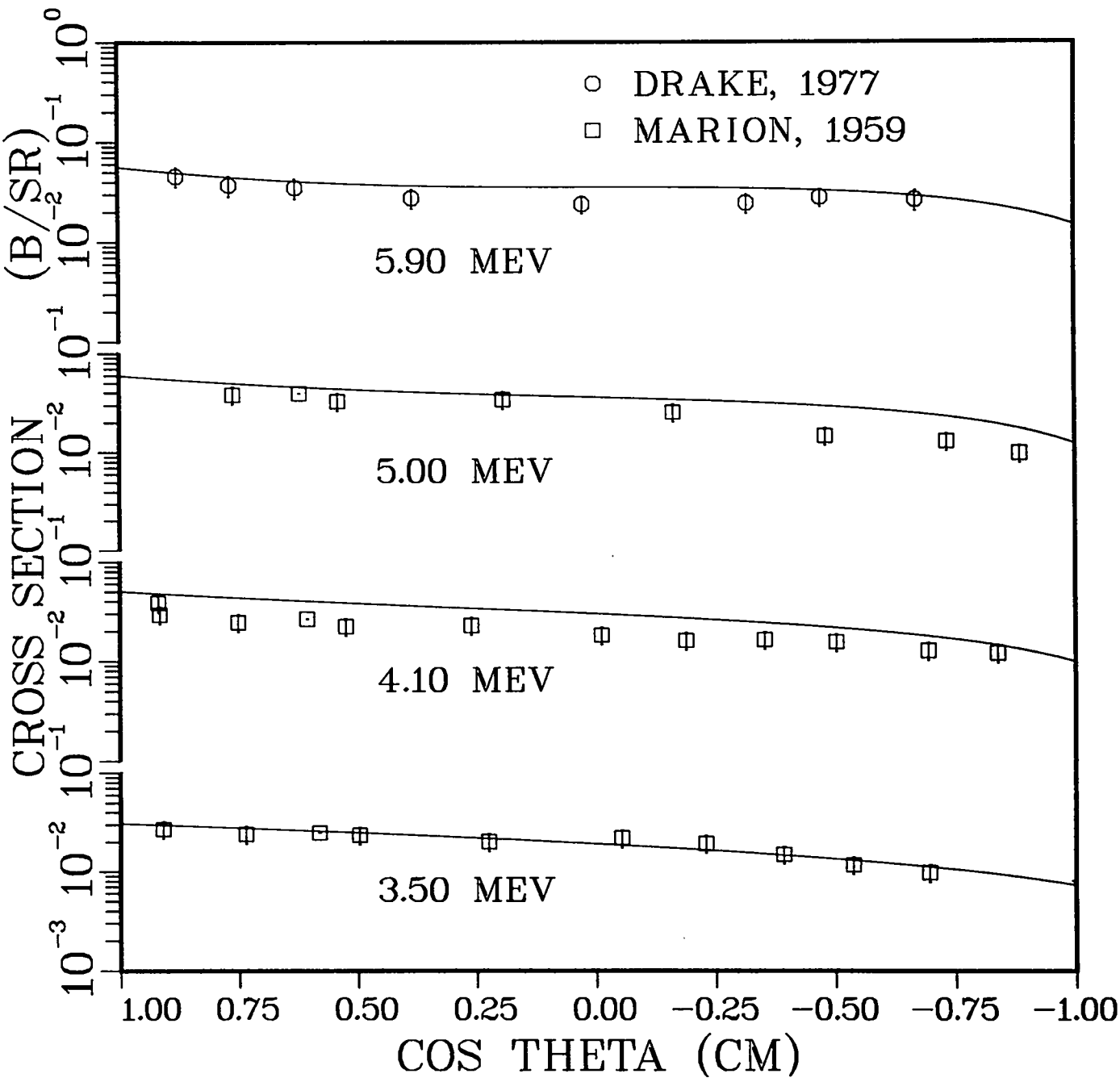


Fig. 35.
Measured and evaluated inelastic angular distributions for $E_x(^9Be)$ = 2.43 MeV and $E_n$ = 3.5-5.9 MeV.

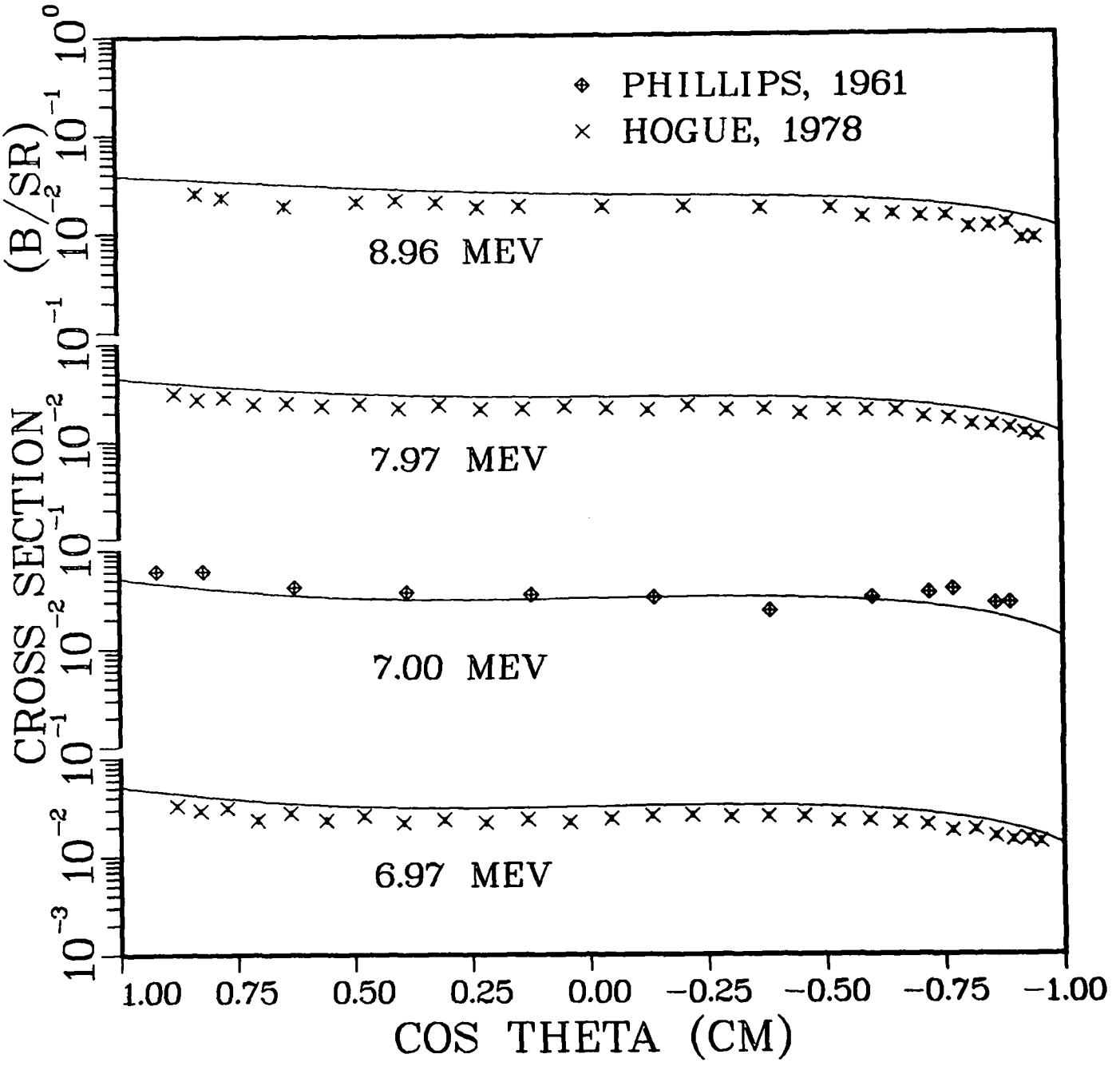


Fig. 36.
Measured and evaluated inelastic angular distributions for $E_x(^9Be)$ = 2.43 MeV and $E_n$ = 6.97-8.96 MeV.

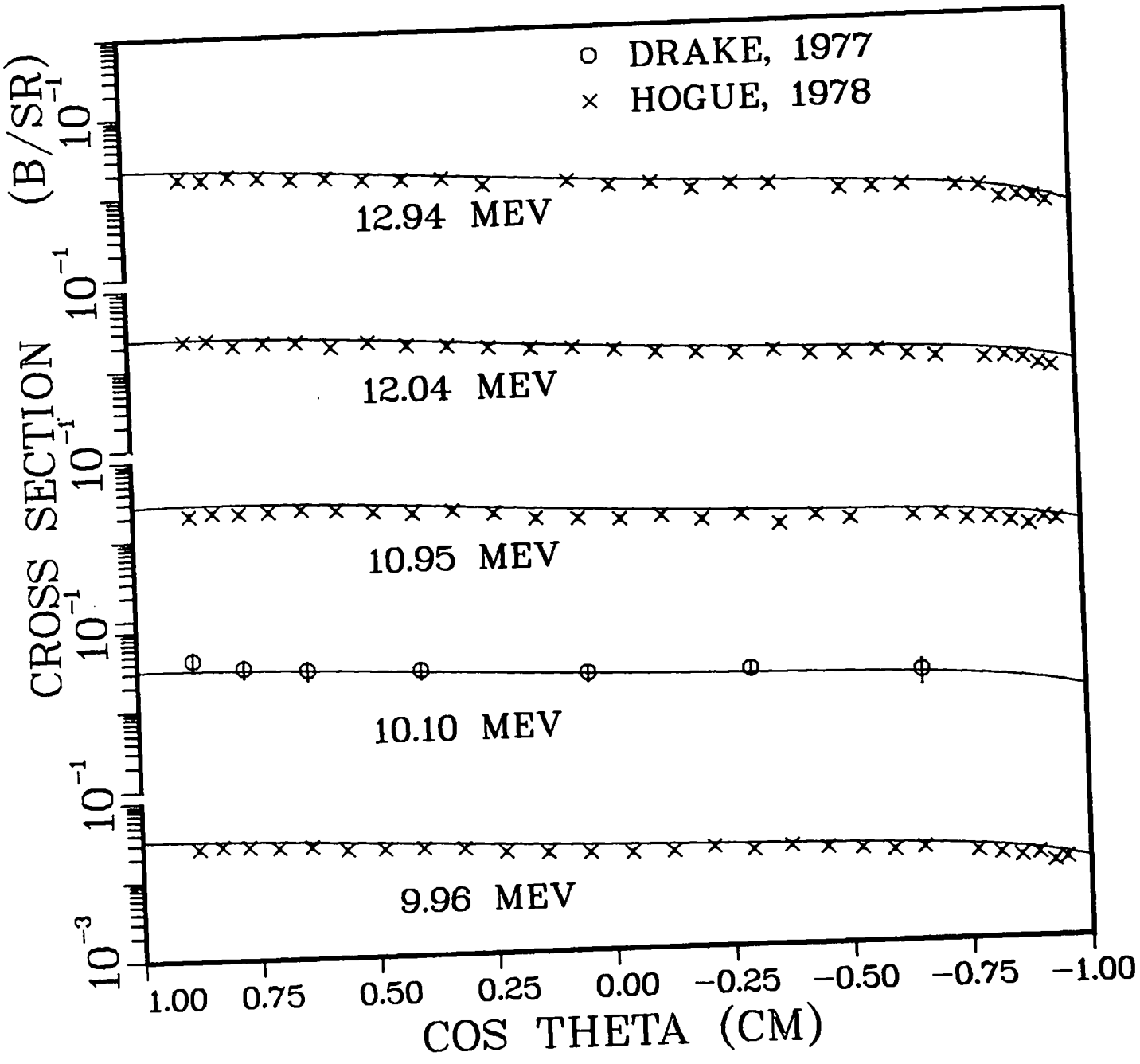


Fig. 37.
Measured and evaluated inelastic angular distributions for $E_x(^9Be)$ = 2.43 MeV and $E_n$ = 9.96-12.94 MeV.

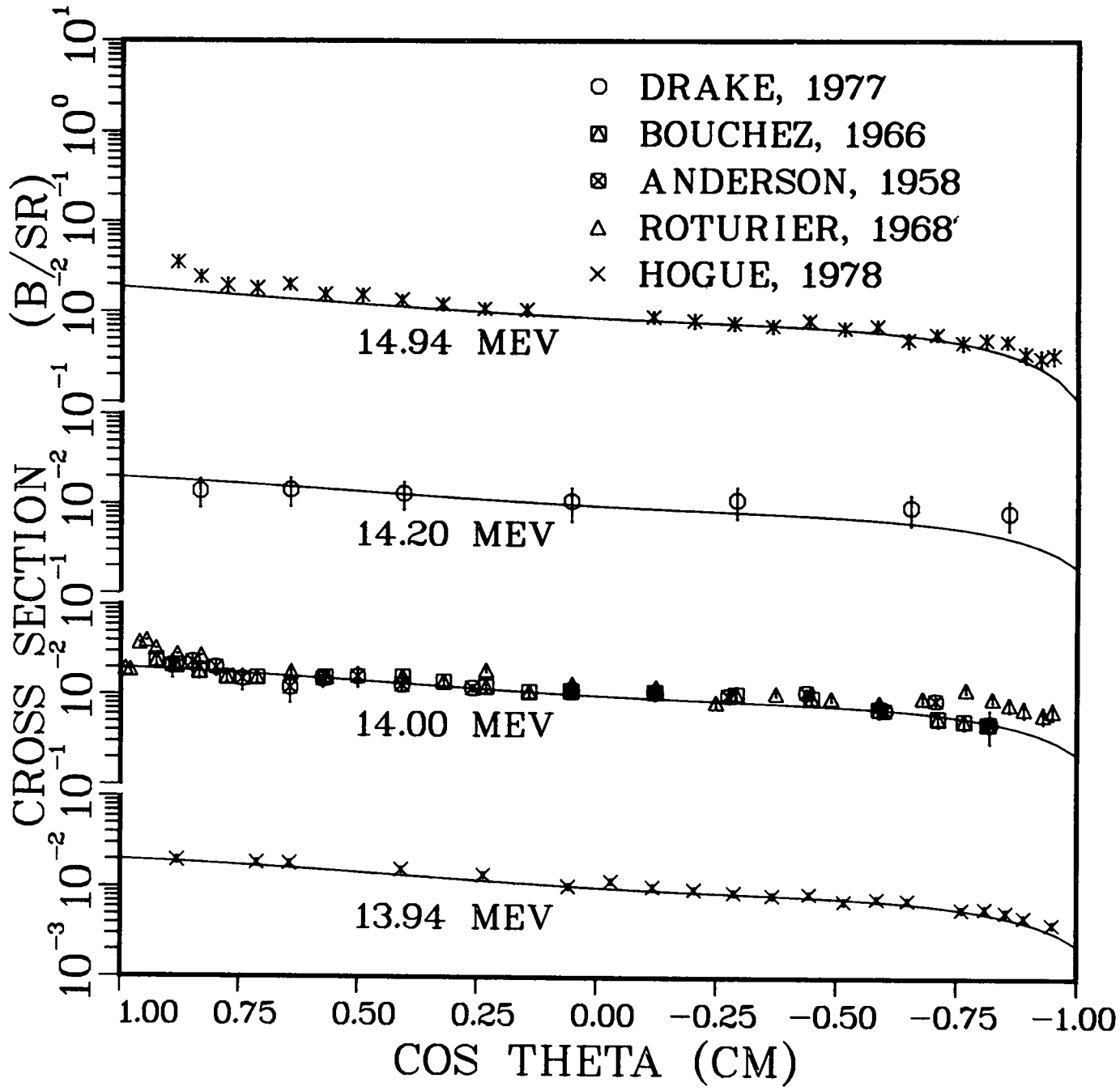


Fig. 38.
Measured and evaluated inelastic angular distributions for $E_x(^9Be)$ = 2.43 MeV and $E_n$ = 13.94-14.94 MeV.

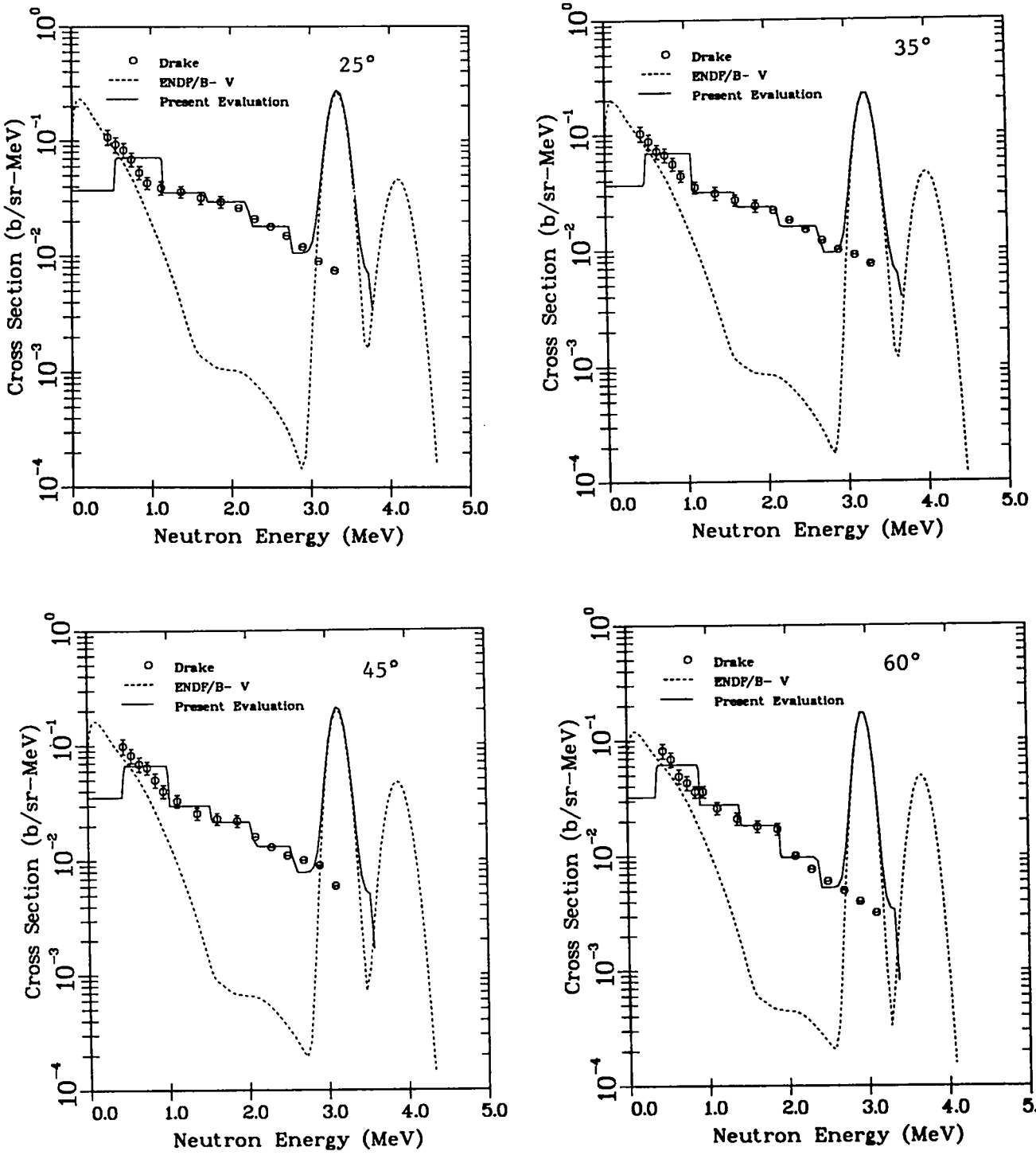


Fig. 39.
Measured and evaluated neutron-emission spectra at 25, 35, 45, and 60° induced by 5.9-MeV neutrons.

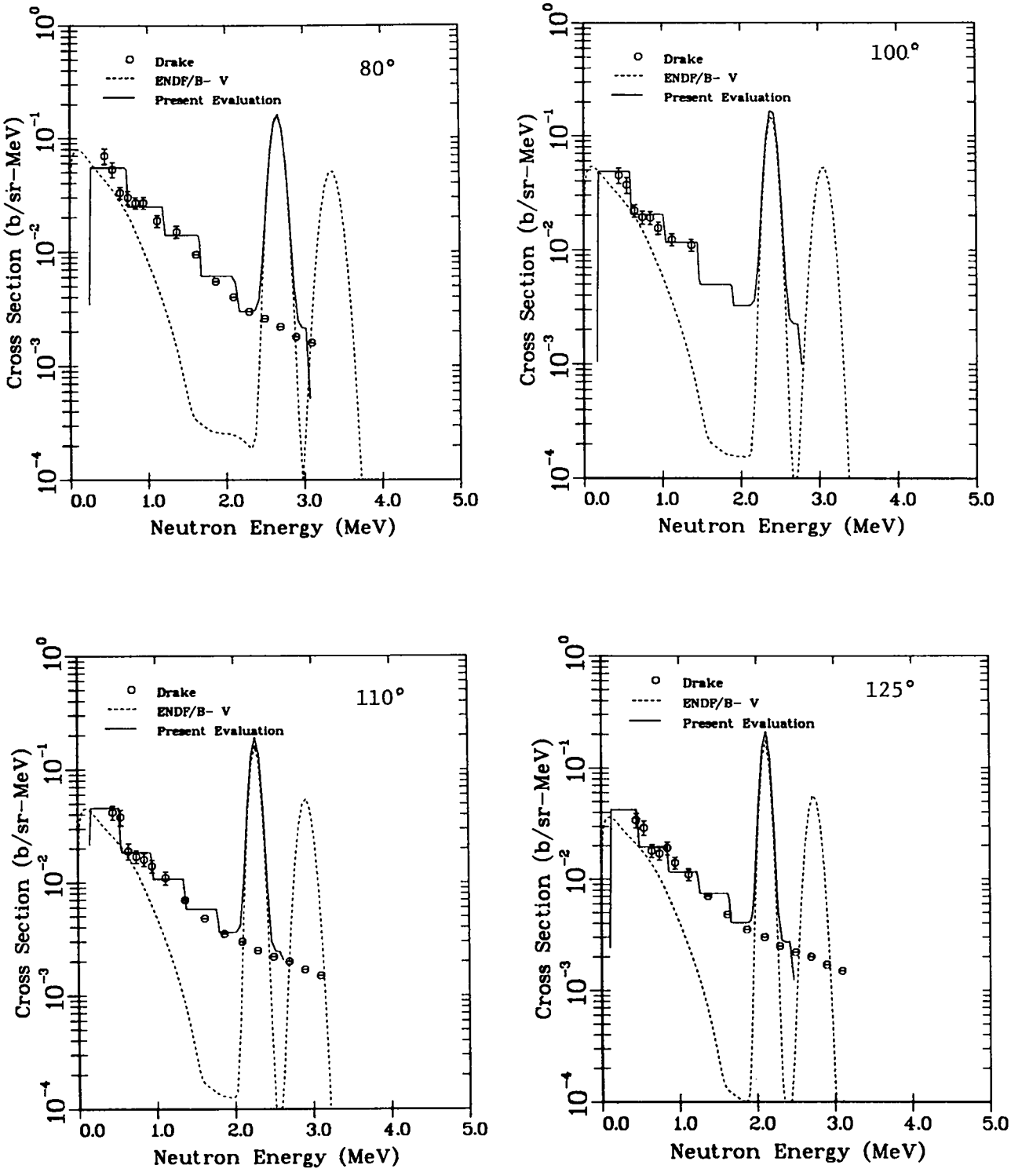


Fig. 40.
Measured and evaluated neutron emission spectra at 80, 100, 110, and 125° induced by 5.9-MeV neutrons.

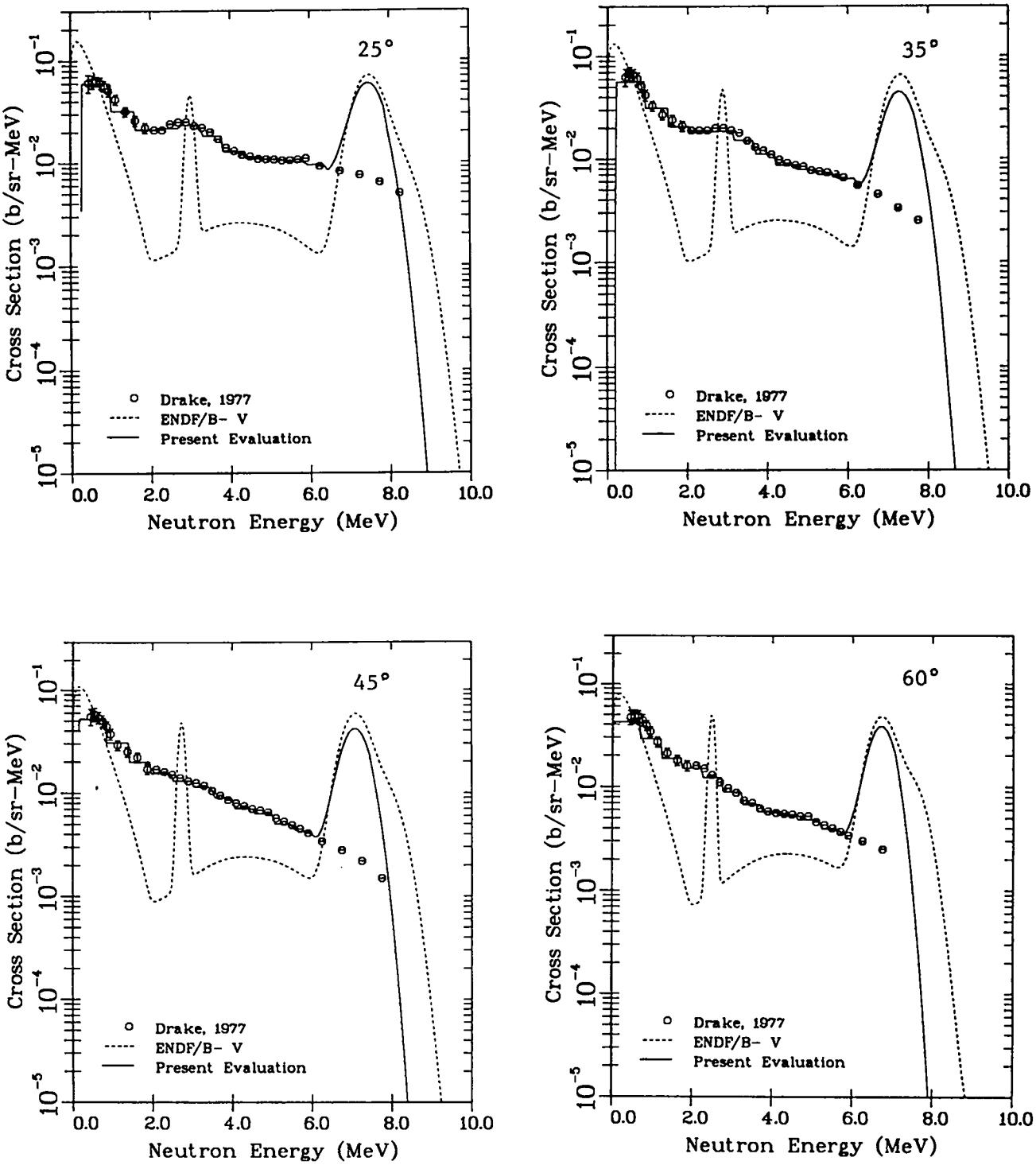


Fig. 41.
Measured and evaluated neutron-emission spectra at 25, 35, 45, and 60° induced by 10.1-MeV neutrons.

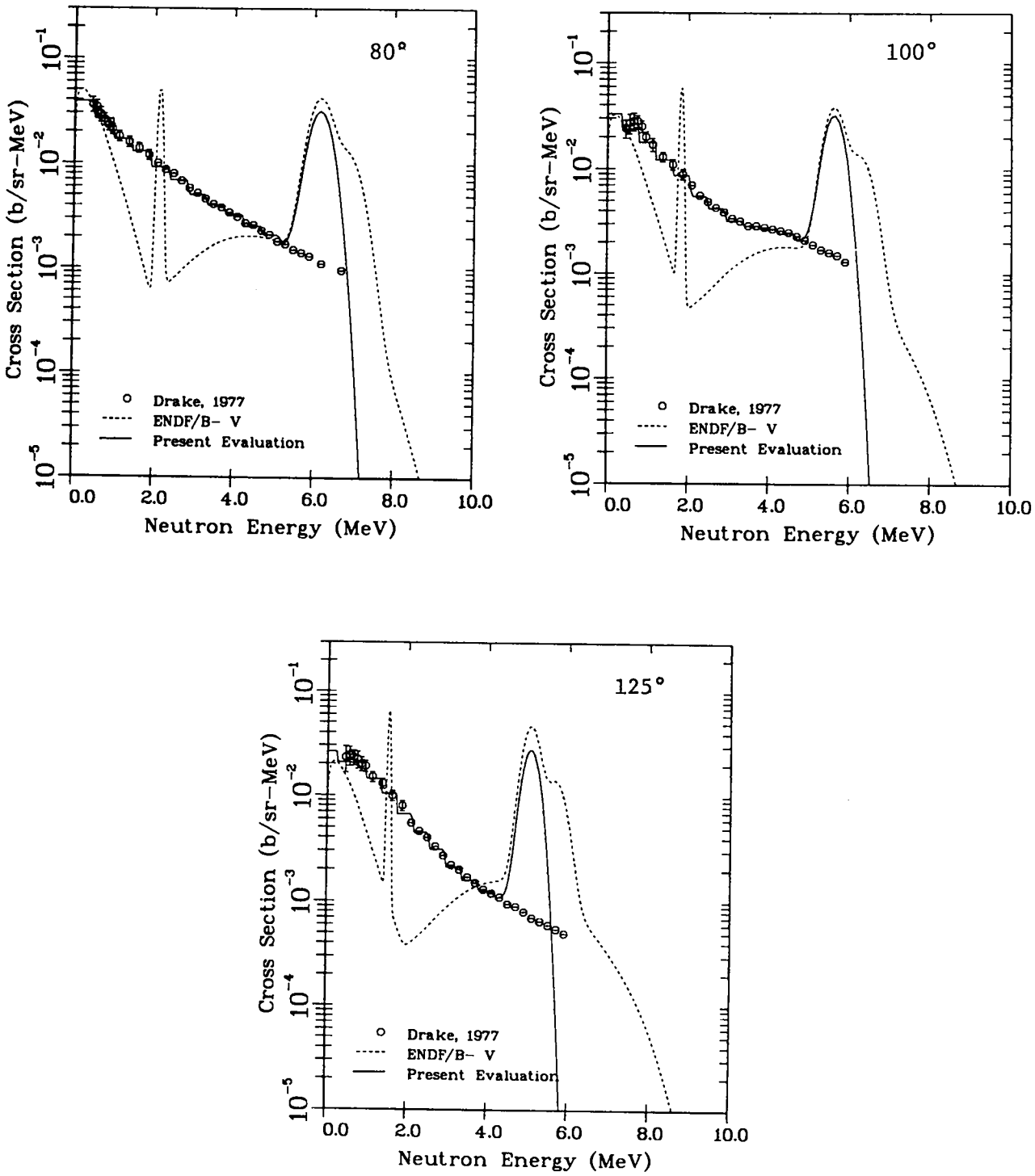


Fig. 42.
Measured and evaluated neutron-emission spectra at 80, 100, and 125° induced by 10.1-MeV neutrons.

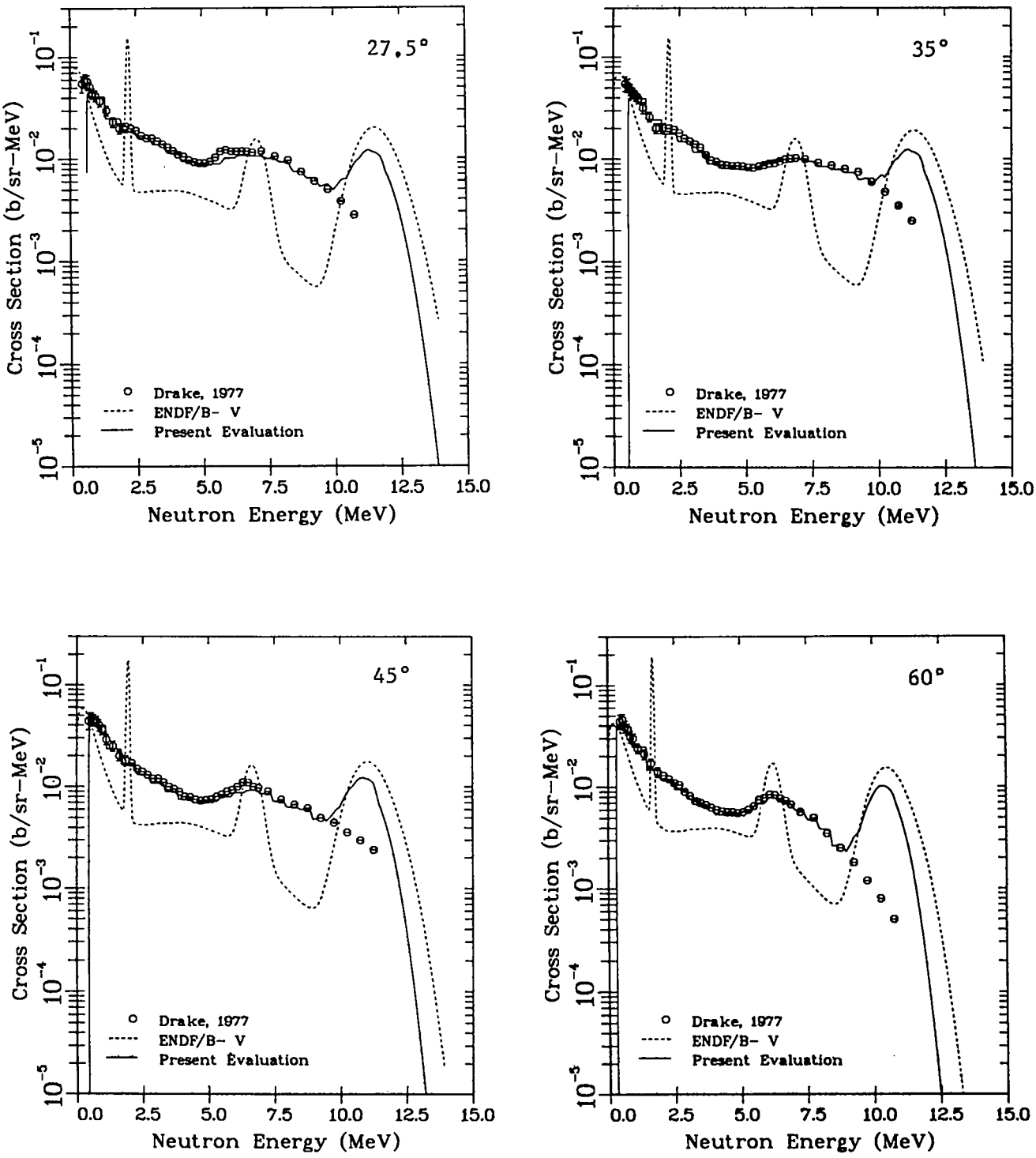


Fig. 43.
Measured and evaluated neutron-emission spectra at 27.5, 35, 45, and 60° induced by 14.2-MeV neutrons.

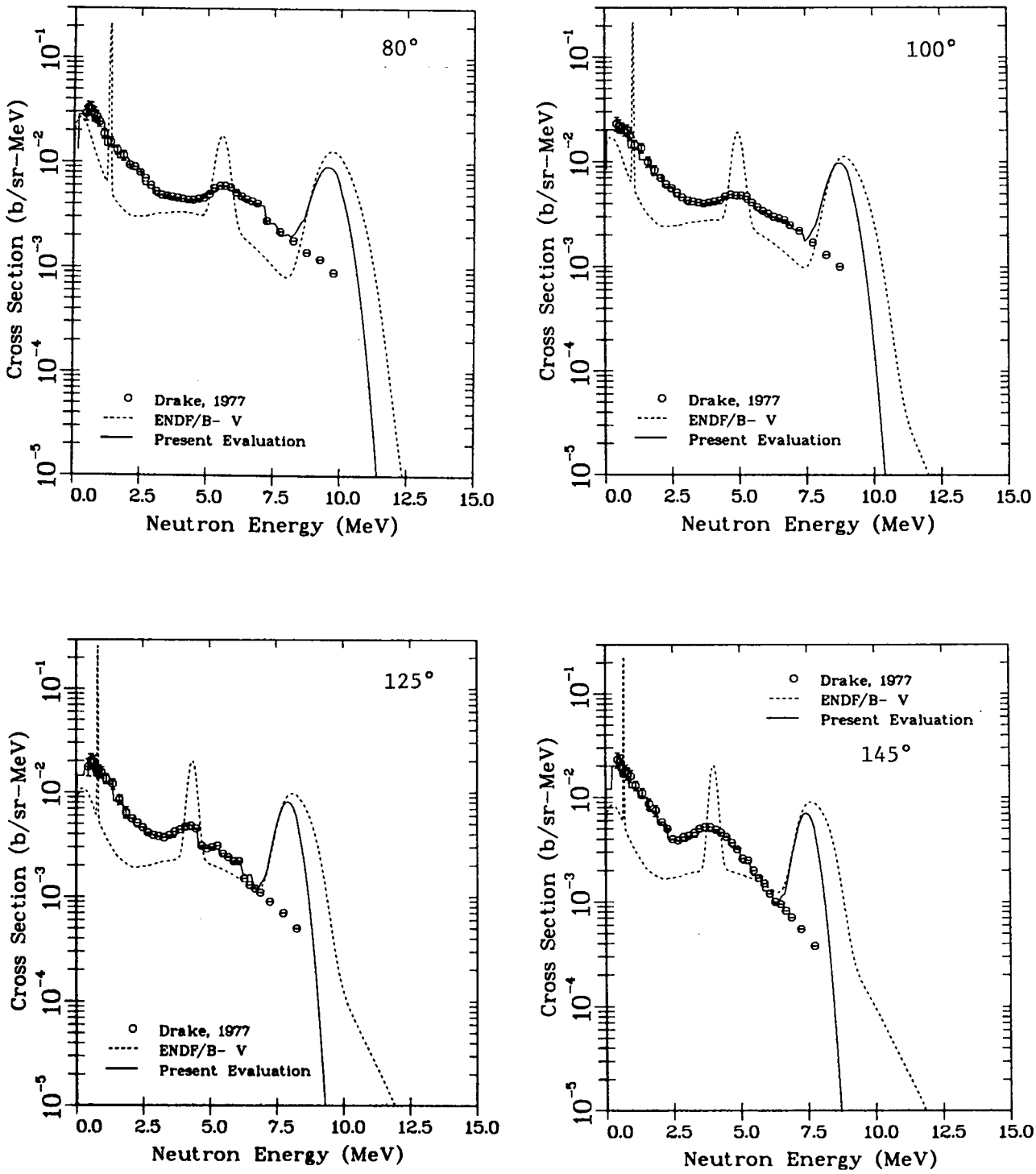


Fig. 44.
Measured and evaluated neutron-emission spectra at 80, 100, 125, and 145° induced by 14.2-MeV neutrons.

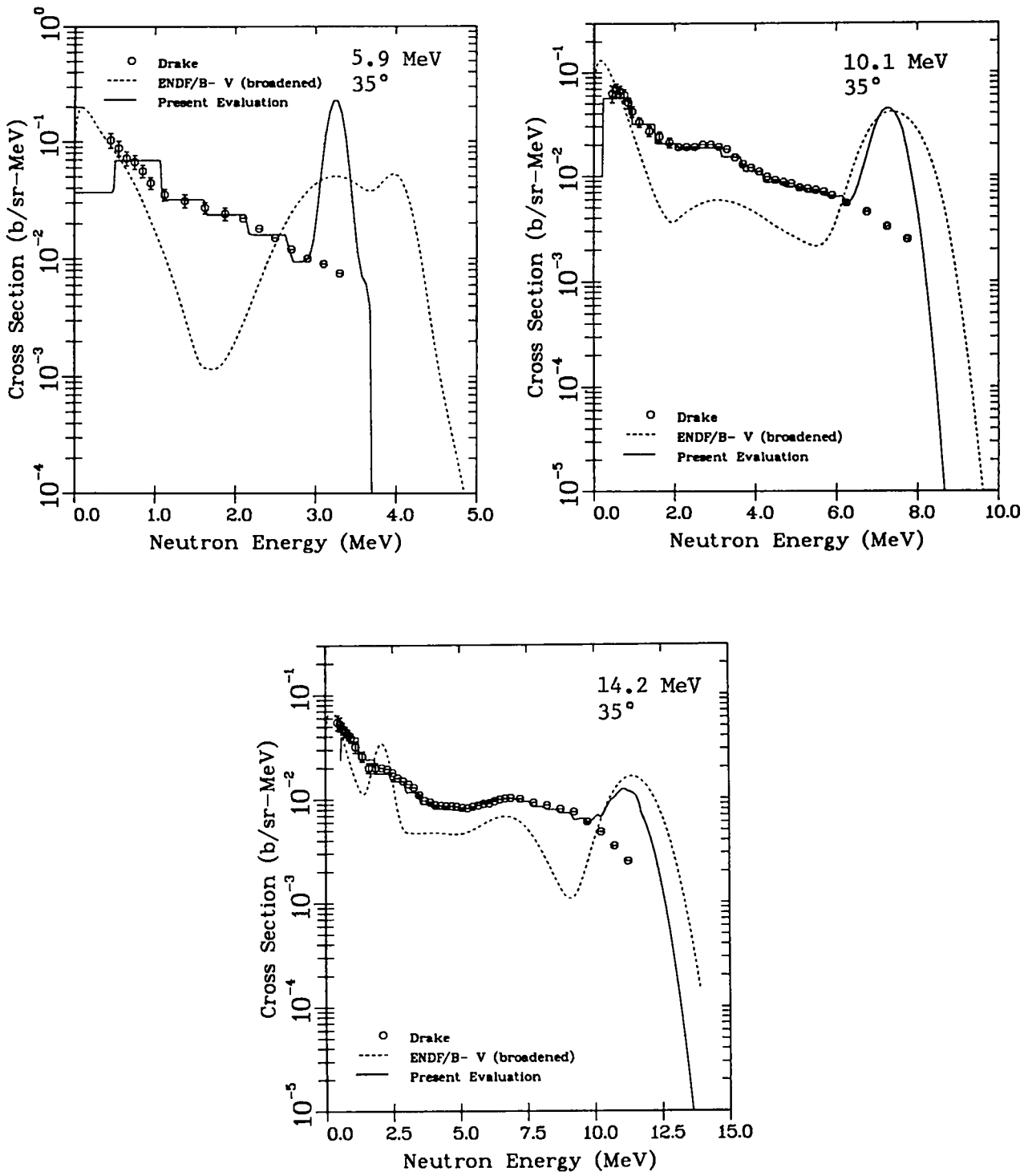


Fig. 45.
Calculated and measured neutron-emission spectra with the ENDF/B-V levels broadened as described in the text.

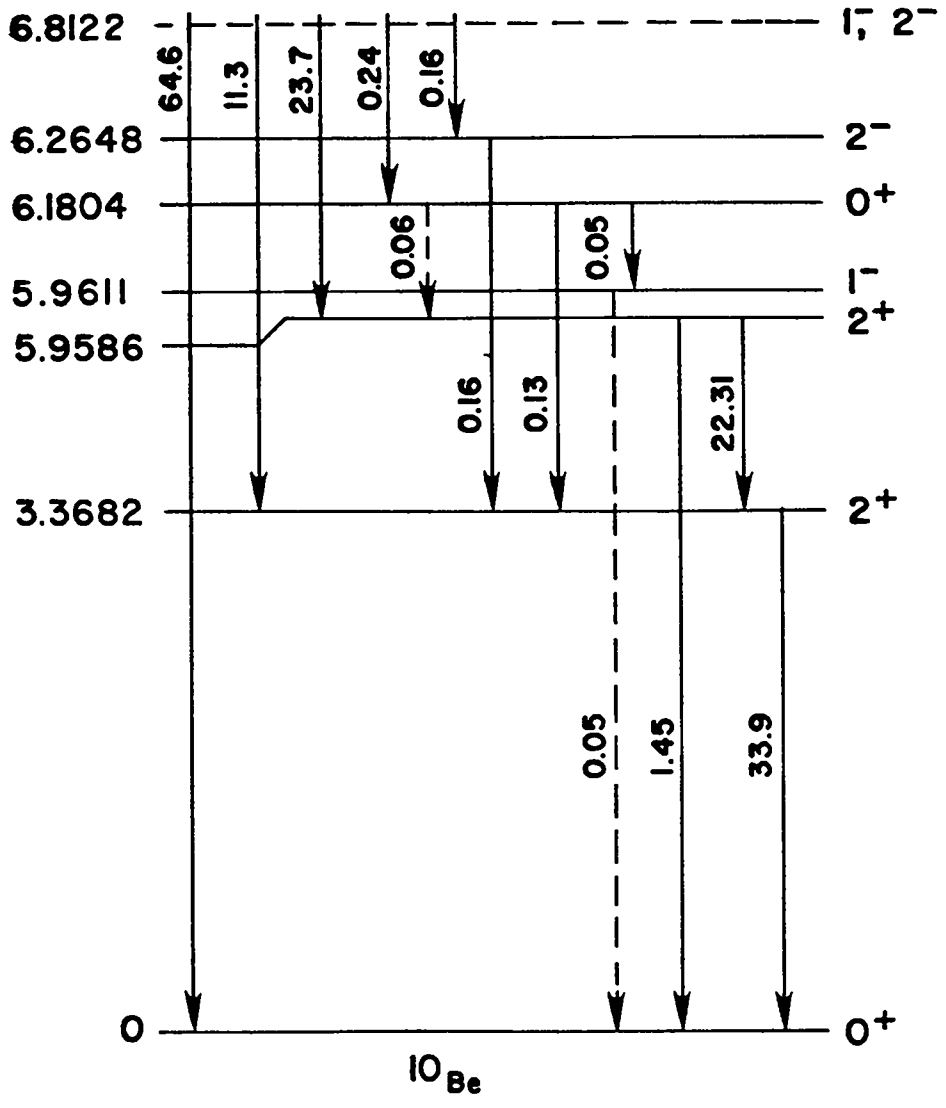


Fig. 46.
Schematic diagram of gamma-ray transitions following radiative capture of thermal neutrons in $^{9}Be$. Energies are given in MeV, and gamma-ray intensities are given in photons per 100 neutron captures.

☆ U.S. Government Printing Office: 1979 —677-013/147

Printed in the United States of America. Available from
National Technical Information Service
US Department of Commerce
5285 Port Royal Road
Springfield, VA 22161

Microfiche $3.00

| | | | | | | | | | |
|---|---|---|---|---|---|---|---|---|---|
| 001-025 | 4.00 | 126-150 | 7.25 | 251-275 | 10.75 | 376-400 | 13.00 | 501-525 | 15.25 |
| 026-050 | 4.50 | 151-175 | 8.00 | 276-300 | 11.00 | 401-425 | 13.25 | 526-550 | 15.50 |
| 051-075 | 5.25 | 176-200 | 9.00 | 301-325 | 11.75 | 426-450 | 14.00 | 551-575 | 16.25 |
| 076-100 | 6.00 | 201-225 | 9.25 | 326-350 | 12.00 | 451-475 | 14.50 | 576-600 | 16.50 |
| 101-125 | 6.50 | 226-250 | 9.50 | 351-375 | 12.50 | 476-500 | 15.00 | 601-up | |

Note: Add $2.50 for each additional 100-page increment from 601 pages up.